Bacteria of a feather floc together: Microbial interactions and function within iron-oxidizing bacterial communities

By

Chequita N. Brooks

May, 2021

Director of Dissertation: Dr. Erin K. Field

Major Department: Department of Biology

The microaerophilic iron-oxidizing bacteria are highly charismatic, forming bright orange structures called iron mats in low flow creeks and streams, in road-side ditches, and marshes. Yet, the study of the microbial communities that exist in the microniches formed by these iron mats has been heretofore lacking. This dissertation addresses ongoing questions regarding the microbial community and its interactions as they take place in iron-oxidizing bacterial communities. We present evidence of the presence of microorganisms previously unobserved in iron mats, including functional groups associated with nitrate-reducing iron-oxidation and methane cycling archaea, adding to the understanding of what major biogeochemical cycles are linked to and within the iron mat system. Furthermore, the possibly syntrophic relationship between iron-oxidizing and sulfate-reducing bacteria can now be studied in the laboratory, as we present in this work a methodology for co-culturing these functional groups. The ability of the iron mat microbial community to respond to anthropogenic stressors was tested using an *in situ* sampling procedure in a hydrocarbon exposed creek. The alpha diversity of exposed mats was found to decrease compared to unexposed mats, and the overrepresentation of common taxa was found to be tied to seasonality. However, the iron mat communities appear to functionally respond to hydrocarbon exposure, as genes associated with benzene degradation were more

abundant in exposed mats and taxa associated with benzene degradation (e.g., *Hydrogenophaga* spp.) were also found. In order to elucidate whether the evolution of microorganisms exposed to hydrocarbons was also influenced, we exposed *Hydrogenophaga taeniospiralis* 2K1 to two different ecologically relevant regimes that are analogous to press and pulse treatment – an intensifying press and repeated pulse - with benzene. We found that both regimes could lead to speciation-level differences in the whole genome sequences of the cultures within 100 generations. Cumulatively, this work serves to further our understanding of the iron mat community, addressing questions regarding structure, function, microbial interactions, and sensitivity to abiotic perturbation.

Bacteria of a feather floc together: Microbial interactions and function within iron-oxidizing bacterial communities

A Dissertation

Presented to the Faculty of the Department of Biology

East Carolina University

In Partial Fulfillment of the Requirements for the Degree

Doctor of Philosophy in the Interdisciplinary Doctoral Program in Biology, Biomedicine, and Chemistry

by

Chequita N. Brooks

May, 2021

Bacteria of a feather floc together: Microbial interactions and function within iron-oxidizing bacterial communities

by

Chequita Nicole Brooks

APPROVED BY:

DIRECTOR OF
DISSERTATION:

Dr. Erin K. Field, Ph.D.

COMMITTEE MEMBER:

Dr. Christopher Balakrishnan, Ph.D.

COMMITTEE MEMBER:

Dr. D. Reide Corbett, Ph.D.

COMMITTEE MEMBER:

Dr. Ariane L. Peralta, Ph.D.

COMMITTEE MEMBER:

Dr. Michael W. McCoy, Ph.D.

CHAIR OF THE
DEPARTMENT OF BIOLOGY:

Dr. David R. Chalcraft, Ph.D.

DEAN OF THE
GRADUATE SCHOOL:

Dr. Paul J. Gemperline, Ph.D.

This dissertation is dedicated to every little girl with big dreams and a big heart. May you go far.

ACKNOWLEDGEMENTS

The process of graduate school is not without its many challenges and if it were not for the help I received, I would not have made it this far. I would like to, first and foremost, thank my advisor Dr. Erin Field for her support. Though we faced many challenges, I will forever be grateful that she picked me to be one of her first graduate students. I would also like to thank my committee, Drs. Christopher Balakrishnan, Reide Corbett, Ariane Peralta, and Mike McCoy for their support and guidance. I would also like to thank some of the many mentors that lent a listening ear during my time as a graduate student, to Drs. Peri Bolton, Michael Brewer, Dave Chalcraft, Ed Stellwag, Thomas Martin, Barbara Ballentine, Jeremy Hyman, and Seán O'Connell I would like to convey my deepest and sincerest gratitude. Thanks to all of you for your time, your energy, and your willingness to help me in finding my way.

I would also like to thank my dearest friends. To Emily Ashe, Rebecca Barnard, and Tyler Bowling: your support has meant the world to me. Thanks to all of you, and all of my friends that will go unnamed here, for reading drafts, listening to my worries, and reminding me to take a minute to breathe. Furthermore, I would like to thank the Center for Counseling and Student Development at ECU. Truly, this dissertation would not exist if it were not for the services provided there. As one of many graduate students that has experienced some form of mental health problem, I cannot overstate the importance of having this resource.

TABLE OF CONTENTS

LIST OF TABLES

LIST OF FIGURES

Chapter 1: Iron Flocs and the Three Domains: Microbial Interactions in Freshwater Iron Mats

Authors: Chequita N. Brooks and Erin K. Field

Citation: Brooks CN, Field EK. 2020. Iron Flocs and the Three Domains: Microbial Interactions in Freshwater Iron Mats. mBio 11:e02720-20.

Abstract

Freshwater iron mats are dynamic geochemical environments with broad ecological diversity, primarily formed by the iron-oxidizing bacteria. The community features functional groups involved in biogeochemical cycles for iron, sulfur, carbon, and nitrogen. Despite this complexity, iron mat communities provide an excellent model system for exploring microbial ecological interactions and ecological theories *in situ*. Syntrophies and competition between the functional groups in iron mats, how they connect cycles, and the maintenance of these communities by taxon outside of bacteria (the eukaryota, archaea, and viruses), has been largely unstudied. Here, we review what is currently known about freshwater iron mat communities, the taxa that reside there, the interactions between these organisms, and propose ways in which future studies may uncover exciting new discoveries. For example, the archaea in these mats may play a greater role than previously thought as they are diverse and widespread in iron mats based on 16S rDNA and include methanogenic taxa. Studies with a wholistic view of the iron mat community members focusing on their diverse interactions will expand our understanding of community functions, such as those involved in pollution removal. To begin addressing questions regarding the fundamental interactions, and identify the conditions in which they occur, more laboratory culturing techniques and co-culture studies, network and keystone species analyses, and the expansion of studies to more freshwater iron mat systems, are necessary. Increasingly accessible bioinformatic, geochemical, and culturing tools now open avenues to address the questions we pose herein.

Introduction

The freshwater iron mat environment epitomizes Darwin's entangled bank (1), with twisted stalks of oxidized iron forming around themselves into charismatic orange mats (2). Iron mats are, as the name implies, comprised of iron-oxyhydroxides, the metabolic byproduct of iron-oxidizing bacteria (FeOB). They are loosely associated, flocculent structures that can be easily disturbed by an increase in flow. These ephemeral structures also exhibit an oxygen (O_2) gradient (2), creating myriad niches. While FeOB are diverse in iron oxidation mechanism (3, 4), the ecology of the microbial communities of freshwater iron mats formed by microaerophilic FeOB are the focus of this review.

Previous studies of iron mats have primarily focused on the FeOB as ecosystem architects, whereas the literature that focuses on the other organisms in iron mats are few (5, 6). Here we discuss the relationships formed between the microaerophilic FeOB and the other microbial members of iron mats because they drive biogeochemical cycling, ecological relationships, and evolution within these systems. We aim to present the current status of what is known about freshwater iron mat microbial communities and to use this framework to add direction for future studies.

Entangled Environments & Geochemical Niches

Iron mats formed by microaerophiles have been collected from groundwater seeps, some as cold as 8ºC (7), while others have been found in caves (8) or engineered water systems (9). The variability among the freshwater environments where the microaerophilic FeOB exist has been explored in other reviews and include freshwater environments with FeOB that do not form "mats" (e.g., in the rhizosphere), brackish and marine environments, acidic streams, and

engineered systems (9-11). The iron mats that are the focus of this review form in streams where there is a high influx of reduced iron, usually from a groundwater seep, and where the oxic-anoxic interface is near the mat surface creating both oxic and anoxic microniches within the iron mat (12). Our focus on freshwater iron mats in slow-flow creeks and streams allows us to characterize the physical and geochemical environment in which the microbial community forms with some specificity.

An intricacy of the iron mat environment is that of the physical conditions under which the mat develops. One of these physical conditions is the rate of flow and its impacts on iron oxidation rates. In studies conducted at Ogilvie Creek, Meilleurs Bay, Ontario, Canada, the presence of established mat led to higher (1.70 ± 0.20 min^{-1}) oxidation kinetics when compared to the ferrous (reduced) iron (Fe^{2+}) oxidation when the iron mat was artificially washed out (0.48 ± 0.14 min^{-1}) (13). This result is perhaps made more interesting by the oxidation kinetics observed for an iron mat formed in a slower flow drainage channel estimated (0.78 ± 0.20 min^{-1}) to be less than half of those of the established mat in Ogilvie Creek, suggesting that oxidation kinetics can be strongly influenced by rate of flow (14). Both studies were conducted in the summer and showed mats dominated by sheaths, indicating that the majority of iron oxidation was carried out by *Leptothrix* spp. It is as-yet unknown how a freshwater mat dominated by *Gallionella* spp., or another microaerophilic FeOB, would compare, perhaps leading to variability in oxidation kinetics throughout the year in following with the ecological succession observed by Fleming et al. (15). However, it is likely that a mat dominated by *Leptothrix ochracea* would have a higher rate of oxidation, considering the rapid production of iron oxides by the species, which is much faster than other FeOB (19 μm min^{-1} compared to 2 μm hr^{-1}) (2). We can draw from this example that the dominant FeOB in the iron mat, as well as the

geochemical and physical conditions surrounding the mat, will influence the further ecology within the system.

Consider, for example, the dynamics of dissolved organic carbon (DOC) in iron mats, which have been suggested to correlate with the dominant FeOB taxa in freshwater iron mats, specifically with the occurrence of *Leptothrix* as opposed to *Gallionella* spp. being closely tied to the presence of higher DOC (15). Because streams are sun-exposed, it has been postulated that the presence of DOC could possibly vary due to photobleaching, which would affect the concentration of DOC that is biologically available (15). This is one of many examples of geochemical drivers of iron mat diversity that should be considered and applied to the ecological approach that we aim to present here.

Another example, that harkens to a familiar concept in microbial ecology, is the presence and biological availability of phosphorous in iron mats. Biogenically produced iron oxides, sometimes referred to as bacteriogenic iron oxides (both use the acronym BIOS) in the literature, have been previously shown to remove phosphorous from solution by adsorption in freshwater as well as other environments such as marine waters and soils (16-18). Interestingly, there is also evidence that DOC may adsorb to the surface of BIOS as well, potentially competing with phosphorous (19, 20) for surface area. While the geochemistry of the iron mat is certainly variable, as shown in the above examples of phosphorous and DOC dynamics, in a freshwater iron mat there are two constants, dissolved oxygen and reduced iron (Fe^{2+}), with opposing gradients (Figure 1.1). The geochemistry of iron mats certainly impacts the survivability within the stream environment, especially in the formed microniches. As explained here there may be at times a paucity of biologically available DOC or phosphorous, which could easily lead to shifts in microbial activity and presence.

Iron Mats: More than Microaerophiles

The flocculent iron mat often seems to elicit the question, who, or what, lives here? Many functional groups of biogeochemical importance reside within the ochreous confines of the mat (Figure 1.1). One functional group that is undeniably present in all neutral, freshwater iron mats are the microaerophilic FeOB. They are keystone taxa, a microbial taxa that exerts a considerable influence on the microbial community structure irrespective of their abundance (21).

The microaerophiles capable of iron oxidation cluster in the class Betaproteobacteria and include members of the genera *Gallionella, Sideroxydans, Ferriphaselus,* and *Leptothrix.* Numerous papers have identified *Gallionella ferruginea* and *Leptothrix ochracea* as the primary producers of iron-oxyhydroxides in freshwater iron mats using 16S rDNA microbial community profiling and characterization of the oxidized iron product (2, 15, 22, 23). *Gallionella* spp. are known to form "stalks," braided chains of iron which the cell rests at the end of, whereas *Leptothrix* spp. produce "sheaths," tubular iron within which the cells reside (2). Members of the genera *Sideroxydans* and *Ferriphaselus* also produce the "stalk" structures, which has likely led to some issues of interpretation in earlier studies that used stalks as definitive markers of *Gallionella ferruginea*'s presence. Interestingly, studies of *Gallionella* and *Leptothrix* spp. have indicated that the two vary in regards to the Fe^{2+} and O_2 niches that they inhabit, where *Leptothrix ochracea* has a more flexible response to imperfect gradients (2). This, paired with their apparent dominance in systems with higher DOC, has led to the line of inquiry that *Leptothrix ochracea* may be a mixotroph or heterotroph, rather than autotrophic like *Gallionella ferruginea* (15, 24). While the microaerophilic FeOB are undeniably the stars of the show in

freshwater iron mats, there is still more to the story of iron-oxidation than that which lies within the micro-oxic region.

Beyond the primary FeOB colonizers, other microbial taxa can be found in the iron mat community. Nitrate-reducing iron-oxidizing bacteria (NRFeOB) functionally exist within the iron mat, though it has been posited many of these mixotrophic organisms are not actively oxidizing iron, but it is instead a chemical reaction with their metabolic byproducts (25). Still, a chemical mechanism of iron-oxidation would likely lead to competition between the nitrate-reducing iron-oxidizing bacterial genera *Acidovorax*, *Aquabacterium*, and *Thiobacillus* that have been identified as present in freshwater, neutral iron mats via clone libraries (6, 26, 27). Notably, the nitrate-reducing genera identified from clone libraries were all from the class Betaproteobacteria, whereas organisms classified as NRFeOB in other classes were not identified. This is unsurprising as the average size of clone libraries from iron mats was 97 and Alphaproteobacteria made up an average of ~9% of the clone libraries, when reported (6, 26-30). The other major iron-oxidizers, the photoferrotrophs are also Alphaproteobacteria (3). This bias could possibly be due to either selection-choices made by experimenters when sampling or due to biases that were perpetuated in clone libraries. Regardless, these results indicate that there is perhaps much to be gained from using methodologies that can incorporate greater proportions of the present microbial community.

Today, it is possible to use amplicon sequencing for microbial community profiling which has aided in the detection of non-dominant FeOB and other taxa. Of the current studies that incorporate iron mat 16S rDNA environmental sequencing most did not report the full community profile or mention Alphaproteobacteria in their results or discussions (15, 22, 31, 32). Only one reported the incidence of Alphaproteobacteria, with an average 9% make-up of

Alaskan iron mat communities (22). While this proportion may seem remarkably low, the sample collection for this study was conducted with great care to only include the leading edge of the iron mat, as the authors were primarily interested in the microaerophilic FeOB that are in greater abundance there (22), which likely led to lost data in regards to the presence of members of the Alphaproteobacteria that were greater in depth within the iron mat. While appropriate for studies focused on FeOB, experimental designs such as this have likely led to under-sampling outside of the Betaproteobacteria within iron mat communities, potentially leading to biases in our wholistic understanding of the iron cycle within the iron mat.

Iron mats feature niches available to organisms other than FeOB, too, which affect where in the iron mat these other organisms are found. Some of the more notable, if understudied, include the predatory bacteria, sulfur-cycling organisms, and methane-cycling organisms (Figure 1.1). The predatory bacteria, *Bacteriovorax* spp., have been identified in freshwater iron mats using bacterial clone sequences (4, 6), and likely have a role in maintaining relative abundances in the ecology of the iron mat. Sulfur-oxidizing (e.g., *Sulfuricurvum* spp.) (6, 27), sulfate-reducing bacteria (e.g., *Desulfobacteraceae*) (29), and methanotrophs (e.g., *Methylophilaceae*) (6) have also been identified using clone libraries. Notably, these include anaerobes and aerobes, possibly competing with the FeOB for niche space or participating in a variety of cryptic nutrient cycles (e.g. carbon, sulfur, nitrogen, phoshorous). It is notably difficult to maintain the structure of an iron mat during sampling, as the flocs are loosely associated and vulnerable to disturbance, and so it is as-yet unknowable where exactly in the iron mat each of these organisms would be observed. Here we present hypotheses based on general knowledge of the organisms' oxygen-sensitivity, dissolved Fe^{2+} requirements, and photosynthetic capability based on the availability

of sunlight (Figure 1.1). Future studies should aim to maintain the structure of iron mats and study these functional groups in situ to tease out their specific niches in the mat.

Why are Microbial Interactions in Iron Mats Important?

Microbial relationships are important to the functioning of aquatic environments (33), biogeochemical cycles (34-37), and in providing colonization resistance against invaders; protecting vulnerable habitats. Microbial communities can be classified using measures of their environmental, functional, and genotypic complexity (38). Using these classifiers for the iron mat community, we can identify knowledge gaps and build a road map for addressing them.

Functional complexity includes considerations of whole community functions such as resource use and trade-offs, which create spatial and temporal structural dynamics in microbial communities (39). FeOB alone have been found to be important to the iron cycle (40) via their biological mediation of iron oxidation, which outpaces rates of chemical oxidation in microaerophilic environments (36). However, the functional complexity within the iron mat is reliant upon other microbial guilds such as the iron-reducing, sulfur-oxidizing, and methanogenic bacteria. How these relationships potentially impact iron cycling has been previously reviewed (41). Because microbial interactions are time-sensitive (42), the variation over time adds another layer of functional complexity to microbial communities, especially those that may have seasonal dynamics (15). Interestingly, many of the functional guilds within the iron mat community are anaerobic, possibly lending to costless, as they do not cause a fitness cost to the producer, metabolic byproducts driving interactions amongst community members, as this is a trend amongst anaerobes (43). For example, the iron-reducing bacteria, as a metabolic byproduct, produce Fe^{2+}, which is then available to other community members or the rapid cycling of sulfate

and sulfur by sulfate-reducing and sulfur-oxidizing bacteria, similar to that in the above example. Through these machinations the iron mat community presents a plethora of potentially tied functions and elemental cycles, which in turn makes it a great model for not only microbial ecologists but biogeochemists.

Of further importance is the sometimes-cryptic biogeochemical cycling that is occurring within these communities. For example, a recent study of freshwater sediment cable bacteria that perform electrogenic sulfide oxidation found that the activity of these organisms enhanced sulfate reduction rates (44). Previously these effects had not been observed as this cycling is typically unobservable *in situ* as they do not lead to an overall increase of sulfate or sulfide concentrations. This example illustrates a commonly observed phenomenon, where the fitness of individuals in a community rely not only on environmental conditions, but also on the other members of the population (45). Similarly, there may be many cryptic cycles ongoing in iron mat communities that are not readily observable by traditional chemical measures, such as cycling between FeOB and FeRB or methanogens and methanotrophs. Using methods of detection, such as 16S sequencing, is often the only way to hypothesize that such cryptic cycles may be occurring, ultimately leading to experimental set-ups that may parse out these cryptic relationships.

Genotypic complexity, used here to describe the overall genetic diversity in the microbial community, is the iron mat black box. As DNA yields are often low from iron mat communities, the full genotypic complexity of these communities has rarely been realized. Among the drivers of genotypic complexity are the presence of keystone taxa and keystone guilds (21), such as the FeOB themselves, which are responsible for niche partitioning (4). Iron mats create niche spaces available to other functional guilds due to the opposing gradients of oxygen and reduced iron

setting the stage for the relationships we will discuss here. According to a study of seasonal changes along a freshwater first-order stream in Boothbay Harbor, ME, the keystone taxa within the FeOB changes temporally, with the dominant iron-oxidizer shifting from *Gallionella* spp. early in the year (April) to *Leptothrix* spp. in the summer (June) (15). This specific trend may not hold true for all iron mat communities, especially iron mat communities in geographical locations not affected by snowpack and subsequent snow melt, which impacts O_2 dissolution in the water column. However, common to all iron mats, beyond the opposing Fe^{2+} and O_2 gradients, are environmental factors such as wastewater runoff, nutrient loading, and flow; these factors are all often variable in the urban environments where many mats are located. How these factors may, independent of season, impact the dominant FeOB and, perhaps subsequently, the colonization by other functional guilds is as-yet unclear.

Each of these classifiers of complexity (environmental, functional, and genotypic) in the community can affect the others. For instance, as the global climate changes the microbial diversity in many types of communities has experienced shifts in response (46). This change in the environmental complexity, where typical conditions are no longer typical, has led to shifts in the observed functional and genotypic complexity. Ostensibly, this changes the rates of mortality within the communities that are sensitive to the removal of keystone species, the colonization by invasive species, and global climate change (47). The iron mat community may be more impervious to the effects of global climate change than many other microbial communities given that the FeOB appear to be adapted to temperate conditions, as in the study in Boothbay Harbor, ME, where the mats are not present in the winter (15); however, the freshwater communities associated with iron mats could still be at risk. As mentioned previously, one of the possible drivers of available DOC in streams with iron mats is photobleaching. This particular condition

can be attenuated with an increase or decrease in rainfall, which would correlate with an increased or decreased albedo, respectively, changing the rate at which DOC is photobleached. Changing weather patterns may also lead to saltwater intrusion in iron mat sites that are upstream of estuaries, one example being the freshwater mat upstream of brackish waters in the Sheepscot River, ME study (23). Sites such as these are vulnerable to increased intrusion due to drought and sea level rise. Changes on a global scale can certainly have local-scale effects that even the freshwater iron mat may experience, leading to shifts in the microbial make-up and function of these ecosystems.

Syntrophy: Community Assembly, Structure, and Function

The study of syntrophic relationships between microbes in iron mat communities lies primarily in theory (48), but many important findings from synthetic microbial communities can be applied toward the study of *in situ* microbial communities such as that of the iron mat. For example, two co-cultured organisms, *Xanthomonas retroflexus* and *Paenibacillus amylolycticus*, developed phenotypes that enhanced their ability to grow in a biofilm together (49). It is likely that similar adaptations, i.e., the bolstering of survival traits, may occur in natural environments, including the iron mat. It is, however, more tractable to study how the co-occurrence and cooperation between microbial groups may drive community structure of established communities (50).

Cooperation is an important driver of community function, especially under environmental stress. It has been observed that generalists, when facing lost advantage due to perturbation, will increase syntrophic processes (51). Syntrophic relationships can also be important for the function of microbial communities in carrying out biodegradation pathways.

Using stable isotope probing, syntrophic relationships leading to the removal of hydrocarbons have been identified between iron-reducing bacteria and sulfate-reducing bacteria (SRB), as well as methanogens and acetate oxidizers (52-56). These relationships are of particular interest as they involve functional groups present in the iron mat system. Such cooperative relationships between microbes may have global import in the form of connecting biogeochemical cycles; potentially extending to many of the Earth's biogenically controlled cycles (57) including sulfur (7, 23, 58), nitrogen (8, 30), manganese (59), and carbon (5, 6, 8).

Syntrophic relationships between the marine FeOB and their community members have been explored to greater depth than the relationships in the freshwater iron mat have. Still, potential syntrophies have been postulated between the FeOB and co-occurring functional groups, including SRB (7, 23) and oxygenic phototrophs (60). The potential for connections extends outside of FeOB; SRB and methanogens are well known for their syntrophic capabilities (61-63). The methanogenic microbes involved in these syntrophic interactions are reliant on other functional groups for electron donors, and their syntrophs are typically H_2 or formate scavengers that can switch to a sulfate-reduction pathway, where they may begin competing for acetate, depending on the carbon-to-sulfate ratios. Methanogens in anoxic cultures from a rice paddy field have also been observed to build syntrophic interactions with FeRB that are facilitated by iron oxide particles (64). The results of the study suggest that *Geobacter* spp. benefit from increased growth, and the methanogen, *Methanosarcina* spp., was able to increase the rate of methanogenesis via an electromethanogenesis pathway (64). Microbial syntrophies in the iron mat likely play a large role in modulating the growth rate *in situ* of organisms and studies designed to capture this would strongly contribute to the literature.

Perhaps of greatest interest are the syntrophic relationships that may form between the ecosystem architects and the community members. There are certainly well-known examples of this, such as the syntrophy between FeOB and the iron-reducing bacteria, reviewed elsewhere (65), but there are other, perhaps overlooked, possibilities that we wish to present here. The syntrophy between FeOB and SRB, where the co-occurrence is well-established in the marine system, is likely mediated by the O_2-Fe-H_2S catalytic cycle (66-68) where reduced iron and sulfate are produced from the reaction of oxidized iron and hydrogen sulfide, making the microbial waste (oxidized iron and hydrogen sulfide) back into microbial food (reduced iron and sulfate) (Figure 1.2-A). The most practical implication of this relationship is that the iron mat's chemistry could feasibly sustain both FeOB and SRB during times of low availability of either reduced iron or sulfate. While first-observed in marine systems, the co-occurrence of FeOB and SRB is noted in freshwater systems as well (7, 23) and could be of great importance during the establishment of iron mats, where the sediment community likely serves as a microbial seedbank (23). This could potentially expand the range of environmental conditions where iron mats could be formed and may add further stability to the iron mat microbial community composition. Novel co-culture conditions have been recommended for marine FeOB and SRB (69), which may be applied to freshwater guilds, but additional cultivation methods may be warranted for future growth-based studies of these two guilds in controlled laboratory settings. While freshwater and marine FeOB communities are disparate in regard to physical, chemical, and biological characters, it may still be informative to draw upon the marine for functional ideas; as this example shows, there is much functional overlap between the two.

Of course, there are other potential syntrophies with FeOB that merit further investigation. FeOB may also form a syntrophic relationship with planktonic cyanobacteria in

the freshwater iron mats. While this has not been explored in freshwater iron mats, it has been suggested under brackish conditions (60). In this instance, the cyanobacteria may be protected from oxidative stress due to the presence of reduced iron species, while the FeOB receive localized O_2 produced by the phototrophs when bulk water O_2 concentrations are too low (60). However, as with any syntrophic relationship, it is possible that this alliance may change in nature under different conditions. In this case, it has also been observed that the growth of acidophilic FeOB in iron mats has been stymied by the presence of cyanobacteria (70). This dynamic is likely due to the degassing of O_2 from acid mine drainage, leading to an increased organic carbon-to-O_2 ratio from the presence of photosynthetic organisms, which ultimately leads to greater competition between the FeOB and organisms bolstered by the increased organic carbon (70). In a neutrophilic freshwater iron mat, it is most likely that the increased O_2 from the presence of phototrophic organisms would be of greater benefit, similar to the brackish conditions previously mentioned. This example demonstrates that not only marine, but acidophilic iron mats, may be useful in hypothesis-generation. However, the ultimate test of these syntrophic relationships will come from further study in the freshwater iron mat system itself.

Competition and Predation: Niche Partitioning and Community Composition

Competition and predation, much like syntrophic relationships, are difficult to study *in situ*; however, these questions are arguably more tractable in a simplified community such as those in the freshwater iron mat, compared to the complexity in, for example, soil systems. It has been noted that competition can increase microbial diversity by competitive exclusion and negative frequency-dependent selection (71). Similar controls are exerted by predation; in a

controlled experiment, it was observed that some typically rare taxa (e.g., *Comamonadaceae*) in a model bacterial community had the highest abundance when the protistan predators were removed (72). It has also been suggested that functional redundancy is, at least in part, maintained by competition and predation (73). These observations could have interesting implications for the interpretation of relative abundance, often used to reconstruct community structure, in freshwater iron mat communities.

One of the most obvious competitions in iron mat communities is that between the microaerophilic FeOB themselves. Those most often studied are *Leptothrix ochracea* and *Gallionella* spp. While these organisms have been shown to coexist in some iron mats (2, 28), they have also been shown to have an almost mutual exclusivity based on current environmental conditions (15), indicating that these organisms share the same niche space and may be competing at the microscopic level (Figure 1.2-B). However, it is easily forgotten that in these same freshwater environments, there are other organisms competing for reduced iron, namely the photoferrotrophs (37, 74-76) and the NRFeOB.

Competition among microbial taxa that utilize the same resources is likely to occur in freshwater iron mats. In a study of coastal iron cycling communities in near-shore marine environments of Aarhus Bay, Denmark, Laufer et al. observed microaerophilic, nitrate-reducing, and phototrophic FeOB coexisting in two different sediment types (77). In a stark difference from what has been observed in a study of iron mats (5), the sediment communities of FeOB observed were not stratified according to O_2, Fe^{2+}, or light conditions (77). The authors postulate that this was due to physical and bioturbation in the marine sediments, which would be less effectual on a typical iron mat. However, this study suggests that the shared niche spaces of the three types of iron-oxidizers in freshwater iron mats, where low-flow streams are less turbulent,

could lead to heretofore unobserved competition between the groups, certainly more studies are warranted.

Other functional groups, the methanotrophs and methylotrophs (5, 6, 8), may also compete with the microaerophilic FeOB for the available oxygen in the iron mats (5). Quaiser et al. found methane-oxidizing bacteria to be a significant proportion of the iron mat microbial communities (5) suggesting that this competition may be widespread and drive oxygen cycling in the mat. This interaction has not been well-studied, and the notable organisms have likely been under-sampled in clone libraries, given that they are not Betaproteobacteria.

The role of predation in altering the biogeochemical potential of the microbial community is likely large, but as yet no studies of predation in the iron mats have been conducted. Notably, *Bacteriovorax* spp. have been identified in iron mat communities (4, 6) and are known to prey on gram-negative bacteria (78), possibly shaping the iron mat community (whose architects, the microaerophilic FeOB, are notably gram-negative) (Figure 1.2-C). Predation by bacterivorous species is typically indiscriminate and has been found to significantly alter relative community compositions (79, 80). This could have important implications for any applied uses of iron mat communities, especially in the transfer of iron mat seed banks to novel locations with higher or lower bacterivorous species incidence than *in situ*.

Eukaryotes, Viruses, and Archaea; Oh My?

What role do micro-eukaryotes, viruses, and archaea play in iron mat microbial communities? The other branches of life are not only largely missing from the iron mat literature, they have often been overlooked in studies of all environments (81, 82). Micro-eukaryotes and archaeal iron mat constituents rarely appear in the literature (5, 6). One study identified nine

archaeal phylotypes (6) and another reported sequencing two archaeal transcripts (5). Micro-eukaryotes identified from iron mat transcripts were associated mostly with freshwater grazing species (e.g., *Tetrahymena* spp.) (5), which have previously been observed to have a role in increasing bacteriophage and bacterial encounters by accumulating both in their phagocytotic vesicles (83). Clearly, the role of microbes other than bacteria in the iron mat should not be brushed off as ancillary. Micro-eukaryotes have also been shown to modify the community structure and abundances in bacterial communities as predation can lead to a rarity of fast-multiplying bacterial taxa *in situ* (72). This predation by micro-eukaryotes may be especially relevant to iron mat communities, where one of the keystone taxa, *Leptothrix ochraceae*, has a rapid doubling time of 5.7 hours (24), which may lead this organism to be under-represented in community sequences. Rare bacterial species in an environment may have invested less in defenses against grazing with bacterial phenotypes such as cell size and cell wall structure (84) and instead invested more energy in quick replication (72). This response to predation can also lead microbial communities to upregulate bioremediation processes (85), which could prove an essential element to the application of iron mat communities to polluted environments. Micro-eukaryotes, it should be noted, do not parody bacterial community members in community structure shifts. While there can be temporal structure and functional change (86), micro-eukaryotes are more likely to respond to deterministic processes in marine ecosystems, unlike bacteria and archaea that appear to respond more strongly to stochastic processes (87). This trend has been hypothesized to be driven by stronger adaptation capabilities in prokaryotes or that environmental factors are not measured that have the most relevant impact on prokaryotic community members (87). In studies of iron mats, it may be of use to use microeukaryotes as "canaries in the coal mine" to identify the relative stress (i.e., deterministic processes) that the

community is facing. For example, facing ecological severity from the Deepwater Horizon oil spill, microbial communities increased in bacterial dominance over archaea and micro-eukaryotes (88). The role of micro-eukaryotes in the freshwater iron mat is largely unexplored, but the datum that is available points to ecologically relevant roles within the ecosystem.

Returning to the prokaryotic amongst the iron mat, there is also a scarcity of information on the archaea present in the freshwater system. It is not clear what role the archaea may play in the iron mats as they currently represent a very small proportion of available iron mat community sequences (5, 6, 31, 32), often only being identified secondarily through the use of bacterial primer sets. As this does not encompass the majority of the archaeal diversity in the environment, and likely in the iron mat, we conducted Illumina MiSeq sequencing of seven freshwater iron mats from Greenville, NC, using archaeal primers A956F (TYAATYGGANTCAACRCC) and A1401R (CRGTGWGTRCAAGGRGCA) (89). Sequences were processed using mothur (v 1.44.1) (90-92), and the MiSeq SOP accessed 2020 APR 13 (https://mothur.org/wiki/miseq_sop/) to identify present taxa (97% OTU threshold). Graphs were generated using the phyloseq package (93) in R v. 3.5.2.

Through the use of a targeted archaeal primer set we were able to amplify a much higher abundance and diversity of archaeal amplicon sequences than the proportions previously reported. Amongst all seven of the iron mat communities included in this analysis, there were 1699 total archaeal OTU's identified, with an average of 400 archaeal OTU's per mat demonstrating that the archaeal diversity is higher than previously shown. The most abundant phylum was Euryarchaeota (Figure 1.3), which accounted for 43% of the total archaeal sequences. 11% and 1% were Methanomicrobiales and Methanobacteriales, respectively. Sequences of these methanogenic archaea were found in all seven iron mats suggesting their

widespread presence in the iron mats may be important for the biogeochemical function of the iron mat community as a whole, and further efforts should be made to recover more complete sequences of archaeal community members from more diverse iron mats. Furthermore, cultivation and co-cultivation techniques should be employed to further delve into the interactions between archaea and bacteria in the iron mat.

Another area of study ripe for investigation is the role of bacteriophages in the iron mat community. Viruses impact microbial communities through varied mechanisms with effects such as community turnover (94) and changing bacterial abundance and function (95). Archaea and Bacteria can also benefit from lateral gene transfer between themselves, and this benefit can be mediated by viruses (94). Functional shifts can occur due to the presence of auxiliary metabolic genes present in both lytic and lysogenic phages (Figure 1.2-D). These genes have been observed to modify host dynamics in marine systems, with auxiliary metabolic genes modifying host metabolic needs or redirecting all cellular energy toward phage replication, further details of these mechanisms have been reviewed by Warwick-Dugdale et al. (96). Similar to micro-eukaryotes, viruses result in top-down pressure in bacterial communities (97). Even a community low in viral diversity can experience a large impact from viruses given the variability in host-specificity (98). Viral community members may also help to maintain and shape communities, even while in a steady-state (84). Interestingly, in the first temporal study of riverine viromes, conducted in three watersheds in British Columbia, Canada, the viral communities were distinct between sites, even those where the geographic distance was markedly close enough for the bacterial communities to be similar (99). Notably, this study also found that the communities of both DNA and RNA viruses were synchronous (99), possibly owing to more similar environmental conditions impacting viral community members that are not analogous in effect to

bacterial community members. As yet there have been no similar studies conducted in iron mats, but in seeking data from a related environment, in this case a river, we have aimed to show the possibility for hypothesis generation from these data sets to be applied to the iron mat system.

The Solution to Pollution is… Iron Mats?

Iron oxyhydroxides produced by FeOB have been studied for their abilities to combat anthropogenic pollution by leaching heavy metals (20, 100-102), degrading aromatic carbons (8), adsorbing hydrophilic pesticides (103), and removing phosphorus (16, 104, 105) from contaminated waters. The iron mat microbial community has a diverse ability to degrade and transform these contaminants ultimately affecting their fate, but the presence of these contaminants will also be a stressor to the community itself and its functioning. The iron oxides are known to remove phosphorous from solution, and the biologically available pool, through sorption mechanisms (16). Because of this, biologically produced iron oxides have also been applied in remediation strategies, where they similarly adsorb arsenic (106). However, few studies have addressed the entire community involved and not only those bacteria identified as responsible for contaminant degradation. By expanding studies to include a more wholistic view of the entire community (e.g. bacteria, eukaryotes, viruses, archaea) in the iron mat, we can better understand how their complex interactions affect community functions such as contaminant degradation and transformation. For example, heavy metals and hydrocarbons can induce the formation of reactive oxygen species which are toxic to bacterial species (107), potentially leading to changes in the overall microbial community in the affected iron mat. Responses of microbial communities to anthropogenic stressors are dynamic (108) and highly context-dependent (107). The responses of microbial communities depend on the pollutant,

whether it be heavy metals, which often lead to decreases in diversity (109, 110), or polycyclic aromatic hydrocarbons (PAH), where communities may decrease (111, 112) or recover diversity after chronic stress (113, 114).

Again, we see the importance of geochemical factors in the regulation of microbial communities when we consider pollution. In the Yangtze Estuary in China, PAH and heavy metals are both contaminating the estuarine sediment. Importantly, not only were the PAH, and heavy metals responsible for regulating the degradation potential of the microbial community, but pH and salinity also played a role (107). Environmental severity, as defined not only by the concentration of pollutants but the surrounding environmental factors, plays a role in the degradation potential of the microbial communities. Key to this study was that the microbes harvested naturally occurred in the polluted area, and still, the environmental factors outside of pollution had significant effects on the degradation potential (107). The functional groups of the iron mat are some commonly thought of as sensitive to oxidative-reductive potential (ORP), dissolved O_2, and physical factors (e.g., flow); how these niche-defining environmental cues interplay with contaminant presence in the iron mat to impact the microbial community is an exciting new avenue for future research.

In urban environments, the presence of all of these contaminants in the same iron mat would come as no great surprise, easily increasing the environmental pressure experienced by the microbial communities of the iron mat. A focus exclusively on degradation potentials of these mats can obscure the importance of these stressors on ecological networks in the iron mats and the role of keystone species. In a study of riverine sediments from Suzhou, China that were contaminated with hydrocarbons the keystone bacteria (e.g., *Dechloromonas* and *Anaerolineaceae* spp.) were able to facilitate interactions, even as the concentration of

hydrocarbons increased (115), supporting the biodegradation of contaminants. As the hydrocarbon concentrations increased, the strength of the species aggregations increased as measured using the Molecular Ecological Network Analysis Pipeline; indicating a greater importance of keystone species to environmental function (115).

Excitingly, functional groups found in the iron mat appear to have potential in the removal of contaminants from waterways. In a study using isolated FeOB and SRB from sewage sludge of Xiangtan City, China, co-cultures were more effective at attenuating antimony (Sb(V)) than isolates (116) indicating the importance of these interactions in contaminant transformations and community function. Similar mechanisms likely play out in iron mats, which are often found in urban environments, such as the North Carolina Piedmont (20), that are prone to increased pollutants. Studies of these and other urban iron mats could lead to the potential application of the wholistic microbial communities, not only the bacteria, toward the attenuation of PAH, heavy metals, or other contaminants. Future avenues of research include using -omics techniques, *in situ* observations, and culturing techniques toward understanding how microbial interactions in the iron mat relate to contaminant remediation.

Concluding Remarks

Community sequencing, both 16S rDNA and metagenomes, can be leveraged to understand the taxonomic and functional diversity within the iron mat. This may be particularly useful where there is not yet geochemical data and cryptic biogeochemical cycles may occur. While we have a strong foundation of the role of iron-oxidizing bacteria in the iron mats, there is still much to be garnered from current and future data sets to expand sequencing and studies beyond these bacterial members, to incorporate other functional guilds, microeukaryotic,

archaeal, and viral members' roles. We also hope to see an inclusion of network ecology approaches, studies of indicator species, and the development of novel co-culture techniques toward discovering and understanding specific interactions within the iron mat community. Applying these approaches may reveal much-needed information about other key taxa in iron mat communities, perhaps also revealing some of the more cryptic relationships and functional roles of these iron mat communities, such as contaminant degradation in these environments. Many research directions remain in the field of iron mat microbial communities, including exploring viral and eukaryotic communities, competition and predation, syntrophic relationships, and the impacts of anthropogenic stressors. While the iron mat is host to a great diversity, it is also simple in comparison to many other freshwater communities and provides an accessible model system for testing ecological theories and interactions between the domains. Here we recommend researchers strike while the iron is hot and work toward building a greater knowledge base for this exciting community.

Acknowledgements

Thanks to Dr. Peri Bolton for her support during the writing of this manuscript. Funding support provided by the Graduate Women in Science National Fellowship Program Nell Mondy, Vessa Notchev, and Monique Braude Fellowship Funds.

References

1. Darwin C. 1859. On the Origin of Species by Means of Natural Selection Or the Preservation of Favoured Races in the Struggle for Life. H. Milford; Oxford University Press.
2. Chan CS, McAllister SM, Leavitt AH, Glazer BT, Krepski ST, Emerson D. 2016. The architecture of iron microbial mats reflects the adaptation of chemolithotrophic iron oxidation in freshwater and marine environments. Front Microbiol 7:796.
3. Hedrich S, Schlömann M, Johnson DB. 2011. The iron-oxidizing proteobacteria. Microbiology 157:1551-1564.
4. Fru EC, Piccinelli P, Fortin D. 2012. Insights into the global microbial community structure associated with iron oxyhydroxide minerals deposited in the aerobic biogeosphere. Geomicrobiol J 29:587-610.
5. Quaiser A, Bodi X, Dufresne A, Naquin D, Francez A-J, Dheilly A, Coudouel S, Pedrot M, Vandenkoornhuyse P. 2014. Unraveling the stratification of an iron-oxidizing microbial mat by metatranscriptomics. PLoS One 9:e102561.
6. Kato S, Kikuchi S, Kashiwabara T, Takahashi Y, Suzuki K, Itoh T, Ohkuma M, Yamagishi A. 2012. Prokaryotic abundance and community composition in a freshwater iron-rich microbial mat at circumneutral pH. Geomicrobiol J 29:896-905.
7. Bruun A-M, Finster K, Gunnlaugsson HP, Nørnberg P, Friedrich MW. 2010. A comprehensive investigation on iron cycling in a freshwater seep including microscopy, cultivation and molecular community analysis. Geomicrobiol J 27:15-34.

8. Baskar S, Baskar R, Thorseth IH, Øvreås L, Pedersen RB. 2012. Microbially induced iron precipitation associated with a neutrophilic spring at Borra Caves, Vishakhapatnam, India. Astrobiology 12:327-346.

9. Emerson D, De Vet W. 2015. The role of FeOB in engineered water ecosystems: a review. J Am Water Works Assoc 107:E47-E57.

10. Emerson D, Fleming EJ, McBeth JM. 2010. Iron-oxidizing bacteria: an environmental and genomic perspective. Annu Rev Microbiol 64:561-583.

11. Johnson DB, Hallberg KB. 2003. The microbiology of acidic mine waters. Res Microbiol 154:466-473.

12. Glazer BT, Rouxel OJ. 2009. Redox speciation and distribution within diverse iron-dominated microbial habitats at Loihi Seamount. Geomicrobiol J 26:606-622.

13. Edwards BA, Shirokova VL, Enright AM, Ferris FG. 2018. Dependence of *in situ* bacterial Fe (II)-oxidation and Fe (III)-precipitation on sequential reactive transport. Geomicrobiol J 35:503-510.

14. Edwards BA, Ferris FG. 2020. Influence of water flow on *in situ* rates of bacterial Fe (II) oxidation. Geomicrobiol J 37:67-75.

15. Fleming EJ, Cetinić I, Chan CS, King DW, Emerson D. 2014. Ecological succession among iron-oxidizing bacteria. ISME J 8:804.

16. Rentz JA, Turner IP, Ullman JL. 2009. Removal of phosphorus from solution using biogenic iron oxides. Water Res 43:2029-2035.

17. Jones C, Nomosatryo S, Crowe SA, Bjerrum CJ, Canfield DE. 2015. Iron oxides, divalent cations, silica, and the early earth phosphorus crisis. Geology 43:135-138.

18. Fink JR, Inda AV, Tiecher T, Barrón V. 2016. Iron oxides and organic matter on soil phosphorus availability. Ciênc agrotec 40:369-379.

19. Sowers TD, Holden KL, Coward EK, Sparks DL. 2019. Dissolved organic matter sorption and molecular fractionation by naturally occurring bacteriogenic iron (oxyhydr)oxides. Environ Sci Technol 53:4295-4304.

20. Field HR, Whitaker AH, Henson JA, Duckworth OW. 2019. Sorption of copper and phosphate to diverse biogenic iron (oxyhydr) oxide deposits. Sci Total Environ 697:134111.

21. Banerjee S, Schlaeppi K, van der Heijden MG. 2018. Keystone taxa as drivers of microbiome structure and functioning. Nat Rev Microbiol 16:567.

22. Emerson D, Scott JJ, Benes J, Bowden WB. 2015. Microbial iron oxidation in the arctic tundra and its implications for biogeochemical cycling. Appl Environ Microbiol 81:8066-8075.

23. McBeth JM, Fleming EJ, Emerson D. 2013. The transition from freshwater to marine iron-oxidizing bacterial lineages along a salinity gradient on the Sheepscot River, Maine, USA. Environ Microbiol Rep 5:453-463.

24. Fleming E, Woyke T, Donatello R, Kuypers MM, Sczyrba A, Littmann S, Emerson D. 2018. Insights into the fundamental physiology of the uncultured Fe-oxidizing bacterium *Leptothrix ochracea*. Appl Environ Microbiol 84:e02239-17.

25. Liu T, Chen D, Li X, Li F. 2019. Microbially mediated coupling of nitrate reduction and Fe (II) oxidation under anoxic conditions. FEMS Microbiol Ecol 95:fiz030.

26. Kato S, Chan C, Itoh T, Ohkuma M. 2013. Functional gene analysis of freshwater iron-rich flocs at circumneutral pH and isolation of a stalk-forming microaerophilic iron-oxidizing bacterium. Appl Environ Microbiol 79:5283-5290.

27. Haaijer SC, Harhangi HR, Meijerink BB, Strous M, Pol A, Smolders AJ, Verwegen K, Jetten MS, Den Camp HJO. 2008. Bacteria associated with iron seeps in a sulfur-rich, neutral pH, freshwater ecosystem. ISME J 2:1231-1242.

28. Duckworth OW, Holmström SJ, Peña J, Sposito G. 2009. Biogeochemistry of iron oxidation in a circumneutral freshwater habitat. Chem Geol 260:149-158.

29. Gault AG, Ibrahim A, Langley S, Renaud R, Takahashi Y, Boothman C, Lloyd JR, Clark ID, Ferris FG, Fortin D. 2011. Microbial and geochemical features suggest iron redox cycling within bacteriogenic iron oxide-rich sediments. Chem Geol 281:41-51.

30. Blöthe M, Roden EE. 2009. Composition and activity of an autotrophic Fe (II)-oxidizing, nitrate-reducing enrichment culture. Appl Environ Microbiol 75:6937-6940.

31. Gagen EJ, Levett A, Shuster J, Fortin D, Vasconcelos PM, Southam G. 2018. Microbial diversity in actively forming iron oxides from weathered banded iron formation systems. Microbes Environ 33:385-393.

32. Levett A, Gagen EJ, Vasconcelos PM, Zhao Y, Paz A, Southam G. 2020. Biogeochemical cycling of iron: Implications for biocementation and slope stabilisation. Sci Total Environ 707:136128.

33. Paerl H, Pinckney J. 1996. A mini-review of microbial consortia: their roles in aquatic production and biogeochemical cycling. Microb Ecol 31:225-247.

34. Overmann J, van Gemerden H. 2000. Microbial interactions involving sulfur bacteria: implications for the ecology and evolution of bacterial communities. FEMS Microbiol Rev 24:591-599.

35. Ho A, Angel R, Veraart AJ, Daebeler A, Jia Z, Kim SY, Kerckhof F-M, Boon N, Bodelier PL. 2016. Biotic interactions in microbial communities as modulators of biogeochemical processes: methanotrophy as a model system. Front Microbiol 7:1285.

36. MacDonald DJ, Findlay AJ, McAllister SM, Barnett JM, Hredzak-Showalter P, Krepski ST, Cone SG, Scott J, Bennett SK, Chan CS. 2014. Using *in situ* voltammetry as a tool to identify and characterize habitats of iron-oxidizing bacteria: from fresh water wetlands to hydrothermal vent sites. Environ Sci Process Impacts 16:2117-2126.

37. Melton ED, Schmidt C, Kappler A. 2012. Microbial iron (II) oxidation in littoral freshwater lake sediment: the potential for competition between phototrophic vs. nitrate-reducing iron (II)-oxidizers. Front Microbiol 3:197.

38. Tecon R, Mitri S, Ciccarese D, Or D, van der Meer JR, Johnson DR. 2019. Bridging the holistic-reductionist divide in microbial ecology. mSystems 4:e00265-18.

39. Litchman E, Edwards KF, Klausmeier CA. 2015. Microbial resource utilization traits and trade-offs: implications for community structure, functioning, and biogeochemical impacts at present and in the future. Front Microbiol 6:254.

40. Emerson D, Roden E, Twining B. 2012. The microbial ferrous wheel: iron cycling in terrestrial, freshwater, and marine environments. Front Microbiol 3:383.

41. Melton ED, Swanner ED, Behrens S, Schmidt C, Kappler A. 2014. The interplay of microbially mediated and abiotic reactions in the biogeochemical Fe cycle. Nat Rev Microbiol 12:797.

42. Pacheco AR, Segrè D. 2019. A multidimensional perspective on microbial interactions. FEMS Microbiol Lett 366:fnz125.

43. Pacheco AR, Moel M, Segrè D. 2019. Costless metabolic secretions as drivers of interspecies interactions in microbial ecosystems. Nat Commun 10:103.

44. Sandfeld T, Marzocchi U, Petro C, Schramm A, Risgaard-Petersen N. 2020. Electrogenic sulfide oxidation mediated by cable bacteria stimulates sulfate reduction in freshwater sediments. ISME J 14:1233-1246.

45. Cavaliere M, Feng S, Soyer OS, Jiménez JI. 2017. Cooperation in microbial communities and their biotechnological applications. Environ Microbiol 19:2949-2963.

46. Cavicchioli R, Ripple WJ, Timmis KN, Azam F, Bakken LR, Baylis M, Behrenfeld MJ, Boetius A, Boyd PW, Classen AT. 2019. Scientists' warning to humanity: microorganisms and climate change. Nat Rev Microbiol:1.

47. Abreu CI, Friedman J, Woltz VLA, Gore J. 2019. Mortality causes universal changes in microbial community composition. Nat Commun 10:2120.

48. Nemergut DR, Schmidt SK, Fukami T, O'Neill SP, Bilinski TM, Stanish LF, Knelman JE, Darcy JL, Lynch RC, Wickey P. 2013. Patterns and processes of microbial community assembly. Microbiol Mol Biol Rev 77:342-356.

49. Røder HL, Herschend J, Russel J, Andersen MF, Madsen JS, Sørensen SJ, Burmølle M. 2018. Enhanced bacterial mutualism through an evolved biofilm phenotype. ISME J 12:2608-2618.

50. Zelezniak A, Andrejev S, Ponomarova O, Mende DR, Bork P, Patil KR. 2015. Metabolic dependencies drive species co-occurrence in diverse microbial communities. Proc Natl Acad Sci U S A 112:6449-6454.

51. Rossa CA, Stratford J, Hodgson DM, Beecroft NJ, Smith A, Marchesi JR. 2018. Disturbance during biofilm community succession promotes cooperation and diversity. bioRxiv:352914.

52. Morris BE, Henneberger R, Huber H, Moissl-Eichinger C. 2013. Microbial syntrophy: interaction for the common good. FEMS Microbiol Rev 37:384-406.

53. Kunapuli U, Lueders T, Meckenstock RU. 2007. The use of stable isotope probing to identify key iron-reducing microorganisms involved in anaerobic benzene degradation. ISME J 1:643-653.

54. Jones D, Head I, Gray N, Adams J, Rowan A, Aitken C, Bennett B, Huang H, Brown A, Bowler B. 2008. Crude-oil biodegradation via methanogenesis in subsurface petroleum reservoirs. Nature 451:176-180.

55. Gray N, Sherry A, Grant R, Rowan A, Hubert C, Callbeck C, Aitken C, Jones D, Adams J, Larter S. 2011. The quantitative significance of *Syntrophaceae* and syntrophic partnerships in methanogenic degradation of crude oil alkanes. Environ Microbiol 13:2957-2975.

56. Westerholm M, Dolfing J, Sherry A, Gray ND, Head IM, Schnürer A. 2011. Quantification of syntrophic acetate-oxidizing microbial communities in biogas processes. Environ Microbiol Rep 3:500-505.

57. Falkowski PG, Fenchel T, Delong EF. 2008. The microbial engines that drive Earth's biogeochemical cycles. Science 320:1034-1039.

58. Li Y-L, Vali H, Yang J, Phelps TJ, Zhang CL. 2006. Reduction of iron oxides enhanced by a sulfate-reducing bacterium and biogenic H_2S. Geomicrobiol J 23:103-117.

59. Carmichael SK, Bräuer SL. 2015. Microbial diversity and manganese cycling: A review of manganese-oxidizing microbial cave communities. Microbial life of Cave Systems Life in Extreme Environments (Book 3) De Gruyter, Berlin.

60. Field E, Kato S, Findlay A, MacDonald D, Chiu B, Luther III G, Chan C. 2016. Planktonic marine iron oxidizers drive iron mineralization under low-oxygen conditions. Geobiology 14:499-508.

61. Ogram A, Bae H-S, Chauhan A. 2019. The ecology of methanogenic archaea in a nutrient-impacted wetland, p 157-172, The Structure and Function of Aquatic Microbial Communities. Springer.

62. Xing L, Zhang W, Gu M, Yin Q, Wu G. 2020. Microbial interactions regulated by the dosage of ferroferric oxide in the co-metabolism of organic carbon and sulfate. Bioresour Technol 296:122317.

63. Liu Y, Gu M, Yin Q, Wu G. 2019. Inhibition mitigation and ecological mechanism of mesophilic methanogenesis triggered by supplement of ferroferric oxide in sulfate-containing systems. Bioresour Technol 288:121546.

64. Kato S, Hashimoto K, Watanabe K. 2012. Methanogenesis facilitated by electric syntrophy via (semi) conductive iron-oxide minerals. Environ Microbiol 14:1646-1654.

65. Roden EE. 2012. Microbial iron-redox cycling in subsurface environments. Biochem Soc Trans 40:1249–1256.

66. Morse JW, Millero FJ, Cornwell JC, Rickard D. 1987. The chemistry of the hydrogen sulfide and iron sulfide systems in natural waters. Earth Sci Rev 24:1-42.

67. Ma S, Noble A, Butcher D, Trouwborst RE, Luther III GW. 2006. Removal of H_2S via an iron catalytic cycle and iron sulfide precipitation in the water column of dead end tributaries. Estuar Coast Shelf Sci 70:461-472.

68. Findlay AJ, Gartman A, MacDonald DJ, Hanson TE, Shaw TJ, Luther III GW. 2014. Distribution and size fractionation of elemental sulfur in aqueous environments: The Chesapeake Bay and Mid-Atlantic Ridge. Geochim Cosmochim Acta 142:334-348.

69. Mumford AC, Adaktylou IJ, Emerson D. 2016. Peeking under the iron curtain: development of a microcosm for imaging the colonization of steel surfaces by *Mariprofundus* sp. strain DIS-1, an oxygen-tolerant Fe-oxidizing bacterium. Appl Environ Microbiol 82:6799-6807.

70. Senko JM, Bertel D, Quick TJ, Burgos WD. 2011. The influence of phototrophic biomass on Fe and S redox cycling in an acid mine drainage-impacted system. Mine Water Environ 30:38-46.

71. Hibbing ME, Fuqua C, Parsek MR, Peterson SB. 2010. Bacterial competition: surviving and thriving in the microbial jungle. Nat Rev Microbiol 8:15-25.

72. Kurm V, van der Putten WH, Weidner S, Geisen S, Snoek BL, Bakx T, Hol WHG. 2019. Competition and predation as possible causes of bacterial rarity. Environ Microbiol 21:1356-1368.

73. Louca S, Polz MF, Mazel F, Albright MB, Huber JA, O'Connor MI, Ackermann M, Hahn AS, Srivastava DS, Crowe SA. 2018. Function and functional redundancy in microbial systems. Nat Ecol Evol 2:936-943.

74. Miot J, Benzerara K, Obst M, Kappler A, Hegler F, Schädler S, Bouchez C, Guyot F, Morin G. 2009. Extracellular iron biomineralization by photoautotrophic iron-oxidizing bacteria. Appl Environ Microbiol 75:5586-5591.

75. Swanner ED, Wu W, Hao L, Wüstner ML, Obst M, Moran DM, McIlvin MR, Saito MA, Kappler A. 2015. Physiology, Fe (II) oxidation, and Fe mineral formation by a marine planktonic cyanobacterium grown under ferruginous conditions. Front Earth Sci (Lausanne) 3:60.

76. Camacho A, Walter XA, Picazo A, Zopfi J. 2017. Photoferrotrophy: remains of an ancient photosynthesis in modern environments. Front Microbiol 8:323.

77. Laufer K, Nordhoff M, Røy H, Schmidt C, Behrens S, Jørgensen BB, Kappler A. 2016. Coexistence of microaerophilic, nitrate-reducing, and phototrophic Fe (II) oxidizers and Fe (III) reducers in coastal marine sediment. Appl Environ Microbiol 82:1433-1447.

78. Chen H, Young S, Berhane T-K, Williams HN. 2012. Predatory *Bacteriovorax* communities ordered by various prey species. PLoS One 7:e34174.

79. Chen H, Laws EA, Martin JL, Berhane T-K, Gulig PA, Williams HN. 2018. Relative contributions of *Halobacteriovorax* and bacteriophage to bacterial cell death under various environmental conditions. mBio 9:e01202-18.

80. Feng S, Tan CH, Constancias F, Kohli GS, Cohen Y, Rice SA. 2017. Predation by *Bdellovibrio bacteriovorus* significantly reduces viability and alters the microbial community composition of activated sludge flocs and granules. FEMS Microbiol Ecol 93:fix020.

81. Spang A, Offre P. 2019. Towards a systematic understanding of differences between archaeal and bacterial diversity. Environ Microbiol Rep 11:9-12.

82. Oikonomou A, Filker S, Breiner HW, Stoeck T. 2015. Protistan diversity in a permanently stratified meromictic lake (Lake Alatsee, SW Germany). Environ Microbiol 17:2144-2157.

83. Aijaz I, Koudelka GB. 2017. Tetrahymena phagocytic vesicles as ecological micro-niches of phage transfer. FEMS Microbiol Ecol 93.

84. Cram JA, Parada AE, Fuhrman JA. 2016. Dilution reveals how viral lysis and grazing shape microbial communities. Limnol Oceanogr 61:889-905.

85. Zhou J, Chen D, Huang R, Huang G, Yuan Y, Fan H. 2019. Effects of bacterial-feeding nematodes on soil microbial activity and the microbial community in oil-contaminated soil. J Environ Manage 234:424-430.

86. Schiaffino M, Diovisalvi N, Molina DM, Fermani P, Puma CL, Lagomarsino L, Quiroga M, Pérez G. 2019. Microbial food-web components in two hypertrophic human-impacted Pampean shallow lakes: interactive effects of environmental, hydrological, and temporal drivers. Hydrobiologia 830:255-276.

87. Liu J, Meng Z, Liu X, Zhang X-H. 2019. Microbial assembly, interaction, functioning, activity and diversification: a review derived from community compositional data. Mar Life Sci Technol:1-17.

88. Handley KM. 2019. Determining microbial roles in ecosystem function: Redefining microbial food webs and transcending kingdom barriers. mSystems 4:e00153-19.

89. Comeau AM, Li WK, Tremblay J-É, Carmack EC, Lovejoy C. 2011. Arctic Ocean microbial community structure before and after the 2007 record sea ice minimum. PLoS One 6.

90. Schloss PD, Gevers D, Westcott SL. 2011. Reducing the effects of PCR amplification and sequencing artifacts on 16S rRNA-based studies. PLoS One 6.

91. Schloss PD, Westcott SL, Ryabin T, Hall JR, Hartmann M, Hollister EB, Lesniewski RA, Oakley BB, Parks DH, Robinson CJ. 2009. Introducing mothur: open-source, platform-independent, community-supported software for describing and comparing microbial communities. Appl Environ Microbiol 75:7537-7541.

92. Kozich JJ, Westcott SL, Baxter NT, Highlander SK, Schloss PD. 2013. Development of a dual-index sequencing strategy and curation pipeline for analyzing amplicon sequence data on the MiSeq Illumina sequencing platform. Appl Environ Microbiol 79:5112-5120.

93. McMurdie PJ, Holmes S. 2013. phyloseq: an R package for reproducible interactive analysis and graphics of microbiome census data. PLoS One 8:e61217.

94. Daly RA, Roux S, Borton MA, Morgan DM, Johnston MD, Booker AE, Hoyt DW, Meulia T, Wolfe RA, Hanson AJ. 2019. Viruses control dominant bacteria colonizing the terrestrial deep biosphere after hydraulic fracturing. Nat Microbiol 4:352.

95. Brown M, Baptista J, Lunn M, Swan D, Smith S, Davenport R, Allen B, Sloan W, Curtis T. 2019. Coupled virus-bacteria interactions and ecosystem function in an engineered microbial system. Water Res 152:264-273.

96. Warwick-Dugdale J, Buchholz HH, Allen MJ, Temperton B. 2019. Host-hijacking and planktonic piracy: how phages command the microbial high seas. Virol J 16:15.

97. Campbell BJ, Yu L, Heidelberg JF, Kirchman DL. 2011. Activity of abundant and rare bacteria in a coastal ocean. Proc Natl Acad Sci U S A 108:12776-12781.

98. Koskella B, Meaden S. 2013. Understanding bacteriophage specificity in natural microbial communities. Viruses 5:806-823.

99. Van Rossum T, Uyaguari-Diaz MI, Vlok M, Peabody MA, Tian A, Cronin KI, Chan M, Croxen MA, Hsiao WW, Isaac-Renton J. 2018. Spatiotemporal dynamics of river viruses, bacteria and microeukaryotes. bioRxiv:259861.

100. Tyagi R, Blais J, Auclair J. 1993. Bacterial leaching of metals from sewage sludge by indigenous iron-oxidizing bacteria. Environmental Pollution 82:9-12.

101. Ishigaki T, Nakanishi A, Tateda M, Ike M, Fujita M. 2005. Bioleaching of metal from municipal waste incineration fly ash using a mixed culture of sulfur-oxidizing and iron-oxidizing bacteria. Chemosphere 60:1087-1094.

102. Whitaker AH, Duckworth OW. 2018. Cu, Pb, and Zn sorption to biogenic iron (oxyhydr) oxides formed in circumneutral environments. Soil Syst 2:18.

103. Søgaard EG, Aruna R, Abraham-Peskir J, Koch CB. 2001. Conditions for biological precipitation of iron by *Gallionella ferruginea* in a slightly polluted ground water. Appl Geochem 16:1129-1137.

104. Takeda I, Somura H, Mori Y. 2010. Recovery of phosphorus from natural water bodies using iron-oxidizing bacteria and woody biomass. Ecol Eng 36:1064-1069.

105. Buliauskaitė R, Wilfert P, Suresh Kumar P, de Vet WW, Witkamp G-J, Korving L, van Loosdrecht MC. 2020. Biogenic iron oxides for phosphate removal. Environ Technol 41:260-266.

106. Omoregie EO, Couture R-M, Van Cappellen P, Corkhill CL, Charnock JM, Polya DA, Vaughan D, Vanbroekhoven K, Lloyd JR. 2013. Arsenic bioremediation by biogenic iron oxides and sulfides. Appl Environ Microbiol 79:4325-4335.

107. Liu X, Liu M, Chen X, Yang Y, Hou L, Wu S, Zhu P. 2019. Indigenous PAH degraders along the gradient of the Yangtze Estuary of China: Relationships with pollutants and their bioremediation implications. Mar Pollut Bull 142:419-427.

108. Bissett A, Brown MV, Siciliano SD, Thrall PH. 2013. Microbial community responses to anthropogenically induced environmental change: towards a systems approach. Ecol Lett 16:128-139.

109. Tyler G. 1974. Heavy metal pollution and soil enzymatic activity. Plant Soil 41:303-311.

110. Lenart-Boroń A, Boroń P. 2014. The effect of industrial heavy metal pollution on microbial abundance and diversity in soils—a review, Environmental risk assessment of soil contamination. IntechOpen.

111. Maila MP, Randima P, Surridge K, Drønen K, Cloete TE. 2005. Evaluation of microbial diversity of different soil layers at a contaminated diesel site. Int Biodeterior Biodegradation 55:39-44.

112. Máthé I, Benedek T, Táncsics A, Palatinszky M, Lányi S, Márialigeti K. 2012. Diversity, activity, antibiotic and heavy metal resistance of bacteria from petroleum hydrocarbon contaminated soils located in Harghita County (Romania). Int Biodeterior Biodegradation 73:41-49.

113. Sun MY, Dafforn KA, Johnston EL, Brown MV. 2013. Core sediment bacteria drive community response to anthropogenic contamination over multiple environmental gradients. Environ Microbiol 15:2517-2531.

114. Nogales B, Lanfranconi MP, Piña-Villalonga JM, Bosch R. 2011. Anthropogenic perturbations in marine microbial communities. FEMS Microbiol Rev 35:275-298.

115. Yan Z, Hao Z, Wu H, Jiang H, Yang M, Wang C. 2019. Co-occurrence patterns of the microbial community in polycyclic aromatic hydrocarbon-contaminated riverine sediments. J Hazard Mater 367:99-108.

116. Li Y, Xu Z, Wu J, Mo P. 2020. Efficiency and mechanisms of antimony removal from wastewater using mixed cultures of iron-oxidizing bacteria and sulfate-reducing bacteria based on scrap iron. Sep Purif Technol:116756.

117. Vollrath S, Behrends T, Van Cappellen P. 2012. Oxygen dependency of neutrophilic Fe (II) oxidation by *Leptothrix* differs from abiotic reaction. Geomicrobiol J 29:550-560.

Figures

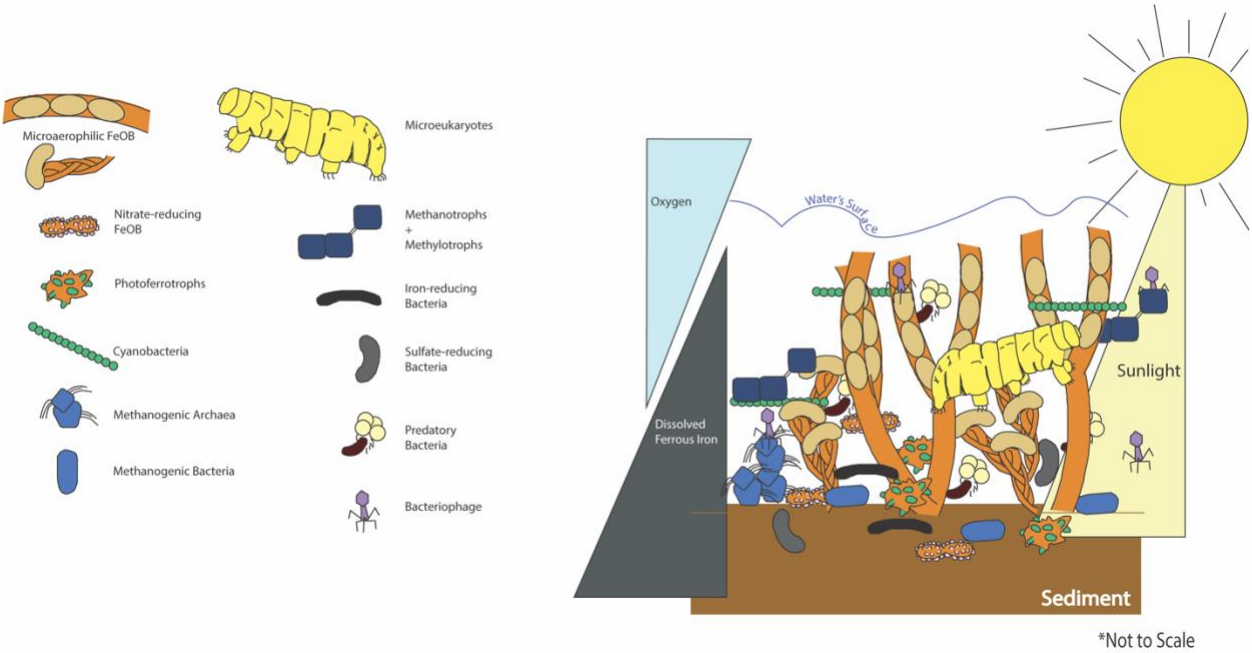

Figure 1.1: An artistic rendition of some of the notable functional groups present in the neutrophilic, freshwater iron mat from eukarya, bacteria, archaea, and viruses. Organisms have been drawn here in their hypothesized niche space based on known functions and abiotic factors such as sunlight, dissolved oxygen (O_2), and dissolved ferrous iron (Fe^{2+}). Notably, for example, the presence of bacteriophage in the mat, and their placement therein, is entirely hypothetical as there is as-yet no literature on the niche spaces inhabited by these community members. There are also missing abiotic factors (e.g., organic carbon, nitrogen, phosphorous) which certainly impact the microbial community composition within the iron mat in low-flow streams, but are less consistent between mats.

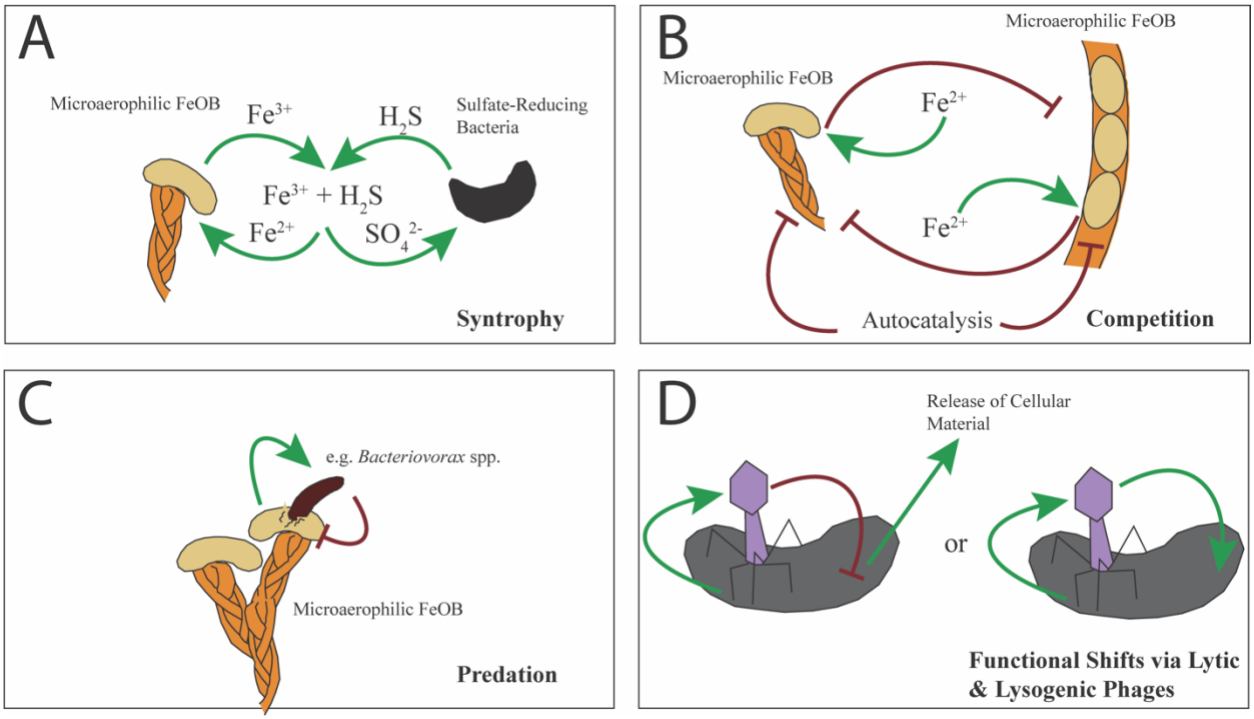

Figure 1.2: A brief graphical summary of some of the potential relationships that could work to maintain the iron mat community. (A) Symbiotic relationships have been proposed for functional groups that coexist within iron mat communities, for example the potential relationship between microaerophilic FeOB (e.g. *Gallionella* spp., *Siderooxydans* spp., *Ferriphaselus* spp., or *Leptothrix* spp.) and sulfate-reducing bacteria that have been identified in freshwater iron mats via 16S sequencing (7, 23). (B) Competitions for niche space and resources is likely prevalent in the iron mat community, though how this competition impacts growth rate is currently unknown. Here the competition is between two different microaerophilic FeOB competing for Fe^{2+} within their shared niche space, this competition is also augmented by the formation of Fe^{3+} chemically known as autocatalysis, the rate of which has been previously investigated (117). (C) Predation within iron mat communities, particularly that of bacterivorous species, such as *Bacteriovorax* spp., has not previously been considered as having a large impact; however, rates of predation may influence dominant taxa or the ecosystem architects, the gram-negative FeOB. (D) Two of

the possible interactions between bacteriophages and their bacterial hosts, either as antagonists (e.g. cell lysis) or symbiotic (e.g. metabolic regulation) that have been shown to modify local ecology. The study of bacteriophage within iron mats is a field as-yet unexplored.

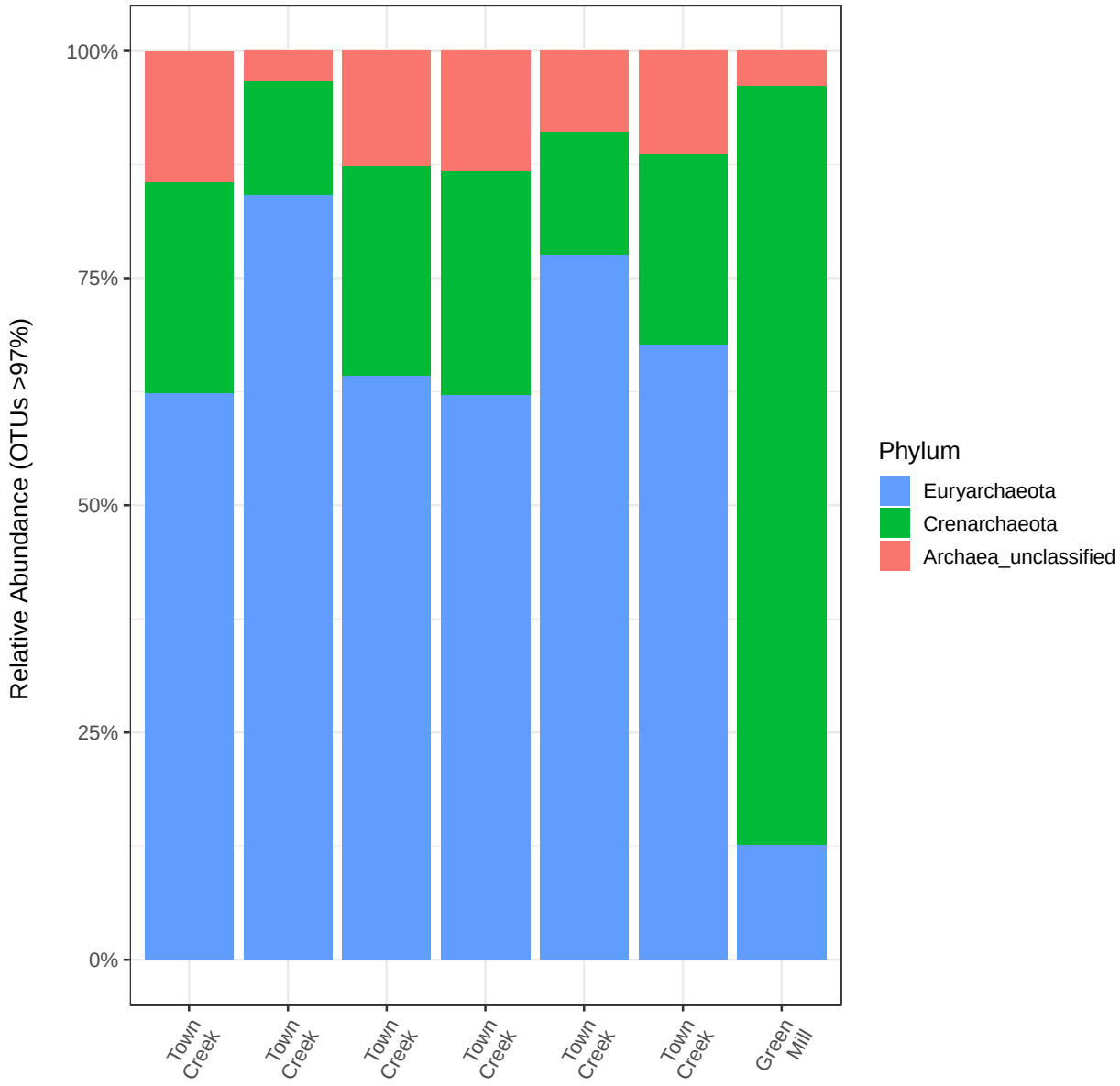

Figure 1.3: Archaeal 16S rDNA was sequenced from seven urban-impacted freshwater iron mats in Greenville, NC. Six of the iron mats were sampled from Town Creek and an out-group from Green Mill Run was included. The relative abundance of the phyla is represented here.

Euryarchaeota (blue) account for 43%, Crenarchaeota (green) account for 24%, and unclassified Archaea (red) account for 33% of the total archaeal sequences from all seven iron mats.

Chapter 2: Community Response to Hydrocarbon Pollution in Iron Oxide Mats: An Environmental Study

Authors: Chequita N. Brooks and Erin K. Field

Prepared for Submission to: *Applied and Environmental Microbiology*

Importance

Bacteria have often been capable of degrading hydrocarbon pollution in the environment, and an increase in the use of oil for heating homes and businesses in the 60's and 70's has led to an epidemic of underground oil storage tanks in disrepair, leaking their leftover contents into groundwater connected to recreational waterways and drinking water infrastructure. This impacts local communities. A final opportunity to remove hydrocarbons is at the oxic-anoxic boundary, where anoxic groundwaters enter surface waters, where we might apply naturally remediating microorganisms to this contamination. The microaerophilic iron-oxidizing bacteria thrive at this interface, and build structures called iron mats that serve to support niches for a wide variety of functionally distinct microorganisms. However, it is unclear whether or not the organisms present in the iron mat would be capable of hydrocarbon degradation or what affect exposure may have on metabolic function.

Abstract

Hydrocarbon pollution is a widespread issue in both groundwater and surface-water systems; however, research on remediation at the interface of these two systems is lacking. This interface is the oxic-anoxic boundary, where hydrocarbon pollution from contaminated groundwaters flows into surface waters, and iron mats are formed by microaerophilic iron-oxidizing bacteria.

Here, iron mats may provide an ecosystem service by remediating hydrocarbons such as benzene before they disseminate. In order to elucidate whether the microbial community in iron mats can function to remove hydrocarbons we sampled from both unexposed and exposed mats. In exposed iron mats we found a negative correlation between the concentration of phosphate and benzene, which was not observed in the reference water samples, that was possibly driven by surface adsorption to iron-oxyhydroxides. Of the geochemical and physical conditions measured, the structure of the iron mat community was driven by dissolved oxygen, pH, and benzene. The alpha diversity and evenness were also significantly lower in hydrocarbon exposed iron mats than unexposed mats, as reflected by an increase in the relative abundance of Betaproteobacteria in the exposed mats. There was also a strong signature of changing taxa between the two collection seasons, spring and summer. 16S amplicon sequences also indicated the presence of taxa associated with hydrocarbon degradation both in exposed and unexposed iron mats, suggesting that unexposed iron mat communities could be functionally responsive upon exposure to hydrocarbons. This suggest that iron mats, and their associated microbial communities, may have application in hydrocarbon polluted freshwater sites and successfully respond to hydrocarbon perturbation where not previously experienced.

Introduction

Hydrocarbon pollution is an international issue, from the Deepwater Horizon Oil Spill to the 500,000+ underground storage tanks leaking oil into groundwaters (as of September 2020) (1, 2). Most clean-up method for these contaminants are expensive, causing delays in remediation or removal. This is highly problematic, as groundwaters can release these toxins into public drinking water or aboveground recreational waterways. In turn, hydrocarbons, such as

benzene, can be highly hazardous to human health, resulting in leukemia and anemia (3). Toward combating this long-standing public health crisis, there is a plethora of work focused on hydrocarbon biodegradation. Efforts have strongly targeted benzene, as it is highly mobile in groundwater (4) and resistant to oxidation, and degradation (5). Benzene biodegradation more readily occurs under aerobic conditions and it occurs via well-studied pathways (6). However, the application of aerobic degradation pathways is limited as oxygen is quickly expended in the water column leading to anoxia in contaminated zones (7). Because it is not limited by oxygen dissolution in groundwater, anaerobic benzene degradation has also been a focus of research (e.g., 7). Previous terrestrial studies have focused primarily on groundwater environments and approaches that attempt to incorporate the oxic-anoxic boundary are notably limited (8). In a study using beach sand from Pensacola Beach, FL, an oxic-anoxic incubation model was found to increase the efficacy of the aerobic hydrocarbon degradation, as it was bolstered following anoxic periods by the byproducts of anaerobic metabolisms (9). As “oxic” and “anoxic” conditions are concurrent in the iron mat, it is possible that a similar bolstering of hydrocarbon degradation occurs over time within this microbial community. Furthermore, the oxic-anoxic boundary where groundwater meets surface water is the last stop prior to widespread contamination by hydrocarbons. In this way, iron mats could be considered the last chance for hydrocarbon remediation using microbial communities before it outspreads.

The use of microorganisms to degrade hydrocarbons does not come without other challenges. Hydrocarbons increase stress in the environment by leading to the production of reactive oxygen species, which can damage microbial DNA (10). This, in turn, can impact the structure of microbial communities exposed to hydrocarbons by decreasing community diversity (11-13). In a study of cyanobacterial mats in Berre lagoon, France, hydrocarbon exposure

decreased the influence of seasonality (14), possibly due to the tendency for hydrocarbon inundated communities to skew toward more extremophilic organisms (15, 16). Microbial communities exposed to hydrocarbon contamination can also decrease in alpha diversity as a result of the decreased probability of horizontal gene transfer compared to communities exposed to other contaminants, such as heavy metals or antibiotics (12).

The microbial communities in freshwater iron mats may already be exposed to high concentrations of heavy metals and increased environmental stress since freshwater iron mats are naturally adsorptive. Iron-oxyhydroxides (FeOOH) produced by iron-oxidizing bacteria (FeOB) adsorb heavy metals (17, 18), aromatic carbons (19), phosphorous (20, 21), and hydrophilic pesticides (22) out of the water column. Due to these adsorptive properties of biogenic FeOOH, iron mats have been suggested as a way to remove benzene and other hydrocarbons from contaminated sites (23, 24). The chemical properties of iron mats are not the only source of potential for benzene removal, as there have been multiple studies that show that functional groups of microorganisms that have been previously identified in iron mats, including sulfate-reducing bacteria (SRB) (7, 25, 26), iron-reducing bacteria (FeRB) (27-29) and nitrate-reducing bacteria (NRB) (30-32), are involved in the biodegradation of benzene and other hydrocarbons in other environments.

The iron mat has connections within and between the biogeochemical cycles of iron, sulfur, and nitrogen. However, whether these connections are maintained under perturbation has yet to be explored. For example, a syntrophic connection between FeOB and SRB has been previously proposed (33), but whether this relationship is retained under stressful conditions is unclear. Still, if hydrocarbon degrading organisms are present and active, then the iron mat community could prove to be an invaluable resource in application toward hydrocarbon

remediation at the oxic-anoxic boundary. Here, we present work from *in situ* samplings of iron mats formed from communities that have been chronically exposed to benzene contamination in Town Creek, Greenville, NC. Using 16S amplicon and metagenomic sequencing, we aim to establish to what extent the microbial communities in iron mats respond to hydrocarbon perturbation. We have paired this molecular data with a battery of physical and chemical parameters in order to establish how hydrocarbon perturbation is mediated by other factors such as seasonal changes. Finally, we examine whether the iron mat communities exhibit hydrocarbon remediation potential through the metagenomic analysis of benzene degradation genes. This work determines if iron mats can be used in application in hydrocarbon impacted streams in novel locations and builds upon our existing knowledge of how iron mat microbial communities respond to perturbation from contamination.

Results and Discussion

Site Conditions

Samples were collected from iron mats up- and downstream of a leaking underground storage tank seepage site in Town Creek, Greenville, NC (Figure 2.1). The upstream mat (U) served as a reference (unexposed) iron mat community within the system that was not impacted by the leaking underground storage tanks. Downstream, benzene-exposed mats (Da and Db) and water samples (W) were collected. Samples were collected twice in March 2018 (S1 and S2)) as well as two sampling efforts in summer (July (S3) and August 2019 (S4)).

Geochemistry

Iron mats were sampled up- and downstream of a hydrocarbon seep resulting from a leaking underground storage tank. An unexposed mat upstream (U), downstream mats (Da and Db), and water samples (W) were collected, and their geochemistry was analyzed (Table S2.1). A noticeable trend amongst the downstream iron mats was lower phosphate concentrations correlating with higher benzene concentrations (R^2=0.95, p=1.6e^{-6}) (Figure 2.2). It is worth mentioning that during sampling day 3 and 4 (S2.3, S2.4) total dissolved phosphate concentrations were beneath the detection limit (0.0001 μM/L) and have been plotted at zero. This negative correlation was stronger in the downstream iron mats than in the reference water sample (R^2=0.58, p=0.028), suggesting that the iron mats are interacting with the benzene and phosphates in the system. It is likely that benzene and phosphate interact antagonistically within the system, since iron mats may adsorb benzene to the surface of the FeOOH particles, similar to phosphate and other contaminants, potentially leading to the observed negative correlation. In other words, if benzene is adsorbed to the surface of the FeOOH particles, then there will be less room for phosphate adsorption. Alternatively, phosphorous addition has been previously observed to increase microbial benzene removal (34), it is therefore possible that at higher benzene concentrations microbial scavenging of phosphorous increases, leading to a measurable decrease. Further studies are needed to understand this negative correlation, and whether it is chemically, physically, or biologically driven. Regardless, these results support the idea that iron mats could be used as a self-renewing resource for sequestering or removing benzene (and possibly other hydrocarbons) from contaminated systems.

The downstream, benzene-exposed iron mats were also divisible into two mat types: flocculent and seep. These mat types were previously established in work by Fleming et al. (35) as flocculent mats being loosely associated and centimeters thick, while seep mats were densely

associated and millimeters thick. Using mat types, we compared the geochemical conditions within each (Figure 2.3). Seep type mats had much higher oxidized and reduced iron concentrations than either the reference downstream water sample or the flocculent mat types. This may reflect a more active iron-cycling community within the seep type mats, possibly owing to a closer association between the aerobic and anaerobic organisms. The flocculent mats were, however, higher in phosphate compared to the seep mats. The average concentration of non-particulate organic carbon was similar in both mat types to that of the water samples. Organic carbon has been previously associated with *Leptothrix ochracea* dominated mats (35), such as those in Town Creek. A compelling result amongst the mats is the lower nitrate and nitrite concentrations when compared with the reference water sample. The low concentration of nitrate and nitrite does not appear to be correlated to the concentration of benzene, ethylbenzene, or total xylenes in the iron mats sampled. It does, however, suggest the possibility of nitrite-reducing organisms and possibly active denitrification processes concentrated within the mats. Likely, the oxygen dynamics in the mats supports this anaerobic metabolism. This may prove to be an important connection between the nitrogen cycle and freshwater iron mats, a connection that is only just being explored in marine iron mats (36).

Community richness and diversity

Bacterial community composition was determined using operational taxonomic unit (OTU) relative abundances and were compared between iron mats up- (U) and downstream (Da and Db). There were six downstream and four upstream samples. The alpha diversity indices (Figure S2.1) and evenness index (Figure S2.2) were significantly lower in downstream than upstream mats (e.g., Simpsons U=0, p=0.01421), which suggests that the within community

diversity of iron mats is strongly impacted by oil perturbation. This is consistent with other oil perturbed communities (11, 12). However, beta diversity did not significantly vary between upstream and downstream ecotypes (ADONIS $R^2 = 0.12644$, $p = 0.234$, strata=location). Interestingly, this suggests that while the overall number of species varies between up- and downstream, the pattern of species change is not that strong. This result, paired with the relative abundance data below, point toward a filtering effect of perturbation on the iron mat microbial community. Still, several OTUs exhibited differential relative abundances between up- and downstream when measured by log Fold Change, with the greatest observed change in the phyla Bacteroidetes and myriad OTUs representing Proteobacteria (Figure 2.4). That these OTUs were from these phyla was unsurprising, as the phylum Proteobacteria had the greatest percent relative abundance amongst downstream mat communities (average 85%) and upstream mat communities (average 69%), followed by Bacteroidetes (average 10% and 19%, respectively) (Figure 2.5). Dominance by Proteobacteria has been previously observed in hydrocarbon-exposed samples; however, the samples from previous studies tend to be dominated by Alphaproteobacteria (37-39), whereas the iron mat sample 16S amplicon sequences (regardless of location) were dominated by Betaproteobacteria (Figure S2.3). Indeed, there was an increase in Betaproteobacteria when iron mats were under hydrocarbon stress, which may be associated with the degradation of lower molecular weight polycyclic aromatic hydrocarbons (40). These results suggest that the hydrocarbons acted as a filter on the iron mat communities and pushed the communities toward an over-representation of the most abundant taxa.

Community composition

Of the genera previously associated with microaerophilic iron-oxidation (41-44), only *Leptothrix* spp. were observed in the iron mats in Town Creek via 16S amplicon sequencing (0.0095% relative abundance downstream, 0.0045% upstream). Microscopy of mat samples revealed some stalk FeOOH (data not shown). Stalks are associated with other genera, such as *Gallionella*, though they may indicate another as yet unknown stalk-forming organism (e.g., 45). That the iron mats in Town Creek are dominated by *Leptothrix* spp. is not necessarily unusual, as there is a previous record of iron mats dominated by *Leptothrix* spp. that have used various 16S regions (V4, V4-V6, V6-V8) (35, 46, 47). It's also not unusual that the other microaerophilic FeOB, such as *Gallionella* would be below the detection limit of the 16S amplicon sequencing, given that these organisms are "rare" community members, even in the iron mat.

Of interest to this study were the hydrocarbonoclastic organisms (generally associated with the obligate use of hydrocarbons) and organisms that have been associated with hydrocarbon degradation overall. Only one genus of hydrocarbonoclast was present in the samples from Town Creek: *Planomicrobium*. These sequences were present in greater relative abundance in the upstream samples, though generally accounted for a very small percent relative abundance (<0.0025%) of any sample. This is in agreement with previous findings in cyanobacterial mats that hydrocarbonoclastic genera are not good indicators of chronic hydrocarbon exposure; rather, they are cosmopolitan (14). There was, however, a greater relative abundance of the genera *Hydrogenophaga* and *Dechloromonas*, which are associated with nitrate-reduction coupled benzene degradation (31, 32, 48), in the downstream (average 5.27%, 0.16% respectively) than upstream mats (average 3.96%, 0.19% respectively). Also present was the iron-reducing benzene degrading genus *Geobacter* (29) (average 0.56% downstream, 0.74% upstream) and sulfate-reducing benzene degrading genus *Desulfobacula* (26) (average 0.0026%

downstream, 0.0010% upstream). These results suggest that the community within the iron mat could contribute to bioremediation of benzene or other hydrocarbons in the creek in the downstream mats. That organisms associated with hydrocarbon remediation were present in iron mats that do not experience hydrocarbon perturbation normally (upstream) also suggests that iron mats in locations currently not experiencing perturbation may be able to maintain biogeochemically important cycles upon exposure. These organisms in total represent connections between hydrocarbons and the nitrogen, iron, and sulfur cycles. Of interest to future studies would be whether the cycling of these elements in the iron mat is as efficient under hydrocarbon perturbation, given the previously discussed loss of diversity.

Of the organisms that may play a role in anaerobic iron oxidation, sequences for the putatively nitrate-reducing iron-oxidizing bacteria genera *Acidovorax*, *Aquabacterium*, *Azospira*, *Paracoccus*, *Thermomonas*, and *Thiobacillus* (49) were recovered from both the downstream and upstream mats. Previously, three of these genera (*Azospira, Paracoccus, and Thermomonas*) were not identified as being present in freshwater iron mats (24), however *Azospira* have been identified previously in paddy soil (50). *Paracoccus* and *Thermomonas* are in the classes Alphaproteobacteria and Gammaproteobacteria, respectively, which are both currently underrepresented in reported iron mat communities, as the majority of reports in the literature are still clone library based (24). There were also possibly photoferrotrophic sequences present in the samples from the genera *Rhodobacter*, *Rhodomicrobium*, and *Rhodovulum* (49). There was a higher proportion of photoferrotrophic genera in the upstream mats. Alternatively, there was a higher proportion of nitrate-reducing iron-oxidizing bacteria in the downstream mats. This difference in community composition may result from site turbidity, as the downstream mats

were under a thin sheen of both oxidized iron and oil that may have decreased irradiance and thus the efficacy of phototrophic organisms.

The iron mat community is of interest not only for the FeOB, but for the biogeochemical cycles that it connects. As such, one of the questions of this research was whether these cycles would be preserved under hydrocarbon perturbation. Two functional guilds that contribute to the iron and sulfur cycles, FeRB and SRB were present, but represented a small proportion of the overall iron mat community amplicon sequences. On average, FeRB genera (Table S2.2) totaled 0.755% and 0.971% relative abundance of downstream and upstream mats, respectively. SRB genera (Table S2.3), on average, totaled 0.143% and 0.209% relative abundance of downstream and upstream mats, respectively. While there was a higher relative abundance of FeRB, there was a greater diversity of SRB in the iron mats both up- and downstream. As mentioned above in discussions of the FeOB, organisms consisting of a low relative abundance in the iron mat community can be of especial importance in cycling major elements (e.g., iron) and should not be discounted in these systems. It is therefore possible that these iron mats are host to connections between the iron and sulfur cycle, as it has been previously suggested that FeOB and SRB participate in a syntrophic interaction within FeOB communities (33) and that these cycles could, based on the detection of these 16S amplicons, be preserved even in the hydrocarbon perturbed iron mats downstream.

Community Structure & Function

Using a Canonical Correspondence Analysis (CCA) we observed that, of the chemical and physical conditions presented in Table S1, dissolved oxygen (DO) (PERMANOVA $F = 2.61$, $p = 0.0033$) had the greatest influence on community structure, followed by pH

(PERMANOVA F = 2.22, p = 0.0192) and then benzene concentration (PERMANOVA F = 1.06, p = 0.4326) (Figure 2.6). Greater separation was seen between upstream and downstream samples along the vertical axis (DO and benzene). The vertical separation was greater between summer (S3 & S4) samples than spring samples (S1 & S2), where the downstream mat samples had a very low average DO compared to all other samples (avg. 2.0 ppm). While benzene was a strong driver of community structure, it makes sense that the iron mat communities, which are assemblages of organisms sensitive to oxygen conditions: microaerophiles, anaerobes, and aerobes, would be sensitive to changes in DO. pH had the greatest effect along the horizontal axis, a result consistent with previous studies showing pH is a strong driver of community structure, even in communities under polycyclic aromatic hydrocarbon influence (51). Still, this result is somewhat surprising given that the pH of this data set only ranged from 6-7.13, which likely falls within the growth range of many of the isolates associated with the retrieved amplicons. Perhaps this result reflects the influence of pH on the biogeochemical cycles that were catalyzed or vice versa. These results highlight that microbial communities under hydrocarbon perturbation in systems such as the one in Town Creek, while structured by the perturbation, are also structured by common drivers such as the ones explored here.

As we were also interested in whether community functions associated with the iron mat system would be persevered under hydrocarbon perturbation, we searched metagenomic sequences for functional gene presence. Assembled contigs from the metagenomic sequences of each sample were assessed for quality (Table S2.4) and functional potential. There was no significant difference between upstream and downstream iron-cycling gene sequence normalized abundances or benzene remediation genes in the assemblies (Figure S2.4, S2.5). This result is in contrast with marine sediment core communities, where the functional potential of iron-cycling

increases under hydrocarbon regimes (38). However, this result underscores iron-cycling as a key process to iron mat community function, where the iron mat community is built upon a foundation of iron-cycling. Furthermore, this result suggests that benzene remediation may readily begin in the upstream mat communities if exposed, indicating that iron mat communities may be useful in hydrocarbon bioremediation in freshwater environments. There were some differences in the gene count for some benzene-remediation associated genes such as 4-hydroxybenzoate octaprenyltransferase and formate dehydrogenase-O major subunit, which were in greater abundance in the exposed than unexposed iron mats. Interestingly, nitrate reductase was detected in greater abundance in the upstream than downstream iron mats. This may have been due to the presence of nitrate-reducing organisms that do not participate in benzene-remediation being lost in the downstream communities.

Recovered MAGs

Metagenomic assembled genomes (MAGs) are highly useful for linking geochemical cycles within a single taxon by identifying how they contribute wholistically. They can also be used for understanding cryptic cycles and rare taxa. MAGs have been found to be useful in identifying rare taxa from data sets that were not previously observed using 16S amplicon sequencing (e.g., 52). Twenty-nine high-quality MAGs were recovered from the iron mat samples (> 59% complete, < 10% contamination) (Table S2.4). Location did not have a large effect on genome size (upstream average 2.57 ± [standard error = SE] 0.24 Mbp; downstream average 2.61 ± SE 0.13 Mbp) or GC content (upstream average 52.67 ± SE 4.68%; downstream average 55.4 ± 2.17%). None of the recovered MAGs appear to be from taxa known for hydrocarbon degradation; however, it is also worth mentioning that the taxa found to be in the

greatest average relative abundance from 16S amplicon sequencing (Figure S2.3) were not represented by the assembled MAGs. This may have been due to currently undiagnosed biases against the assembly of these MAGs from the iron mat environment. That said, seven MAGs (one upstream/six downstream) were classified as belonging to the genus *Gallionella*, which were not identified as part of the communities using 16S amplicon sequencing, thus providing a fuller profile of the FeOB that were present in the iron mats. Eight MAGs (one upstream/seven downstream) were classified as belonging to the family Burkholderiaceae, which could be poorly assigned *Leptothrix* spp. genomes. Seven of these eight, excluding only MAG #13, were positive for iron oxidation genes based on the FeGenie analysis (Table S2.5). This result suggests that these seven MAGs were likely related to the microaerophilic *Leptothrix ochracea*, within the context of the iron mat system. Greater taxonomic diversity in the MAGs was recovered from the upstream mat location, including two MAGS that were classified as the protist endosymbiont (53), *Phycorickettsia* spp. The presence of these endosymbionts from MAGs indicates the presence protists or other microeukaryotes in the upstream iron mats that would host these organisms.

Seasonal Influences

In order to assess if sampling period had an effect on the resultant data, alpha diversity (Figure S2.6) and evenness indices (Figure S2.7) were also compared by season, as this study occurred over sampling periods in the spring and summer. While alpha diversity and evenness was not significantly different between spring and summer, we tested a model for Pielou's evenness using both season and location (up- or downstream) as factors. When both factors were included, evenness was significantly different between season ($F = 28.77$, $p = 0.001$) and

location (upstream vs. downstream) ($F = 42.58$, $p = 0.0003$). This result indicates that there is an interaction between season and location, since the difference between locations was increased when separated by season. Evenness also increased for up- and downstream locations in the summer compared to their spring counterparts. A similar trend has been shown in riverine microbial communities to be associated with changes in flow resulting from seasonal precipitation differences (54) or could also be due to hydrological factors such as groundwater discharge (55). Beta diversity was also significantly different in the iron mat communities when assessed seasonally (ADONIS $R^2 = 0.25$, $p = 0.004$, strata = season) (Figure S2.8), suggesting that there is a strong signature in taxon changes between seasons. These signatures have been previously observed in iron mat communities (35). The Town Creek iron mat samples, however, did not have the confounding variable of dominant microaerophilic FeOB, which was observed in the previous study by Fleming et al. to also change with the seasons (35), as Town Creek was consistently dominated by *Leptothrix* spp. This result provides further evidence that iron mat communities, not just FeOB, are sensitive to conditions such as dissolved oxygen (DO) which was observed to shift between seasons in the Town Creek iron mats (Figure S2.9). This is exemplified by the log Fold Change results for season, where multiple taxa representing both high and low abundance phyla were over- and under-expressed in either season (Figure S2.10). It is, however, important to note that season was not independently descriptive of the iron mat communities as the effects of hydrocarbon perturbation were great, but also because season may have some influence on the hydrocarbons themselves. Previous work has found that the concentration and type of hydrocarbon present in watersheds in Mexico varied with season (spring and summer) that was attributed to increased precipitation and motor traffic (56). While we did not identify differences in the types of hydrocarbons present in the downstream mats by

season, the concentrations of benzene, ethylbenzene, and xylenes were all higher in summer (0.015 ± 0.001, 0.007 ± 0.000, 0.037 ± 0.005) than spring (0.005 ± 0.003, 0.000 ± 0.000, 0.001 ± 0.001). The average precipitation during March 2018 (0.47 mm) and July and August 2019 (0.41 mm) were very similar and flow was negligible at all sites, making it is less clear why season would impact the concentrations of hydrocarbons in Town Creek. Precipitation and other factors will be important to consider for future work involving iron mats and hydrocarbons.

Conclusions

Iron mat communities may have application in currently hydrocarbon polluted systems. The iron mat microbial communities in Town Creek Greenville, NC consisted of genera associated with benzene remediation and functional genes were found from metagenomic contig assemblies. There was also a negative correlation between phosphate and benzene concentrations, that provides further support that the iron mat system has properties that can lead to a decrease in benzene concentrations. However, this may come at the cost of other ecosystem functions, as iron mats exposed to hydrocarbons had less diverse communities. The difference between exposed and unexposed communities was increased when samples were separated by season, where spring had an increase in over-represented taxa in the 16S amplicon data, suggesting an even greater loss in ecosystem function is possible during certain seasonal periods. These results are encouraging to research on iron mats toward application in systems that are currently unbuffered from hydrocarbon pollution. With over 500,000 leaking storage tanks in the United States, it is inevitable that these pollutants will reach above ground reservoirs, where, as indicated here, the iron mat microbial community may be successfully applied.

Materials and Methods

Site description and sample collection

The creek site, Town Creek, Greenville, NC (Figure 2.1) was in a residential area and consisted of a low-flow creek with high banks lined with riprap. Sampling of iron mats took place over four time points over two years, in March of 2018 and July and August of 2019. Samples for biological molecular analysis were collected aseptically and stored on ice until they were transported to the lab and stored at -80ºC. Samples of iron mats were also processed via filtration in an acid-washed top-bottle filter using pre-ashed (500ºC, 4h) Whatman glass microfiber filters, Grade 934-AH (1.5 µm pore size, GE Healthcare Bio-Sciences, Marlborough, MA) and filtrates were stored on ice for transport to the lab where they were stored at -20ºC until they could be analyzed. Sample analysis for phosphate, ammonia, nitrates/nitrites (SmartChem 170 and 200 Discrete Analyzer, Unity Scientific), and dissolved organic carbon (DOC) (ASI-L Autosampler, Shimadzu Scientific Instruments, Inc.) was carried out by the Environmental Research Lab at East Carolina University, Greenville, NC. Iron mat was also collected in pre-treated bottles containing ascorbic acid provided by the Environment 1, Inc. lab in Greenville, NC. Immediately after collection, hydrochloric acid was added to the samples, and they were stored at 4ºC until they were analyzed using EPA method 602 (57). Measurements of Total Iron, oxidized iron (Fe^{3+}), and reduced iron (Fe^{2+}) for all sampling sites were conducted immediately following sampling using the ferrozine method (58). Measurements of pH, conductivity, dissolved oxygen, and water temperature were taken using a YSI Quatro Professional Plus (YSI Inc., Yellow Springs, OH). Precipitation data (mm) (Station ID: US1NCPT0005) were obtained from the National Climactic Data Center (https://www.ncdc.noaa.gov/cdo-web/search; Accessed 2021 APR 15).

DNA extraction, 16S rDNA sequencing, and phylogenetic analysis

The Qiagen DNeasy PowerSoil Kit (Qiagen, Germantown, MD) was used according to the manufacturer instructions for each mat sample with the following modifications: DNA was eluted in 60 µL, and cell lysis occurred using a 10-minute cycle in a Disruptor Genie (Scientific Industries, Inc., Bohemia, NY) set to maximum speed. 16S rDNA sequencing of the V4-V5 region was performed at the Comparative Genomics and Evolutionary Bioinformatics' Integrated Microbiome Resource (CGEB-IMR, Halifax, NS) using universal primers 515FB and 926R (59, 60). Sequences were processed and annotated using mothur v. 1.44.1 (61-63) and the SILVA database v. 138.1 (64). The MiSeq SOP was accessed 2020 April 13 (https://mothur.org/wiki/miseq_sop/) and used to identify present taxa (97% OTU threshold). Further analyses were performed in R v. 3.5.2 using phyloseq v. 1.26.1 (65) to import mothur data into R, perform quality checks, calculate alpha diversity indices, ordination, and calculate relative abundances. All samples were rarified to even depth (sample size of 6883) based on the smallest sample with a set seed prior to alpha diversity and evenness calculations. The package microbiome v. 1.4.2 (66) was used to convert data into a centered log ratio format for beta diversity indices and calculate Pielou's Evenness. Prior to calculating beta diversity indices, a centered log ratio was used to transform the count data to dominance of taxa compared to the geometric mean of all taxa on a log scale and the principle coordinates analysis was performed using a redundancy analysis (RDA). The package vegan v. 2.5-6 (67) was used to convert phyloseq objects into Euclidean distance, beta dispersion and calculate statistics for the Canonical Correspondence Analysis (CCA). A permutation ANOVA (PERMANOVA) was used to test each of the margins (factors) (number of permutations = 9999) variance inflation factor

was calculated using *vif.cca()*. CCA was chosen to show overall community structuring as it was most useful in building a model of community structuring in response to the numerous environmental factors measured. The package picante v. 1.8.2 (68) was used to create a data frame with alpha diversity measurements. The package edgeR v. 3.24.3 (69, 70) was used to calculate the log Fold Change (logFC) of OTUs between benzene exposed and unexposed sites. Phyloseq objects were converted to edgeR objects using the phyloseq extension accessed 2020 January 6 (https://joey711.github.io/phyloseq-extensions/edgeR.html). Samples were filtered for independence using a variance threshold set to $1e^{-7}$ prior to calculating logFC. Visuals were generated using ggplot2 v. 3.3.2 (71), and relative abundances were converted to percentages for visualization using the package scales v. 1.1.1 (72). Color blind accessible palettes were applied to graphs using ggthemes v. 4.2.0 (73-75).

Metagenomic sequencing, assembly, and annotation

DNA extraction methods for metagenomic sequencing were performed as for 16S amplicon sequencing. Metagenomes were sequenced at CGEB-IMR using the Illumina Nextera Flex for the NextSeq at 3x depth paired-end reads. Sequence adapters were trimmed using TrimGalore v. 0.4.5 (76), and sequence loss was assessed using FastQC v. 0.11.5 (77). Reads were assembled using SPAdes v. 3.13.0 (78), unpaired reads were preserved. Assembly quality was assessed using the MetaQUAST function in QUAST v. 5.0.2 (79) (Table S2.6). Assemblies were binned into MAGs using MaxBin v. 2.2.7 (80), CONCOCT v. 1.0.0 (81), and Metabat2 v. 2.14 (82). All bins were aggregated using DAS Tool v. 1.1.2 (83). The quality of each MAG was checked using the CheckM v. 1.0.18 (84) lineage-specific workflow (Table S4). Bin identities of high-quality (> 59% complete, < 10% contamination) MAGs were determined using the

MetaSanity v. 1.2.0 (85) PhyloSanity pipeline. MAG genome size and GC content were calculated using the RASTtk server (86-88) accessed 2021 January.

Hidden Markov Models

Assembled and unpaired reads from SPAdes were filtered to remove contigs with fewer than 500 base pairs using filter_contigs.py (accessed 2020 AUG 5; https://github.com/tinybio/filter_contigs) and was subsequently filtered for contigs that had at least 1.5x coverage using another python script (accessed 2020 AUG 5; https://microsizedmind.wordpress.com/2015/03/05/removing-small-low-coverage-contigs-from-a-spades-assembly/) (89). The remaining contigs were annotated using prokka v. 1.14.5 (90) using the --*metagenome* flag. The UniProtKB database (Accessed 2021 JAN 28; https://www.uniprot.org/) (91) was used to find benzene-metabolism related genes. The search term “taxonomy:"Bacteria [2]" (benzene metabolism) AND reviewed:yes” was used, and the reviewed sequences were downloaded. Sequences for anaerobic benzene carboxylase (ubiD) (30), periplasmic nitrate reductase (napA) (92), and aerobic toluene-4-monooxygenase (tmoABCDEF) (30) were also retrieved from the database. As toluene-4-monooxygenase did not have a reviewed representative, the unreviewed sequences were used. Using MMseqs2 v. 12.113e3 (93), the sequences were collapsed using a 70% sequence identity cutoff to remove overrepresented protein sequences. The sequences were then aligned using Clustal Omega v. 1.2.4 (94, 95) and returned in Stockholm format using --*outfmt=st.* A Hidden Markov Model (HMM) was built from this file using the hmmbuild function of HMMER v. 3.2.1 (96). The HMM was used to search the annotated contigs using the hmmsearch function of HMMER v. 3.2.1 (96). Gene counts were normalized for total open reading frame number using OrfM v.

0.7.1 (97). Assemblies were also analyzed for iron-cycling related genes using FeGenie v. 1 (98). Assemblies were annotated using Prodigal v. 2.6.3 (99) using *-contig_source meta*. Gene counts were normalized using *-norm y*.

Visuals for both HMM and FeGenie results were generated using ggplot2 v. 3.3.2 (71), ggpubr v. 0.4.0 (100), and reshape v. 0.8.8 (101). Gene count normalizations were converted to percentages for visualization using the package scales v. 1.1.1 (72). Color blind accessible palettes were applied to graphs using rcartocolor v. 2.0.0 (102).

Acknowledgements

Funding support was provided by the Graduate Women in Science National Fellowship Program and the Nell Mondy, Vessa Notchev, and Monique Braude Fellowship Funds to CNB. The funders had no role in study design, data collection and interpretation, or the decision to submit this work for publication. We would like to thank the Field and Peralta Labs for assisting with field sampling.

References

1. Office of Underground Storage Tanks DC. 2020. Semiannual Report Of UST Performance Measures: End Of Fiscal Year 2020 (October 1, 2019 – September 30, 2020). U.S. E.P.A.,
2. Meegoda JN, Hu L. 2011. A review of centrifugal testing of gasoline contamination and remediation. Int J Environ Res Public Health 8:3496-3513.
3. Badham HJ, Winn LM. 2007. Investigating the role of the aryl hydrocarbon receptor in benzene-initiated toxicity in vitro. Toxicology 229:177-185.
4. Minetti RCP, Macaño HR, Britch J, Allende MC. 2017. In situ chemical oxidation of BTEX and MTBE by ferrate: pH dependence and stability. J Hazard Mater 324:448-456.
5. Johnson S, Woolhouse K, Prommer H, Barry D, Christofi N. 2003. Contribution of anaerobic microbial activity to natural attenuation of benzene in groundwater. Engineering Geology 70:343-349.
6. Jindrova E, Chocova M, Demnerova K, Brenner V. 2002. Bacterial aerobic degradation of benzene, toluene, ethylbenzene and xylene. Folia Microbiol (Praha) 47:83-93.
7. Keller AH, Kleinsteuber S, Vogt C. 2018. Anaerobic benzene mineralization by nitrate-reducing and sulfate-reducing microbial consortia enriched from the same site: Comparison of community composition and degradation characteristics. Microb Ecol 75:941-953.
8. Bradley PM. 2012. Perils of categorical thinking: “Oxic/anoxic” conceptual model in environmental remediation. Remediation Journal 22:9-18.
9. Karthikeyan S, Kim M, Heritier-Robbins P, Hatt JK, Spain JC, Overholt WA, Huettel M, Kostka JE, Konstantinidis KT. 2020. Integrated Omics Elucidate the Mechanisms

Driving the Rapid Biodegradation of Deepwater Horizon Oil in Intertidal Sediments Undergoing Oxic–Anoxic Cycles. Environ Sci Technol 54:10088-10099.

10. Liu X, Liu M, Chen X, Yang Y, Hou L, Wu S, Zhu P. 2019. Indigenous PAH degraders along the gradient of the Yangtze Estuary of China: Relationships with pollutants and their bioremediation implications. Mar Pollut Bull 142:419-427.
11. Maila MP, Randima P, Surridge K, Drønen K, Cloete TE. 2005. Evaluation of microbial diversity of different soil layers at a contaminated diesel site. Int Biodeterior Biodegradation 55:39-44.
12. Máthé I, Benedek T, Táncsics A, Palatinszky M, Lányi S, Márialigeti K. 2012. Diversity, activity, antibiotic and heavy metal resistance of bacteria from petroleum hydrocarbon contaminated soils located in Harghita County (Romania). Int Biodeterior Biodegradation 73:41-49.
13. Sun MY, Dafforn KA, Johnston EL, Brown MV. 2013. Core sediment bacteria drive community response to anthropogenic contamination over multiple environmental gradients. Environ Microbiol 15:2517-2531.
14. Aubé J, Senin P, Pringault O, Bonin P, Deflandre B, Bouchez O, Bru N, Biritxinaga-Etchart E, Klopp C, Guyoneaud R, Goñi-Urriza M. 2016. The impact of long-term hydrocarbon exposure on the structure, activity, and biogeochemical functioning of microbial mats. Mar Pollut Bull 111:115-125.
15. Paissé S, Coulon F, Goñi-Urriza M, Peperzak L, McGenity TJ, Duran R. 2008. Structure of bacterial communities along a hydrocarbon contamination gradient in a coastal sediment. FEMS Microbiol Ecol 66:295-305.

16. Abed RMM, Al-Kharusi S, Prigent S, Headley T. 2014. Diversity, Distribution and Hydrocarbon Biodegradation Capabilities of Microbial Communities in Oil-Contaminated Cyanobacterial Mats from a Constructed Wetland. PLoS One 9:e114570.

17. Field HR, Whitaker AH, Henson JA, Duckworth OW. 2019. Sorption of copper and phosphate to diverse biogenic iron (oxyhydr) oxide deposits. Sci Total Environ 697:134111.

18. Li Y, Xu Z, Wu J, Mo P. 2020. Efficiency and mechanisms of antimony removal from wastewater using mixed cultures of iron-oxidizing bacteria and sulfate-reducing bacteria based on scrap iron. Sep Purif Technol:116756.

19. Baskar S, Baskar R, Thorseth IH, Øvreås L, Pedersen RB. 2012. Microbially induced iron precipitation associated with a neutrophilic spring at Borra Caves, Vishakhapatnam, India. Astrobiology 12:327-346.

20. Takeda I, Somura H, Mori Y. 2010. Recovery of phosphorus from natural water bodies using iron-oxidizing bacteria and woody biomass. Ecol Eng 36:1064-1069.

21. Buliauskaitė R, Wilfert P, Suresh Kumar P, de Vet WW, Witkamp G-J, Korving L, van Loosdrecht MC. 2020. Biogenic iron oxides for phosphate removal. Environ Technol 41:260-266.

22. Søgaard EG, Aruna R, Abraham-Peskir J, Koch CB. 2001. Conditions for biological precipitation of iron by *Gallionella ferruginea* in a slightly polluted ground water. Appl Geochem 16:1129-1137.

23. Abbas A, Abussaud BA, Ihsanullah, Al-Baghli NAH, Khraisheh M, Atieh MA. 2016. Benzene Removal by Iron Oxide Nanoparticles Decorated Carbon Nanotubes. Journal of Nanomaterials 2016:5654129.

24. Brooks CN, Field EK. 2020. Iron Flocs and the Three Domains: Microbial Interactions in Freshwater Iron Mats. mBio 11:e02720-20.

25. Edwards EA, Grbić-Galić D. 1992. Complete mineralization of benzene by aquifer microorganisms under strictly anaerobic conditions. Appl Environ Microbiol 58:2663-2666.

26. Chakraborty R, Coates JD. 2004. Anaerobic degradation of monoaromatic hydrocarbons. Appl Microbiol Biotechnol 64:437-446.

27. Jahn MK, Haderlein SB, Meckenstock RU. 2005. Anaerobic Degradation of Benzene, Toluene, Ethylbenzene, and *o*-Xylene in Sediment-Free Iron-Reducing Enrichment Cultures. Appl Environ Microbiol 71:3355-3358.

28. Lovley DR, Woodward JC, Chapelle FH. 1996. Rapid Anaerobic Benzene Oxidation with a Variety of Chelated Fe(III) Forms. Appl Environ Microbiol 62:288-291.

29. Tremblay P, Zhang T. 2020. Functional Genomics of Metal-Reducing Microbes Degrading Hydrocarbons. *In* Boll M (ed), Anaerobic Utilization of Hydrocarbons, Oils, and Lipids Handbook of Hydrocarbon and Lipid Microbiology doi:https://doi.org/10.1007/978-3-319-50391-2_13. Springer, Cham.

30. Atashgahi S, Hornung B, van der Waals MJ, da Rocha UN, Hugenholtz F, Nijsse B, Molenaar D, van Spanning R, Stams AJM, Gerritse J, Smidt H. 2018. A benzene-degrading nitrate-reducing microbial consortium displays aerobic and anaerobic benzene degradation pathways. Sci Rep 8:4490.

31. Coates JD, Chakraborty R, Lack JG, O'Connor SM, Cole KA, Bender KS, Achenbach LA. 2001. Anaerobic benzene oxidation coupled to nitrate reduction in pure culture by two strains of *Dechloromonas*. Nature 411:1039-1043.

32. Fahy A, Ball A, Lethbridge G, Timmis K, McGenity T. 2008. Isolation of alkali-tolerant benzene-degrading bacteria from a contaminated aquifer. Lett Appl Microbiol 47:60-66.

33. Koeksoy E, Halama M, Hagemann N, Weigold PR, Laufer K, Kleindienst S, Byrne JM, Sundman A, Hanselmann K, Halevy I. 2018. A case study for late Archean and Proterozoic biogeochemical iron-and sulphur cycling in a modern habitat—the Arvadi Spring. Geobiology 16:353-368.

34. Xiong W, Mathies C, Bradshaw K, Carlson T, Tang K, Wang Y. 2012. Benzene removal by a novel modification of enhanced anaerobic biostimulation. Water Res 46:4721-4731.

35. Fleming EJ, Cetinić I, Chan CS, King DW, Emerson D. 2014. Ecological succession among iron-oxidizing bacteria. ISME J 8:804.

36. McAllister SM, Vandzura R, Keffer JL, Polson SW, Chan CS. 2020. Aerobic and anaerobic iron oxidizers together drive denitrification and carbon cycling at marine iron-rich hydrothermal vents. ISME J doi:10.1038/s41396-020-00849-y.

37. Saul DJ, Aislabie JM, Brown CE, Harris L, Foght JM. 2005. Hydrocarbon contamination changes the bacterial diversity of soil from around Scott Base, Antarctica. FEMS Microbiol Ecol 53:141-155.

38. Zhao R, Summers ZM, Christman GD, Yoshimura KM, Biddle JF. 2020. Metagenomic views of microbial dynamics influenced by hydrocarbon seepage in sediments of the Gulf of Mexico. Sci Rep 10:5772.

39. Eze MO. 2021. Metagenome Analysis of a Hydrocarbon-Degrading Bacterial Consortium Reveals the Specific Roles of BTEX Biodegraders. Genes 12:98.

40. Sun X, Chu L, Mercando E, Romero I, Hollander D, Kostka JE. 2019. Dispersant Enhances Hydrocarbon Degradation and Alters the Structure of Metabolically Active

Microbial Communities in Shallow Seawater From the Northeastern Gulf of Mexico. Front Microbiol 10.

41. Kato S, Krepski S, Chan C, Itoh T, Ohkuma M. 2014. Ferriphaselus amnicola gen. nov., sp. nov., a neutrophilic, stalk-forming, iron-oxidizing bacterium isolated from an iron-rich groundwater seep. Int J Syst Evol Microbiol 64:921-925.

42. Weiss JV, Rentz JA, Plaia T, Neubauer SC, Merrill-Floyd M, Lilburn T, Bradburne C, Megonigal JP, Emerson D. 2007. Characterization of neutrophilic Fe (II)-oxidizing bacteria isolated from the rhizosphere of wetland plants and description of *Ferritrophicum radicicola* gen. nov. sp. nov., and *Sideroxydans paludicola* sp. nov. Geomicrobiol J 24:559-570.

43. Fabisch M, Beulig F, Akob DM, Küsel K. 2013. Surprising abundance of *Gallionella*-related iron oxidizers in creek sediments at pH 4.4 or at high heavy metal concentrations. Front Microbiol 4:390.

44. Fleming E, Woyke T, Donatello R, Kuypers MM, Sczyrba A, Littmann S, Emerson D. 2018. Insights into the fundamental physiology of the uncultured Fe-oxidizing bacterium *Leptothrix ochracea*. Appl Environ Microbiol 84:e02239-17.

45. Krepski ST, Hanson TE, Chan CS. 2012. Isolation and characterization of a novel biomineral stalk-forming iron-oxidizing bacterium from a circumneutral groundwater seep. Environ Microbiol 14:1671-1680.

46. Emerson D, Scott JJ, Benes J, Bowden WB. 2015. Microbial iron oxidation in the arctic tundra and its implications for biogeochemical cycling. Appl Environ Microbiol 81:8066-8075.

47. Gagen EJ, Levett A, Shuster J, Fortin D, Vasconcelos PM, Southam G. 2018. Microbial diversity in actively forming iron oxides from weathered banded iron formation systems. Microbes Environ 33:385-393.

48. Fahy A, McGenity TJ, Timmis KN, Ball AS. 2006. Heterogeneous aerobic benzene-degrading communities in oxygen-depleted groundwaters. FEMS Microbiol Ecol 58:260-270.

49. Hedrich S, Schlömann M, Johnson DB. 2011. The iron-oxidizing proteobacteria. Microbiology 157:1551-1564.

50. Li X, Zhang W, Liu T, Chen L, Chen P, Li F. 2016. Changes in the composition and diversity of microbial communities during anaerobic nitrate reduction and Fe(II) oxidation at circumneutral pH in paddy soil. Soil Biology and Biochemistry 94:70-79.

51. Wu Y, Zeng J, Zhu Q, Zhang Z, Lin X. 2017. pH is the primary determinant of the bacterial community structure in agricultural soils impacted by polycyclic aromatic hydrocarbon pollution. Sci Rep 7:40093.

52. Wilkins LGE, Ettinger CL, Jospin G, Eisen JA. 2019. Metagenome-assembled genomes provide new insight into the microbial diversity of two thermal pools in Kamchatka, Russia. Sci Rep 9:3059.

53. Yurchenko T, Ševčíková T, Přibyl P, El Karkouri K, Klimeš V, Amaral R, Zbránková V, Kim E, Raoult D, Santos LMA, Eliáš M. 2018. A gene transfer event suggests a long-term partnership between eustigmatophyte algae and a novel lineage of endosymbiotic bacteria. ISME J 12:2163-2175.

54. Luo X, Xiang X, Yang Y, Huang G, Fu K, Che R, Chen L. 2020. Seasonal effects of river flow on microbial community coalescence and diversity in a riverine network. FEMS Microbiol Ecol 96.

55. Valett HM, Dahm CN, Campana ME, Morrice JA, Baker MA, Fellows CS. 1997. Hydrologic Influences on Groundwater-Surface Water Ecotones: Heterogeneity in Nutrient Composition and Retention. Journal of the North American Benthological Society 16:239-247.

56. Narciso-Ortiz L, Vargas-García KA, Vázquez-Larios AL, Quiñones-Muñoz TA, Hernández-Martínez R, Lizardi-Jiménez MA. 2020. Coral reefs and watersheds of the Gulf of Mexico in Veracruz: Hydrocarbon pollution data and bioremediation proposal. Regional Studies in Marine Science 35:101155.

57. Warner B, Finke J, Gable R, Strobel J, Snyder A. 1984. EPA (Environmental Protection Agency) method study 25, method 602, purgeable aromatics. Report for Sep 79-Dec 82. Monsanto Co., Dayton, OH (USA),

58. Lovley DR, Phillips EJ. 1987. Rapid assay for microbially reducible ferric iron in aquatic sediments. Appl Environ Microbiol 53:1536-1540.

59. Parada AE, Needham DM, Fuhrman JA. 2016. Every base matters: assessing small subunit rRNA primers for marine microbiomes with mock communities, time series and global field samples. Environ Microbiol 18:1403-1414.

60. Walters W, Hyde ER, Berg-Lyons D, Ackermann G, Humphrey G, Parada A, Gilbert JA, Jansson JK, Caporaso JG, Fuhrman JA. 2016. Improved bacterial 16S rRNA gene (V4 and V4-5) and fungal internal transcribed spacer marker gene primers for microbial community surveys. mSystems 1:e00009-15.

61. Schloss PD, Westcott SL, Ryabin T, Hall JR, Hartmann M, Hollister EB, Lesniewski RA, Oakley BB, Parks DH, Robinson CJ. 2009. Introducing mothur: open-source, platform-independent, community-supported software for describing and comparing microbial communities. Appl Environ Microbiol 75:7537-7541.

62. Schloss PD, Gevers D, Westcott SL. 2011. Reducing the effects of PCR amplification and sequencing artifacts on 16S rRNA-based studies. PLoS One 6.

63. Kozich JJ, Westcott SL, Baxter NT, Highlander SK, Schloss PD. 2013. Development of a dual-index sequencing strategy and curation pipeline for analyzing amplicon sequence data on the MiSeq Illumina sequencing platform. Appl Environ Microbiol 79:5112-5120.

64. Quast C, Pruesse E, Yilmaz P, Gerken J, Schweer T, Yarza P, Peplies J, Glöckner FO. 2013. The SILVA ribosomal RNA gene database project: improved data processing and web-based tools. Nucleic Acids Res 41:D590-D596.

65. McMurdie PJ, Holmes S. 2013. phyloseq: an R package for reproducible interactive analysis and graphics of microbiome census data. PLoS One 8:e61217.

66. Lahti L, Shetty S, Blake T, Salojarvi J. 2017. Tools for microbiome analysis in R, v2.1.26. http://microbiome.github.com/microbiome.

67. Oksanen J, Guillame Blanchet F, Friendly M, Kindt R, Legendre P, McGlinn D, Minchin PR, O'Hara RB, Simpson GL, Solymos P, Stevens MHH, Szoecs E, Wagner H. 2019. vegan: Community Ecology Package. R package version 2.5-6., https://CRAN.R-project.org/package=vegan.

68. Kembel SW, Cowan PD, Helmus MR, Cornwell WK, Morlon H, Ackerly DD, Blomberg SP, Webb CO. 2010. Picante: R tools for integrating phylogenies and ecology. Bioinformatics 26:1463-1464.

69. Robinson MD, McCarthy DJ, Smyth GK. 2009. edgeR: a Bioconductor package for differential expression analysis of digital gene expression data. Bioinformatics 26:139-140.

70. McCarthy DJ, Chen Y, Smyth GK. 2012. Differential expression analysis of multifactor RNA-Seq experiments with respect to biological variation. Nucleic Acids Res 40:4288-4297.

71. Wickham H. 2016. ggplot2: Elegant Graphics for Data Analysis. Springer-Verlag New York.

72. Wickham H, Seidel D. 2020. scales: Scale Functions for Visualization, vR package version 1.1.1. https://CRAN.R-project.org/package=scales.

73. Chang W. 2013. R graphics cookbook. O'Reilly, Beijing.

74. Arnold JB. 2019. ggthemes: Extra Themes, Scales and Geoms for 'ggplot2', vR package version 4.2.0. https://CRAN.R-project.org/package=ggthemes.

75. Ichihara Y, Okabe M, Iga K, Tanaka Y, Musha K, Ito K. 2008. Color universal design: the selection of four easily distinguishable colors for all color vision types, vol 6807. SPIE.

76. Galore KFT. 2015. A wrapper tool around Cutadapt and FastQC to consistently apply quality and adapter trimming to FastQ files.

77. Andrews S. 2010. FastQC: a quality control tool for high throughput sequence data. Babraham Bioinformatics, Babraham Institute, Cambridge, United Kingdom.

78. Bankevich A, Nurk S, Antipov D, Gurevich AA, Dvorkin M, Kulikov AS, Lesin VM, Nikolenko SI, Pham S, Prjibelski AD. 2012. SPAdes: a new genome assembly algorithm and its applications to single-cell sequencing. J Comput Biol 19:455-477.

79. Gurevich A, Saveliev V, Vyahhi N, Tesler G. 2013. QUAST: quality assessment tool for genome assemblies. Bioinformatics 29:1072-1075.

80. Wu Y-W, Tang Y-H, Tringe SG, Simmons BA, Singer SW. 2014. MaxBin: an automated binning method to recover individual genomes from metagenomes using an expectation-maximization algorithm. Microbiome 2:26.

81. Alneberg J, Bjarnason BS, de Bruijn I, Schirmer M, Quick J, Ijaz UZ, Loman NJ, Andersson AF, Quince C. 2013. CONCOCT: clustering contigs on coverage and composition. arXiv preprint arXiv:13124038.

82. Kang DD, Li F, Kirton E, Thomas A, Egan R, An H, Wang Z. 2019. MetaBAT 2: an adaptive binning algorithm for robust and efficient genome reconstruction from metagenome assemblies. PeerJ 7:e7359.

83. SIEBER C. 2017. Dereplication, Aggregation and Scoring Tool (DAS Tool) v1. 0. Lawrence Berkeley National Lab.(LBNL), Berkeley, CA (United States),

84. Parks DH, Imelfort M, Skennerton CT, Hugenholtz P, Tyson GW. 2015. CheckM: assessing the quality of microbial genomes recovered from isolates, single cells, and metagenomes. Genome Res 25:1043-1055.

85. Neely CJ, Graham ED, Tully BJ. 2020. MetaSanity: an integrated microbial genome evaluation and annotation pipeline. Bioinformatics 36:4341-4344.

86. Aziz RK, Bartels D, Best AA, DeJongh M, Disz T, Edwards RA, Formsma K, Gerdes S, Glass EM, Kubal M. 2008. The RAST Server: rapid annotations using subsystems technology. BMC Genomics 9:1-15.

87. Overbeek R, Olson R, Pusch GD, Olsen GJ, Davis JJ, Disz T, Edwards RA, Gerdes S, Parrello B, Shukla M. 2014. The SEED and the Rapid Annotation of microbial genomes using Subsystems Technology (RAST). Nucleic Acids Res 42:D206-D214.

88. Brettin T, Davis JJ, Disz T, Edwards RA, Gerdes S, Olsen GJ, Olson R, Overbeek R, Parrello B, Pusch GD. 2015. RASTtk: a modular and extensible implementation of the RAST algorithm for building custom annotation pipelines and annotating batches of genomes. Sci Rep 5:8365.

89. Gihawi A, Rallapalli G, Hurst R, Cooper CS, Leggett RM, Brewer DS. 2019. SEPATH: benchmarking the search for pathogens in human tissue whole genome sequence data leads to template pipelines. Genome Biol 20:1-15.

90. Seemann T. 2014. Prokka: rapid prokaryotic genome annotation. Bioinformatics 30:2068-2069.

91. Boutet E, Lieberherr D, Tognolli M, Schneider M, Bairoch A. 2007. Uniprotkb/swiss-prot, p 89-112, Plant bioinformatics. Springer.

92. Schaedler F, Lockwood C, Lueder U, Glombitza C, Kappler A, Schmidt C. 2018. Microbially mediated coupling of Fe and N cycles by nitrate-reducing Fe (II)-oxidizing bacteria in littoral freshwater sediments. Appl Environ Microbiol 84:e02013-17.

93. Steinegger M, Söding J. 2017. MMseqs2 enables sensitive protein sequence searching for the analysis of massive data sets. Nat Biotechnol 35:1026-1028.

94. Sievers F, Wilm A, Dineen D, Gibson TJ, Karplus K, Li W, Lopez R, McWilliam H, Remmert M, Söding J. 2011. Fast, scalable generation of high-quality protein multiple sequence alignments using Clustal Omega. Mol Syst Biol 7:539.

95. Sievers F, Higgins DG. 2018. Clustal Omega for making accurate alignments of many protein sequences. Protein Sci 27:135-145.

96. Eddy SR. 1998. Profile hidden Markov models. Bioinformatics (Oxford, England) 14:755-763.

97. Woodcroft BJ, Boyd JA, Tyson GW. 2016. OrfM: a fast open reading frame predictor for metagenomic data. Bioinformatics (Oxford, England) 32:2702-2703.

98. Garber AI, Nealson KH, Okamoto A, McAllister SM, Chan CS, Barco RA, Merino N. 2020. FeGenie: A Comprehensive Tool for the Identification of Iron Genes and Iron Gene Neighborhoods in Genome and Metagenome Assemblies. Front Microbiol 11.

99. Hyatt D, Chen G-L, LoCascio PF, Land ML, Larimer FW, Hauser LJ. 2010. Prodigal: prokaryotic gene recognition and translation initiation site identification. BMC Bioinformatics 11:119.

100. Kassambara A. 2020. ggpubr: 'ggplot2' Based Publication Ready Plots, vR package version 0.4.0. https://CRAN.R-project.org/package=ggpubr.

101. Wickham H. 2007. Reshaping Data with the reshape Package. 2007 21:20.

102. Nowosad J. 2018. 'CARTOColors' Palettes, vR package version 2.0.0. https://nowosad.github.io/rcartocolor.

103. Humphrey C, Blackmon J, Kelley T, Driscoll M, Iverson G. 2018. Environmental health threats associated with drainage from a coastal urban watershed. Environmental Natural Resources Research 8:52-60.

Figures

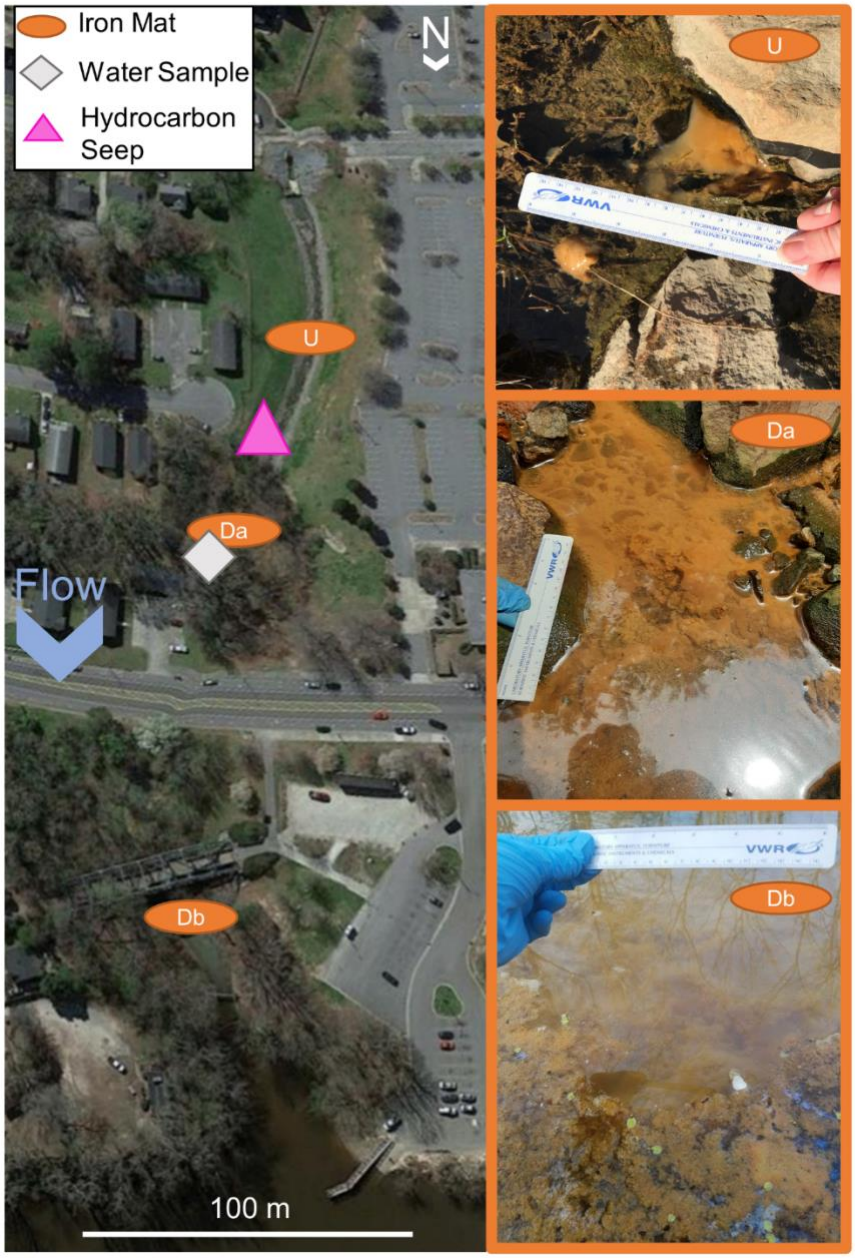

Figure 2.1: A map of Town Creek, Greenville, NC. Iron mat sampling locations indicated with orange ovals labeled with iron mat location ID: Upstream (U) unexposed, Downstream A (Da) benzene-exposed, or Downstream B (Db) benzene-exposed. The water sampling site (W) benzene-exposed is indicated by a grey diamond and was chosen so as to be as far across the

creek cross-section from iron mat sample as possible to avoid confounding results. The hydrocarbon seeps are indicated by the pink triangle. Seep location based on Humphrey et al. (103). Map obtained from Google Earth Pro v. 7.3.3.7786 and modified with iron mat, benzene seep, and water sample locations and inset images.

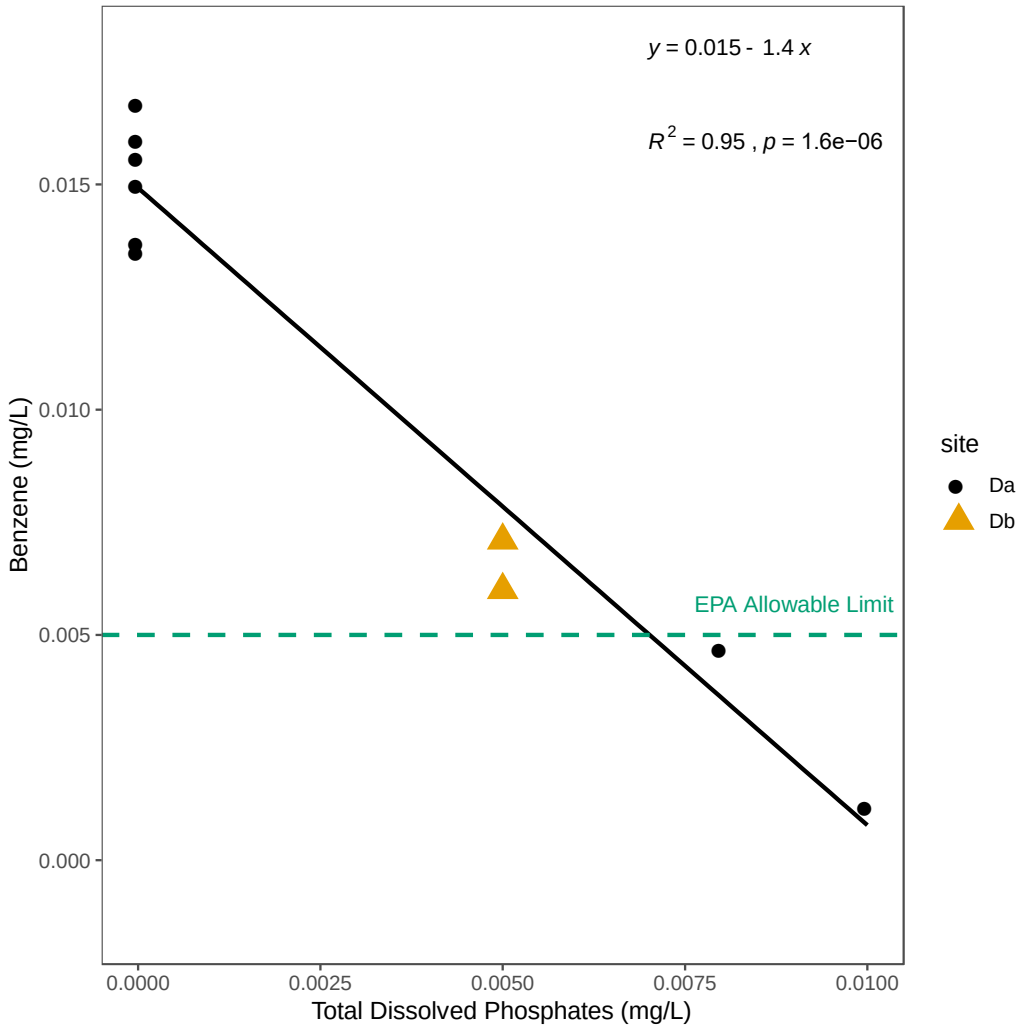

Figure 2.2: Total dissolved phosphates (mg/L) from filtered samples and benzene concentrations (mg/L) from the downstream iron mats, Da (black circle) and Db (yellow triangle). The EPA allowable limit for benzene (0.005 mg/L) is designated by a green-dashed line. Db was only measured during the first two time points (S1 and S2). Phosphate and benzene concentrations in the downstream mats have a significant negative correlation ($R^2 = 0.95$, $p = 1.6e^{-6}$), which was stronger than the correlation in the water sample (W) reference (not shown; $R^2 = 0.58$, $p = 0.028$). This correlation indicates an as-yet undefined antagonistic effect between phosphate and benzene in the iron mat system.

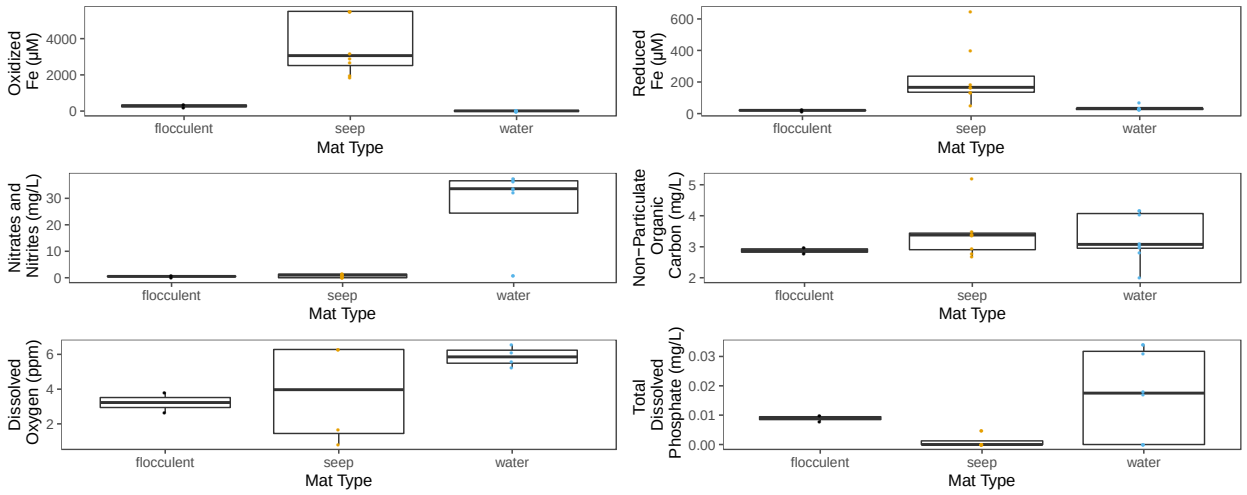

Figure 2.3: Concentrations of analytes in downstream, benzene-exposed iron mats by mat type. Iron mats were designated to a mat type, either flocculent (black) or seep (yellow) as previously defined by Fleming et al. (35) the flocculent mats were in looser association and centimeters thick, whereas seep mats were denser and millimeters thick. Mat types are plotted here compared to the reference water sample (blue) for concentration of oxidized iron, reduced iron, nitrates and nitrites, non-particulate organic carbon, dissolved oxygen, and total dissolved phosphate. Only two of the sampled iron mats were classifiable as flocculent and both were sampled in the spring. Flocculent mats were high in non-particulate organic carbon, dissolved oxygen, and phosphate compared to seep mats. Seep mats were higher in both oxidized and reduced iron. Both mat types had a much lower concentration of nitrates and nitrites than the downstream water sample.

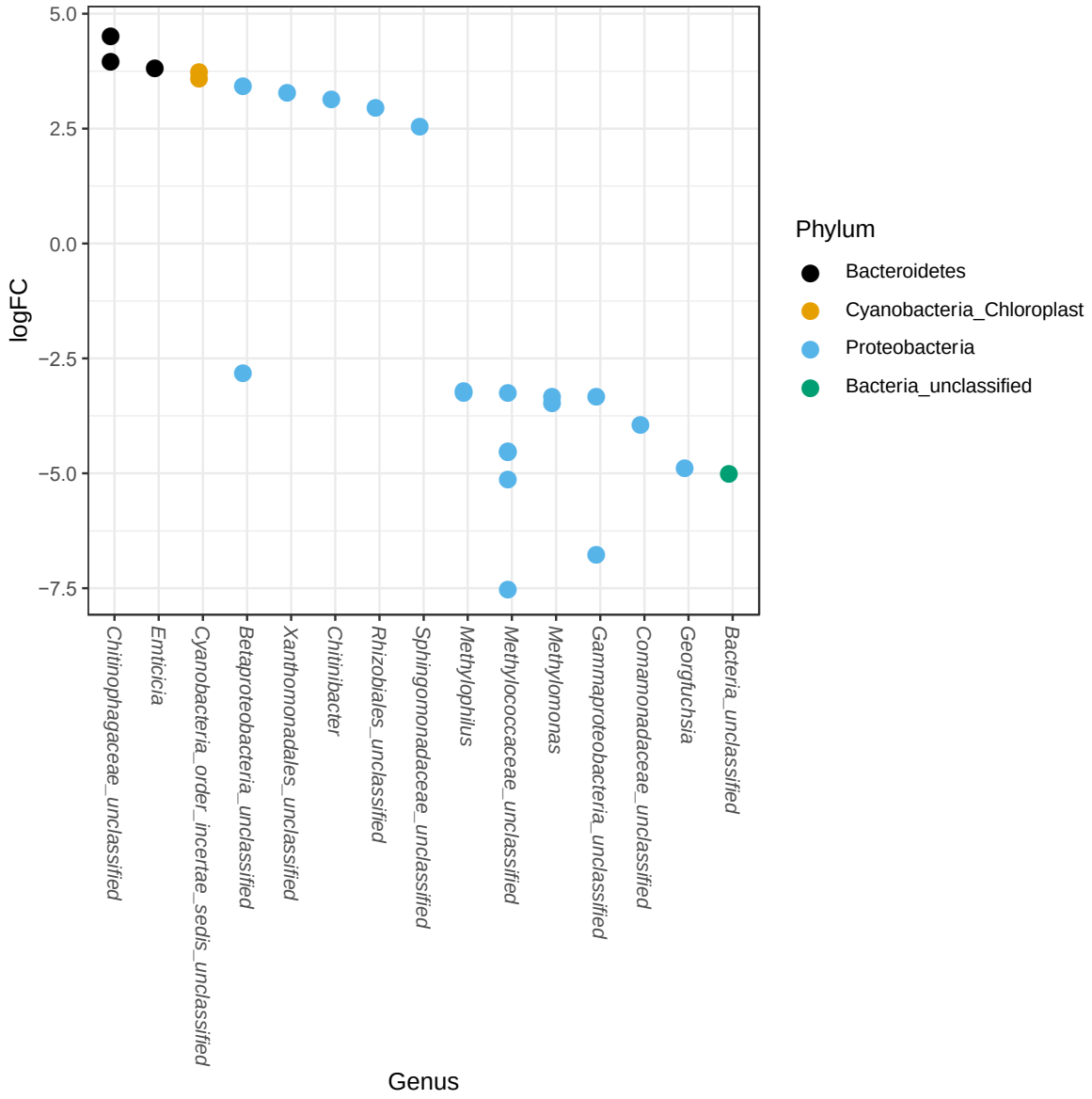

Figure 2.4: Differential abundances of taxa between upstream and downstream mats were calculated from an independently filtered data set. Genera with differential abundances with an alpha < 0.05 were plotted. Each point on the plot represents a single OTU sequence. Points with a log Fold Change greater than zero are under-expressed in the downstream iron mat communities, whereas points with a log-fold change less than 0 are over-expressed in downstream communities relative to upstream communities. The largest fold-changes were in OTUs downstream and were observed in the highly represented taxa, Proteobacteria.

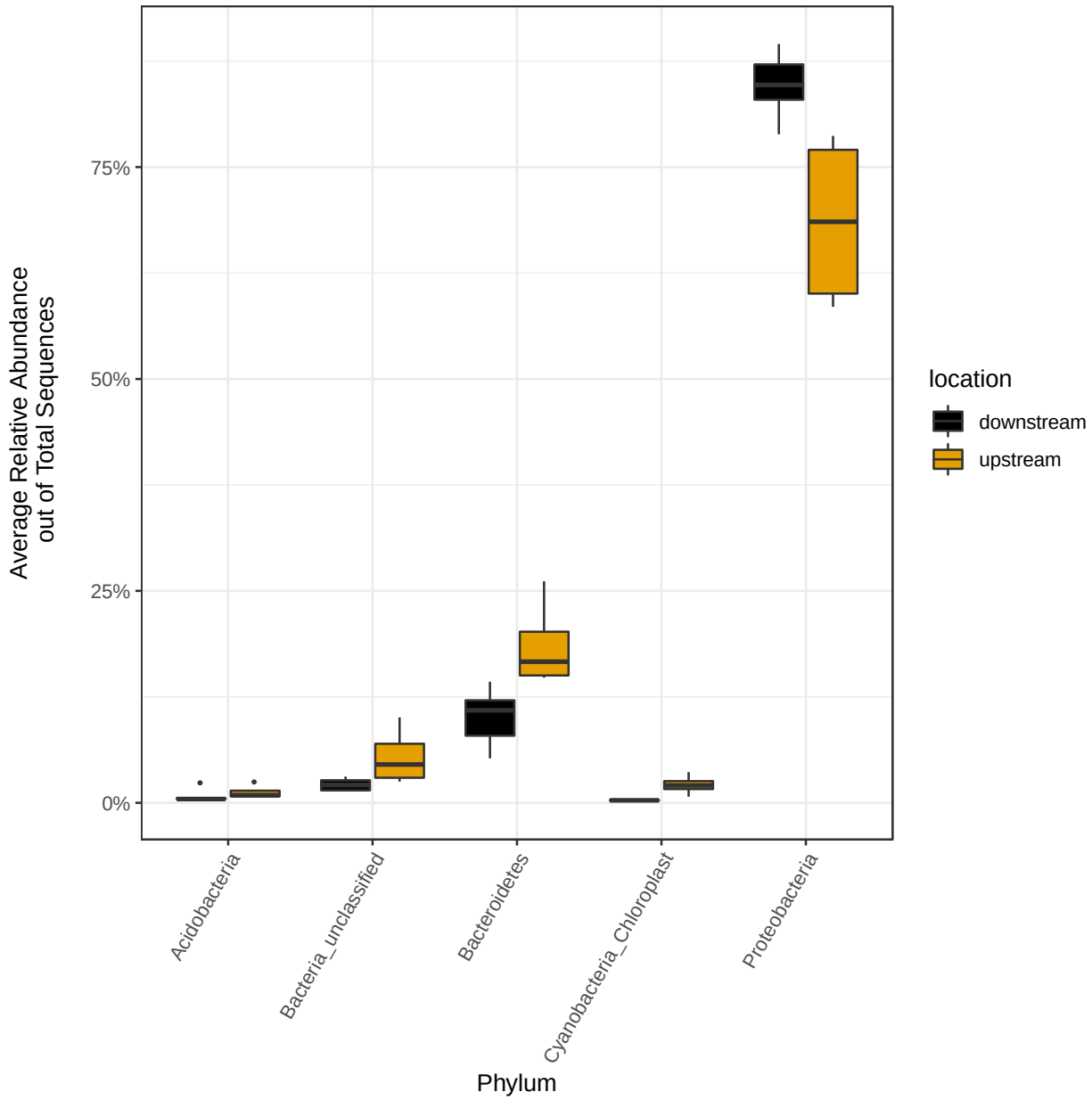

Figure 2.5: Relative abundances of phyla greater than two percent were calculated out of total sequences for each sample and averaged by location (up- or downstream). Averages for present phyla are presented in yellow (upstream) or black (downstream). The average relative abundance of all phyla except Proteobacteria are greater in upstream samples. The increased relative abundance of Proteobacteria in the downstream iron mats reflects the decreased overall diversity.

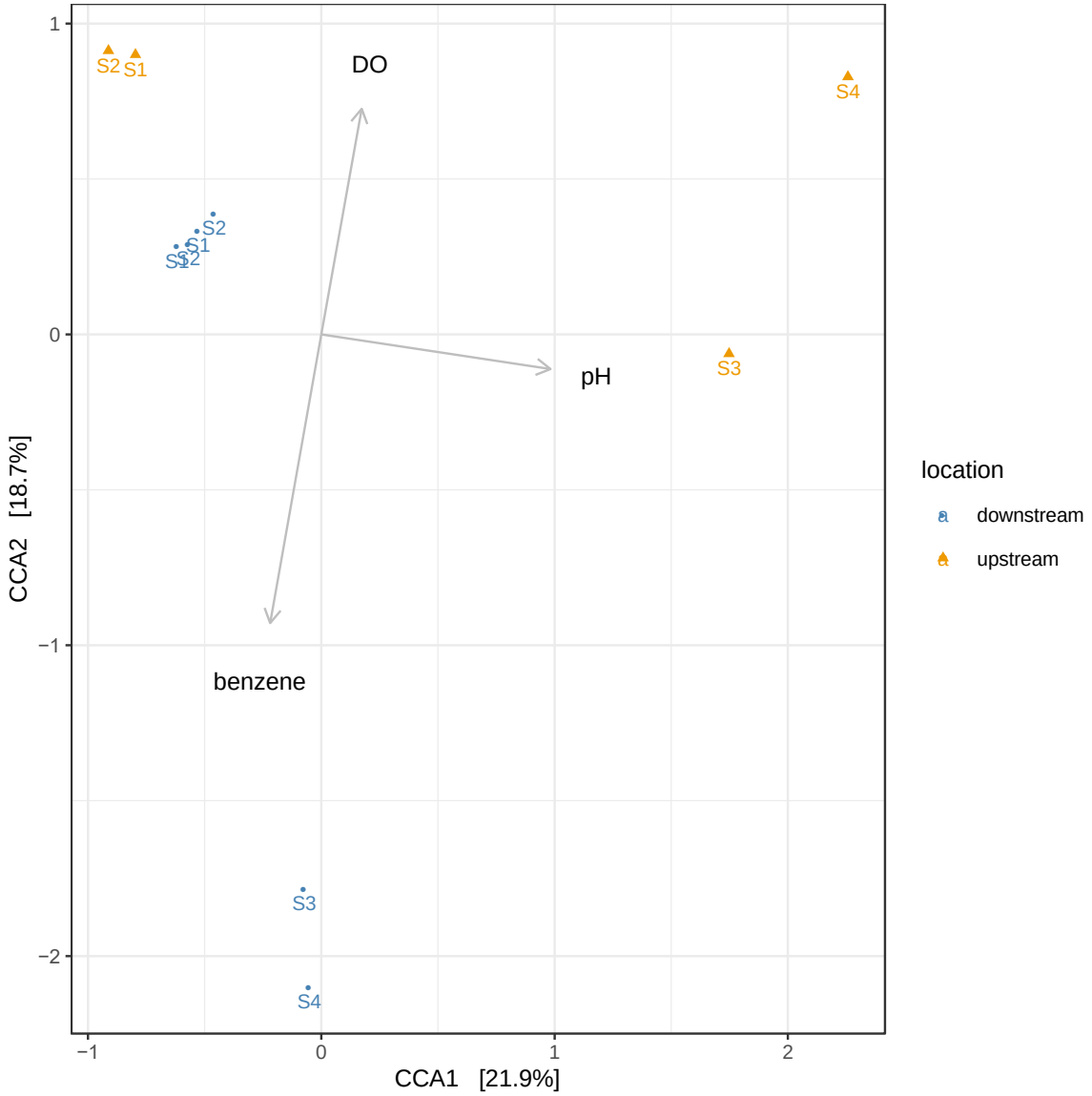

Figure 2.6: A canonical correspondence analysis (CCA) was used to calculate eigenvalues for the environmental conditions of iron mats. The overall model presented above is a good fit of the data (PERMANOVA F = 1.95, p = 0.002) and the variance inflation factor for each explanatory term is less than 3. Results indicate that the greatest effect on microbial community structure is from DO, followed by pH then benzene concentration. Sampling efforts (1-4) are labeled on each point.

Chapter 3: Orange leads to black: Evaluating the efficacy of co-culturing iron-oxidizing and sulfate-reducing bacteria to discern ecological relationships

Authors: Chequita N. Brooks and Erin K. Field

Citation: Brooks CN, Field EK. 2021. Orange leads to black: evaluating the efficacy of co-culturing iron-oxidizing and sulfate-reducing bacteria to discern ecological relationships. Environmental Microbiology Reports.

Originality-Significance Statement

This study has developed a novel technique for co-culturing iron-oxidizing bacteria and sulfate-reducing bacteria from the same source inocula. It is the first time, to the author's knowledge, that these two functional groups have been cultured together in a controlled media environment. The successful modification of agarose-stabilized gradient tubes for the co-culture of these biogeochemically important groups allowed us to further explore potential relationships between them that could have applications for studying their interactions as they relate not only to biogeochemical cycling, but to microbially influenced corrosion.

Summary

Two global cycles, iron and sulfur, are critically interconnected in estuarine environments by microbiological actors. To this point, the methods of laboratory study of this interaction have been limited. Here we propose a methodology for co-culturing from numerous coastal environments, from the same source inocula, iron-oxidizing and sulfate-reducing bacteria. The use of same source inocula is largely beneficial to understanding real-world interactions that are likely occurring *in situ*. Through the use of this methodology the ecological interactions between these groups can be studied in a more controlled environment. Here, we characterize the oxygen and hydrogen sulfide concentrations using microelectrode depth profiling in the co-cultures of iron-oxidizing bacteria and sulfate-reducing bacteria. These results suggest that while oxygen drives the relationship between these organisms and sulfate-reducers are reliant on iron-oxidizers in this culture to create an anoxic environment, there is likely another environmental driver that also influences the interaction as the two remain spatially distinct, as trends in FeS precipitation changed within the anoxic zone relative to the presence of Fe(III) oxyhydroxides. Understanding

the relationship between iron-oxidizing and sulfate-reducing bacteria will ultimately have implications for understanding microbial cycling in estuarine environments as well as in processes such as controlling microbially influenced corrosion.

Introduction

Estuaries are important hot spots of nutrient cycling, water purification, and carbon sequestration (Barbier et al., 2011). Trace nutrients, such as biologically available iron (Fe(II)), also fluctuate in availability, owing to the dynamic nature of estuarine water tables (Williams et al., 1994). Similarly, a fluctuating tide has implications for the oxic-anoxic boundary in the water column or sediment and creates a reliance on anoxic microenvironments in anaerobic bacteria (Murray et al., 1989; Hines, 2006; Field et al., 2016). Two of the major cycles in estuaries are the iron and sulfur cycles, which are both sensitive to these environmental fluctuations, as well as the actions of microorganisms.

Microaerophilic iron-oxidizing bacteria (FeOB) are prevalent in these fresh to saltwater transition zones (Erbs and Spain, 2002; McBeth et al., 2013; MacDonald et al., 2014b; Field et al., 2016; McBeth and Emerson, 2016; Garrison et al., 2019) and are found in a variety of environments such as plant rhizospheres and soils (Neubauer et al., 2002), freshwater catchments (Lin et al., 2012), sediments (Sobolev and Roden, 2004), microbial mats (Chan et al., 2016), living planktonically in water columns (Field et al., 2016; Chiu et al., 2017), and have been associated with biocorrosion (Emerson, 2018). FeOB likely play key roles in organic carbon consumption (Laufer et al., 2016a) and in nutrient cycling, as the iron-oxides produced can impact phosphorous dynamics by reducing bioavailability and mobility through adsorption (Pan et al., 2019) in estuaries. FeOB are also players in microbially influenced corrosion, where their

role is to serve as an ecosystem engineers on mild steel (Emerson, 2018). Mild steels are used in estuarine environments for various infrastructure, making replacing steels that fall prey to microbial influenced corrosion a costly endeavor (Little and Lee, 2007).

FeOB have been hypothesized to interact, either directly or indirectly, with a variety of functional guilds including iron-reducing, sulfur-oxidizing, and methanogenic bacteria (Melton et al., 2014). Potential symbioses have also been proposed between FeOB and oxygenic phototrophs (Field et al., 2016) as well as between FeOB and sulfate-reducing bacteria (SRB) (Li et al., 2006; Bruun et al., 2010; McBeth et al., 2013; Mumford et al., 2016; Koeksoy et al., 2018). A symbiotic relationship between FeOB and other functional guilds could have important implications for biogeochemical cycling in coastal environments. An important step in understanding the impacts these microbes have on cycling, is studying these relationships in microbial lab cultures.

In the instance of FeOB and SRB, a potential symbiosis could provide resource stability to each group in these dynamic environments. Resources may be recycled amongst the FeOB and SRB through the O_2-Fe-H_2S catalytic cycle (Morse et al., 1987; Ma et al., 2006; Findlay et al., 2014; MacDonald et al., 2014a; MacDonald et al., 2014b). FeOB oxidize Fe(II) to Fe(III) and SRB reduce SO_4^{2-} to H_2S. Fe(III) and H_2S chemically react to produce Fe(II) and SO_4^{2-}, thus recycling the necessary nutrients. FeOB would be essential to these reactions, as the oxidation of Fe(II) to Fe(III) has been observed as the rate limiting step in estuarine environments (Ma et al., 2006). The oxidation of H_2S is greatly rate-limited without present metals where it has been measured at approximately one day (Millero et al., 1987; Vazquez et al., 1989), whereas in the presence of $Fe(OH)_3$ the oxidation of H_2S has been measured at approximately 30 minutes (Pyzik and Sommer, 1981). FeOB have also been suggested to be primary colonizers in instances

of biocorrosion, creating niche spaces that allow SRB to subsequently exploit carbon and stainless steels (McBeth and Emerson, 2016; Garrison et al., 2019). This synergy has been observed to increase the severity of pitting on these steels (Lv et al., 2019). As our understanding of the niche spaces inhabited by FeOB expands, the question of active growth maintenance during periods of low Fe(II) remains.

The microaerophilic FeOB live at the oxic-anoxic boundary in the water column or in the sediment, where oxygen concentrations are as low as 2-3 µM (Druschel et al., 2008; Busigny et al., 2014; MacDonald et al., 2014b; Chan et al., 2016). The oxygen conditions where FeOB are active can vary as in Chan et al. (2016) where the observed O_2 concentrations varied from 21-99.3 µM at the surface of freshwater and marine iron mats, where active FeOB were at the leading edge. Comparatively, the atmosphere is approximately 21% O_2. The solubility of O_2 in estuarine waters at 25ºC and atmospheric pressure, ranges from approximately 250.7-217.4 µM (Ramsing and Gundersen, 1994). Traditional culturing methods for microaerophilic FeOB rely on setting up specific oxygen conditions in the culture headspace that undergoes no further active maintenance representing static conditions including the agarose-stabilized gradient tube method (Emerson and Floyd, 2005; Saini and Chan, 2013; Barco and Edwards, 2014; Lueder et al., 2017). These culturing methods are intended to create a gradient of low oxygen concentrations in the culture media and is assisted, as in the study of Krepski et al. (2013) where the media was exposed to an atmospheric headspace, by the reducing properties of the Fe(II) at the bottom of the media. The chosen headspace has varied in studies of microaerophilic FeOB between an atmospheric gas mix (Emerson and Moyer, 1997; Emerson and Floyd, 2005; Lin et al., 2012; Laufer et al., 2016b) or a gaseous mix of $N_2/CO_2/O_2$ where oxygen was 1% (Kato et al., 2014; Field et al., 2016; Chiu et al., 2017). Using a gaseous headspace mix with a lower oxygen

concentration new FeOB were isolated (Field et al., 2016; Chiu et al., 2017). SRB, on the other hand, are usually strictly anaerobic. Therefore, any gradient of oxygen is less than ideal for culturing these organisms. In order to elucidate the relationship between FeOB and SRB they first must be cultured together. Here we present a method of co-culturing FeOB and SRB from estuarine environments using a headspace maintenance method that alters oxygen concentrations during culturing and provide a framework for studying the relationship between these two functional guilds of bacteria in the laboratory.

Results & Discussion

Development of a novel co-culture method for iron-oxidizing and sulfate-reducing bacteria

Samples from two estuarine sites, Cedar Island (35.024974, -76.327171) and Fisher's Landing (35.012718, -76.980697), NC (Fig. S3.1), were used as inoculum for co-culture growth trials. While both sites are estuarine in nature, the salinities at each site differ in that Fisher's Landing is oligohaline (0.5-5 ppt) and Cedar Island is mesohaline (5-18 ppt) to polyhaline (18-30 ppt). The trials were carried out in both 0 ppt Modified Wolfe's Mineral Media (Emerson and Floyd, 2005) and 18 ppt Estuary Media (Field et al., 2016). These salinities were chosen for testing as Fisher's Landing has a very low average salinity, whereas Cedar Island is considerably more saline. After a second week of incubation tubes were assessed for the presence of orange precipitates (FeOB; poorly soluble Fe(III) oxyhydroxides) and black precipitates (SRB; likely Fe(II) Sulfides (FeS)) (Fig. 3.1) and microbial growth from each visibly different layer was confirmed via fluorescence microscopy by sampling 10 µL from each layer (Fig. S3.2). Because discrete layers were often narrow, multiple sampling from the same tube was infeasible. As this methodology application appears to successfully observe FeS production modulated by SRB

presence, it likely also has useful application in furthering the understanding of SRB influence on mackinawite and greigite minerals, which has been previously demonstrated (Picard et al., 2018; Thiel et al., 2019).

Incubating one week under a 1% O_2 mix followed by one week under an atmospheric headspace was found to be a consistent and reliable method of culturing FeOB and SRB from the same sample (Table 3.1). The appearance of the orange precipitate always preceded the black precipitate by one week (i.e., the black precipitate only developed after the headspace change) and no SRB grew in gradient tubes that did not have FeOB growth. Notably, while none of our samples were isolates (Fig. S3.3) and bacteria with unique cellular morphologies were observed in the precipitate-free zone of the gradient tubes (Fig. S3.2), the presence of heterotrophic organisms alone does not seem to be sufficient in creating an appropriate environment for the SRB in the gradient tube, as evidenced by the absence of SRB in tubes also lacking FeOB. Similarly, it seems unlikely that organisms such as iron-reducing bacteria were responsible for the precipitate-free zone, as they have previously been observed not to compete with SRB (Bruun et al., 2010), and therefore should not have affected the production of the FeS precipitate. This work, however, only lays the groundwork for more direct studies of isolated FeOB and SRB using this culture method.

We hypothesize this result reflects an establishment effect, where the FeOB were able to both multiply and create an iron-oxide structure prior to the introduction of a greater concentration of oxygen. As FeOB must compete with the abiotic oxidation of Fe(II) (Emerson and Revsbech, 1994; Edwards et al., 2004; James and Ferris, 2004; Ferris, 2005), greater numbers of active FeOB would increase their capacity for oxygen consumption and provide a microenvironment for out-competition of abiotic iron oxidation. The increased rate of Fe(II)

oxidation in the presence of FeOB (James and Ferris, 2004) likely then leads to a more favorably anoxic environment for SRB growth. This technique has proven successful for these estuarine environments and sample types, meriting broadened testing. A gradient tube method may not be an effective method for culturing SRB from environments where microaerophilic FeOB are not present (e.g., strictly anaerobic). However, we were able to propagate cultures from all four sampling sites suggesting that, after initial inoculation, SRB cultures could be isolated from FeOB, whose absence was confirmed using 16S rDNA (Fig. S3.3), following dilution-to-extinction culturing methods. Thus, for the successful co-culture and eventual isolation of both FeOB and SRB from environmental samples, the gradient tube method can be applied utilizing the dynamic headspace technique presented here. Through the application of this technique, strides may be made in the study of these two organisms in their roles in both microbially influenced corrosion and connecting two major biogeochemical cycles.

Measuring Gradient Dynamics in Oxygen and Hydrogen Sulfide

The FeOB were able to grow to the surface of the semi-solid top layer which never exceeded 350 µM O_2 (Fig. 3.2), and growth was restricted to oxic environments in the gradient tube (Fig. 3.2-B, D, Fig. S3.4-D). H_2S profiles from gradient tubes that were an abiotic control (no inocula) or FeOB only (no SRB) had a consistent H_2S profile of approximately 10 µM throughout the depth of the gradient tube, which we interpret as an artifact of the detection limit of the microelectrode (Fig. 3.2-A, B, Fig. S3.4-A, B). This provided the baseline for the interpretation of SRB cultures as well as FeOB and SRB co-culture. These samples showed an increasing, then decreasing trend in H_2S concentrations, peaking around 20-25 mm in depth (Fig. 3.2-C, D, Fig. S3.4-C, D). This trend suggested that SRB are actively metabolizing SO_4^{2-} to H_2S

in the gradient tubes, and that this activity was restricted below the oxic-anoxic boundary, defined by where the O_2 concentrations fell beneath the detection limit, again confirming an anaerobic metabolism.

Despite the O_2 gradients following a similar pattern in SRB cultures and co-cultures, the FeS produced as a function of the presence of SRB was never observed within the 5 mm anoxic precipitate-free zone (i.e. lacking FeS or Fe(III)) beneath the Fe(III) band. This pattern did not appear to reflect a shift in the available niche space for formation of Fe(III) oxyhydroxides by FeOB, rather in FeS production as a result of the SRB presence. In cultures without FeOB, FeS precipitated up to the anoxic boundary (Fig. 3.2-C, S3.4-C). However, when FeOB were present and forming Fe(III) oxyhydroxides, FeS was observed approximately 5 mm below the anoxic boundary (Fig. 3.2-D, S3.4-D). As it has been previously observed that the presence of SRB cells (either live or dead) increased concentrations of FeS minerals, this indicates that it is likely that SRB cells were not present within the precipitate-free zone in either culture. While our spatial resolution in this study was low, we argue that these measurements are still useful in hypothesis generation in regard to the patterning of growth as it was observed consistently. One potential hypothesis is that there may be a secondary metabolite or oxidative-reductive-potential difference in the tubes containing co-cultures that is altering the growth pattern of SRB. Alternatively, as our samples were mixed cultures, it is possible that another microorganism was otherwise sequestering the poorly crystalline FeS prior to diffusion to the anoxic boundary and Fe(III) oxyhydroxide band. Further characterization with increased spatial resolution, as well as further analyses of oxidative-reductive potential, in this precipitate-free zone will likely lead to a further understanding of the potential relationship between FeOB and SRB, which could assist in efforts to inhibit the growth of SRB and FeOB on steel surfaces in estuarine environments (Li et

al., 2019) or in manipulating microbial communities to take advantage of protective microbial action, known as microbially influenced corrosion inhibition (Ma et al., 2020).

Conclusion

The co-occurrence of FeOB and SRB, as was demonstrated here from various estuarine samples, has led to the suggestion that these organisms may potentially interact within their micro-environments (Li et al., 2006; Bruun et al., 2010; McBeth et al., 2013; Mumford et al., 2016). Such an interaction would have large implications for iron and sulfur cycling and microbially influenced corrosion. Our technique leverages the use of changes in the oxygen environment in the headspace of gradient tubes, providing a more dynamic environment which encourages the secondary formation of a SRB niche. We present the foundations for how we may elucidate the relationship between the FeOB and SRB in culture by characterizing the co-culture environment. The results from our initial characterization suggests that the co-culture dynamics between FeOB and SRB is not driven solely by O_2 but may be due to an as-yet unmeasured metabolite or culture condition that leads to the formation of these microniches.

Here, we present a methodology for successfully culturing both FeOB and SRB from the same environmental sample. Using the agarose-stabilized gradient tube method (Emerson and Floyd, 2005) the co-culture of FeOB and SRB will have improved success in media closely resembling the sampling site salinity. We recommend the use of either Modified Wolfe's Mineral Media (0ppt), Estuary Media (18 ppt), or Artificial Sea Water Media (34 ppt) (Emerson and Floyd, 2005; Field et al., 2016) depending on the salinity of the sampling site. However, the observed decoupling under salinity stress presents possible other avenues of further research. The headspace of the gradient tubes should be modified from a 1% O_2 mix to atmospheric

oxygen once a solid band of Fe(III) oxyhydroxides has precipitated. While our study did not focus on the relationship between isolated representatives from the FeOB and SRB groups, we recommend further studies consider the use of presently isolated cultures to implement these techniques. Isolates of SRB may also be easier to generate using a modified media in the gradient tubes with increased concentrations of SO_4^{2-}, as this would likely increase the replication rate of these organisms over that of heterotrophs for greater success with dilutions-to-extinction. FeOB can also be isolated using liquid plate media, which can be employed only after the initial culture from sediment if one aims to co-isolate FeOB and SRB from the same source. However, not all FeOB can utilize all reduced iron media additives (e.g., zero valent iron, FeS, $FeCl_2$) and it may be necessary to employ a series of dilutions-to-extinction for both the FeOB and SRB. As studies of these biogeochemically important functional guilds continue, we anticipate that these results will set the stage for further discovery by providing a baseline for hypothesis generation and a method for co-culture enrichments, aiding in our understanding of real-world issues such as that of microbially influenced corrosion and nutrient cycling.

Acknowledgements

This work was supported by funding from the ECU Coastal Maritime Council. Thanks to the staff at Unisense, Denmark, for their assistance and teaching on microsensor profiling. Thanks to Dr. Cassandra Marnocha for providing comments that improved this manuscript. The authors declare no conflict of interest.

References

Barbier, E.B., Hacker, S.D., Kennedy, C., Koch, E.W., Stier, A.C., and Silliman, B.R. (2011) The value of estuarine and coastal ecosystem services. *Ecol Monogr* **81**: 169-193.

Barco, R.A., and Edwards, K.J. (2014) Interactions of proteins with biogenic iron oxyhydroxides and a new culturing technique to increase biomass yields of neutrophilic, iron-oxidizing bacteria. *Front Microbiol* **5**: 259.

Bruun, A.-M., Finster, K., Gunnlaugsson, H.P., Nørnberg, P., and Friedrich, M.W. (2010) A comprehensive investigation on iron cycling in a freshwater seep including microscopy, cultivation and molecular community analysis. *Geomicrobiol J* **27**: 15-34.

Busigny, V., Planavsky, N.J., Jézéquel, D., Crowe, S., Louvat, P., Moureau, J. et al. (2014) Iron isotopes in an Archean ocean analogue. *Geochim Cosmochim Acta* **133**: 443-462.

Chan, C.S., McAllister, S.M., Leavitt, A.H., Glazer, B.T., Krepski, S.T., and Emerson, D. (2016) The architecture of iron microbial mats reflects the adaptation of chemolithotrophic iron oxidation in freshwater and marine environments. *Front Microbiol* **7**: 796.

Chiu, B.K., Kato, S., McAllister, S.M., Field, E.K., and Chan, C.S. (2017) Novel pelagic iron-oxidizing Zetaproteobacteria from the Chesapeake Bay oxic–anoxic transition zone. *Front Microbiol* **8**: 1280.

Druschel, G.K., Emerson, D., Sutka, R., Suchecki, P., and Luther III, G.W. (2008) Low-oxygen and chemical kinetic constraints on the geochemical niche of neutrophilic iron (II) oxidizing microorganisms. *Geochim Cosmochim Acta* **72**: 3358-3370.

Edwards, K.J., Bach, W., McCollom, T.M., and Rogers, D.R. (2004) Neutrophilic iron-oxidizing bacteria in the ocean: their habitats, diversity, and roles in mineral deposition, rock alteration, and biomass production in the deep-sea. *Geomicrobiol J* **21**: 393-404.

Emerson, D. (2018) The role of iron-oxidizing bacteria in biocorrosion: a review. *Biofouling* **34**: 989-1000.

Emerson, D., and Revsbech, N.P. (1994) Investigation of an iron-oxidizing microbial mat community located near Aarhus, Denmark: field studies. *Appl Environ Microbiol* **60**: 4022-4031.

Emerson, D., and Moyer, C. (1997) Isolation and characterization of novel iron-oxidizing bacteria that grow at circumneutral pH. *Appl Environ Microbiol* **63**: 4784-4792.

Emerson, D., and Floyd, M.M. (2005) Enrichment and isolation of iron-oxidizing bacteria at neutral pH. *Methods Enzymol* **397**: 112-123.

Erbs, M., and Spain, J. (2002) Microbial iron metabolism in natural environments. *Microbial Diversity*: 1-19.

Ferris, F. (2005) Biogeochemical properties of bacteriogenic iron oxides. *Geomicrobiol J* **22**: 79-85.

Field, E., Kato, S., Findlay, A., MacDonald, D., Chiu, B., Luther III, G., and Chan, C. (2016) Planktonic marine iron oxidizers drive iron mineralization under low-oxygen conditions. *Geobiology* **14**: 499-508.

Findlay, A.J., Gartman, A., MacDonald, D.J., Hanson, T.E., Shaw, T.J., and Luther III, G.W. (2014) Distribution and size fractionation of elemental sulfur in aqueous environments: The Chesapeake Bay and Mid-Atlantic Ridge. *Geochim Cosmochim Acta* **142**: 334-348.

Garrison, C.E., Price, K.A., and Field, E.K. (2019) Environmental Evidence and Genomic Insight of Iron-oxidizing Bacteria Preference Towards More Corrosion Resistant Stainless Steel at Higher Salinities. *Appl Environ Microbiol*: AEM. 00483-00419.

Hines, M.E. (2006) Microbially mediated redox cycling at the oxic–anoxic boundary in sediments: comparison of animal and plants habitats. *Water, Air, & Soil Pollution: Focus* **6**: 523-536.

James, R., and Ferris, F. (2004) Evidence for microbial-mediated iron oxidation at a neutrophilic groundwater spring. *Chem Geol* **212**: 301-311.

Kato, S., Krepski, S., Chan, C., Itoh, T., and Ohkuma, M. (2014) Ferriphaselus amnicola gen. nov., sp. nov., a neutrophilic, stalk-forming, iron-oxidizing bacterium isolated from an iron-rich groundwater seep. *Int J Syst Evol Microbiol* **64**: 921-925.

Koeksoy, E., Halama, M., Hagemann, N., Weigold, P.R., Laufer, K., Kleindienst, S. et al. (2018) A case study for late Archean and Proterozoic biogeochemical iron-and sulphur cycling in a modern habitat—the Arvadi Spring. *Geobiology* **16**: 353-368.

Krepski, S., Emerson, D., Hredzak-Showalter, P., Luther Iii, G., and Chan, C. (2013) Morphology of biogenic iron oxides records microbial physiology and environmental conditions: toward interpreting iron microfossils. *Geobiology* **11**: 457-471.

Laufer, K., Byrne, J.M., Glombitza, C., Schmidt, C., Jørgensen, B.B., and Kappler, A. (2016a) Anaerobic microbial Fe (II) oxidation and Fe (III) reduction in coastal marine sediments controlled by organic carbon content. *Environ Microbiol* **18**: 3159-3174.

Laufer, K., Nordhoff, M., Røy, H., Schmidt, C., Behrens, S., Jørgensen, B.B., and Kappler, A. (2016b) Coexistence of microaerophilic, nitrate-reducing, and phototrophic Fe (II) oxidizers and Fe (III) reducers in coastal marine sediment. *Appl Environ Microbiol* **82**: 1433-1447.

Li, X., Xiao, H., Zhang, W., Li, Y., Tang, X., Duan, J. et al. (2019) Analysis of cultivable aerobic bacterial community composition and screening for facultative sulfate-reducing bacteria in marine corrosive steel. *Journal of Oceanology and Limnology* **37**: 600-614.

Li, Y.-L., Vali, H., Yang, J., Phelps, T.J., and Zhang, C.L. (2006) Reduction of iron oxides enhanced by a sulfate-reducing bacterium and biogenic H_2S. *Geomicrobiol J* **23**: 103-117.

Lin, C., Larsen, E.I., Nothdurft, L.D., and Smith, J.J. (2012) Neutrophilic, microaerophilic Fe (II)-oxidizing bacteria are ubiquitous in aquatic habitats of a subtropical Australian coastal catchment (ubiquitous FeOB in catchment aquatic habitats). *Geomicrobiol J* **29**: 76-87.

Little, B.J., and Lee, J.S. (2007) *Microbiologically influenced corrosion*: John Wiley & Sons.

Lueder, U., Druschel, G., Emerson, D., Kappler, A., and Schmidt, C. (2017) Quantitative analysis of O_2 and Fe^{2+} profiles in gradient tubes for cultivation of microaerophilic Iron(II)-oxidizing bacteria. *FEMS Microbiol Ecol* **94**: fix177.

Lv, M., Du, M., Li, X., Yue, Y., and Chen, X. (2019) Mechanism of microbiologically influenced corrosion of X65 steel in seawater containing sulfate-reducing bacteria and iron-oxidizing bacteria. *Journal of Materials Research and Technology* **8**: 4066-4078.

Ma, S., Noble, A., Butcher, D., Trouwborst, R.E., and Luther III, G.W. (2006) Removal of H_2S via an iron catalytic cycle and iron sulfide precipitation in the water column of dead end tributaries. *Estuar Coast Shelf Sci* **70**: 461-472.

Ma, Y., Zhang, Y., Zhang, R., Guan, F., Hou, B., and Duan, J. (2020) Microbiologically influenced corrosion of marine steels within the interaction between steel and biofilms: A brief view. *Appl Microbiol Biotechnol* **104**: 515-525.

MacDonald, D.J., Findlay, A.J., McAllister, S.M., Barnett, J.M., Hredzak-Showalter, P., Krepski, S.T. et al. (2014a) Using *in situ* voltammetry as a tool to identify and characterize habitats of iron-oxidizing bacteria: from fresh water wetlands to hydrothermal vent sites. *Environ Sci Process Impacts* **16**: 2117-2126.

MacDonald, D.J., Findlay, A.J., McAllister, S.M., Barnett, J.M., Hredzak-Showalter, P., Krepski, S.T. et al. (2014b) Using *in situ* voltammetry as a tool to identify and characterize habitats of iron-oxidizing bacteria: from fresh water wetlands to hydrothermal vent sites. *Environ Sci Process Impacts* **16**: 2117-2126.

McBeth, J.M., and Emerson, D. (2016) *In situ* microbial community succession on mild steel in estuarine and marine environments: exploring the role of iron-oxidizing bacteria. *Front Microbiol* **7**: 767.

McBeth, J.M., Fleming, E.J., and Emerson, D. (2013) The transition from freshwater to marine iron-oxidizing bacterial lineages along a salinity gradient on the Sheepscot River, Maine, USA. *Environ Microbiol Rep* **5**: 453-463.

Melton, E.D., Swanner, E.D., Behrens, S., Schmidt, C., and Kappler, A. (2014) The interplay of microbially mediated and abiotic reactions in the biogeochemical Fe cycle. *Nat Rev Microbiol* **12**: 797.

Millero, F.J., Hubinger, S., Fernandez, M., and Garnett, S. (1987) Oxidation of H_2S in seawater as a function of temperature, pH, and ionic strength. *Environ Sci Technol* **21**: 439-443.

Morse, J.W., Millero, F.J., Cornwell, J.C., and Rickard, D. (1987) The chemistry of the hydrogen sulfide and iron sulfide systems in natural waters. *Earth Sci Rev* **24**: 1-42.

Mumford, A.C., Adaktylou, I.J., and Emerson, D. (2016) Peeking under the iron curtain: development of a microcosm for imaging the colonization of steel surfaces by *Mariprofundus* sp. strain DIS-1, an oxygen-tolerant Fe-oxidizing bacterium. *Appl Environ Microbiol* **82**: 6799-6807.

Murray, J., Jannasch, H., Honjo, S., Anderson, R., Reeburgh, W., Top, Z. et al. (1989) Unexpected changes in the oxic/anoxic interface in the Black Sea. *Nature* **338**: 411-413.

Neubauer, S.C., Emerson, D., and Megonigal, J.P. (2002) Life at the energetic edge: kinetics of circumneutral iron oxidation by lithotrophic iron-oxidizing bacteria isolated from the wetland-plant rhizosphere. *Appl Environ Microbiol* **68**: 3988-3995.

Pan, F., Liu, H., Guo, Z., Li, Z., Wang, B., Cai, Y., and Gao, A. (2019) Effects of tide and season changes on the iron-sulfur-phosphorus biogeochemistry in sediment porewater of a mangrove coast. *Journal of hydrology* **568**: 686-702.

Picard, A., Gartman, A., Clarke, D.R., and Girguis, P.R. (2018) Sulfate-reducing bacteria influence the nucleation and growth of mackinawite and greigite. *Geochim Cosmochim Acta* **220**: 367-384.

Pyzik, A.J., and Sommer, S.E. (1981) Sedimentary iron monosulfides: kinetics and mechanism of formation. *Geochim Cosmochim Acta* **45**: 687-698.

Ramsing, N., and Gundersen, J. (1994) Seawater and Gases: Tabulated physical parameters of interest to people working with microsensors in marine systems. In. Unisense Internal Report.

Saini, G., and Chan, C. (2013) Near-neutral surface charge and hydrophilicity prevent mineral encrustation of F e-oxidizing micro-organisms. *Geobiology* **11**: 191-200.

Sobolev, D., and Roden, E.E. (2004) Characterization of a neutrophilic, chemolithoautotrophic Fe (II)-oxidizing β-proteobacterium from freshwater wetland sediments. *Geomicrobiol J* **21**: 1-10.

Thiel, J., Byrne, J.M., Kappler, A., Schink, B., and Pester, M. (2019) Pyrite formation from FeS and H_2S is mediated through microbial redox activity. *Proc Natl Acad Sci U S A* **116**: 6897-6902.

Vazquez, F.G., Zhang, J.-z., and Millero, F.J. (1989) Effect of metals on the rate of the oxidation of H_2S in seawater. *Geophys Res Lett* **16**: 1363-1366.

Williams, T., Bubb, J., and Lester, J. (1994) Metal accumulation within salt marsh environments: a review. *Mar Pollut Bull* **28**: 277-290.

Figures & Tables

Table 3.1: Summary of varied growth conditions used for initial culturing of environmental samples of FeOB and SRB in co-culture. All samples were allowed to incubate at 25ºC in the dark for two weeks before growth was assessed. Each treatment of media, headspace, and environmental inocula had two replicates. If FeOB growth was observed in a treatment condition it is denoted as either none (0), one (1), or both (2) of the replicates under the column "FeOB". If SRB growth was observed in a treatment condition it is denoted as either none (0), one (1), or both (2) of the replicates under the column "SRB".

	Estuary Media						**Modified Wolfe's Mineral Media**					
Headspace	**Atm O_2 (21%)**		**1% O_2 Gas Mix**		**Gas Mix 1 Week / Atm O_2 1 Week**		**Atm O_2 (21%)**		**1% O_2 Gas Mix**		**Gas Mix 1 Week / Atm O_2 1 Week**	
	FeOB	**SRB**	**FeOB**	**SRB**	**FeOB**	**SRB**	**FeOB**	**SRB**	**FeOB**	**SRB**	**FeOB**	**SRB**
Cedar Island (10.5 ppt)	1	0	2	2	2	2	0	0	0	0	1	0
Fisher's Landing (3.2 ppt)	2	1	1	1	2	1	2	0	2	1	2	2

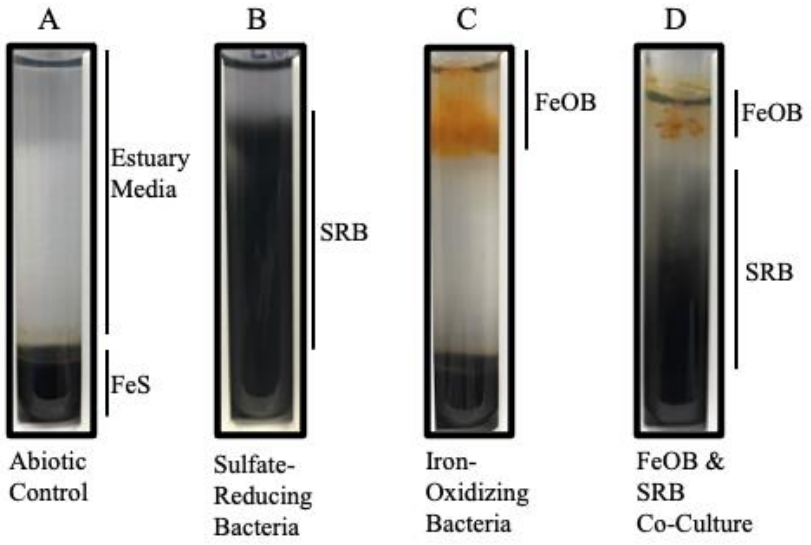

Figure 3.1: Agarose-stabilized gradient tubes made with an iron sulfide (FeS) plug and an estuary medium (A). The growth of bacteria in the gradient tube is usually indicated by the formation of a precipitate in what is typically a banded pattern, where the band is depends on the growth requirements of the organism. SRB growth is indicated by the formation of a black precipitate (FeS) (B), while FeOB growth is indicated by the formation of an orange precipitate (Fe(III) oxyhydroxides) in the estuary media (C). When cultures of FeOB and SRB are mixed there is an intermediate zone where no growth appears (D).

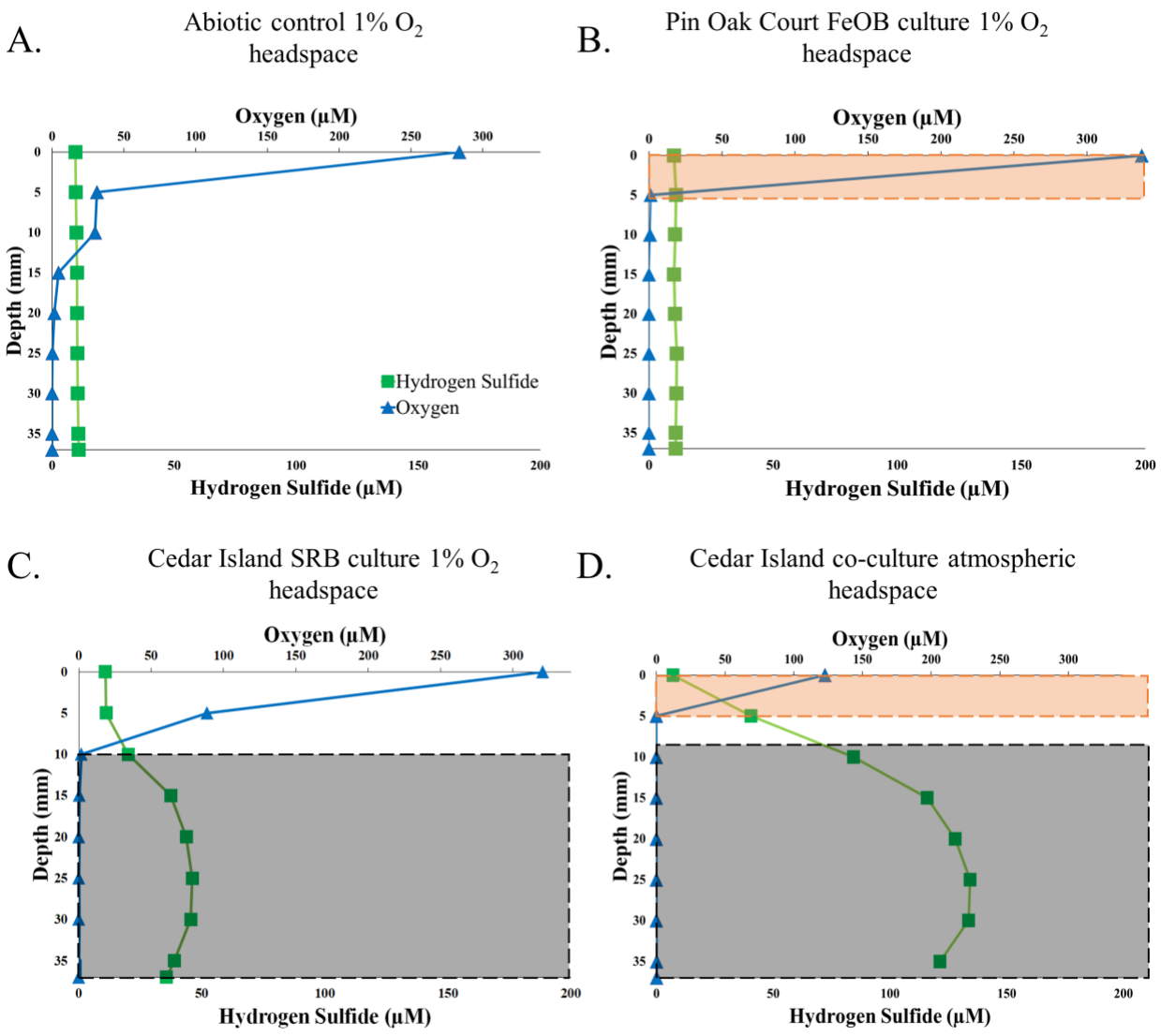

Figure 3.2: Measurements of the H2S (gray) and O2 (blue) concentrations (µmol/L) at depth in the gradient tube starting at the surface (0 mm). In panels representing cultures with FeOB (B, C) the orange shaded box indicates presence of iron-oxide precipitate (Fe(III) oxyhydroxides). Cultures with SRB (C, D) have a black shaded box indicating the presence of a black precipitate (FeS). Samples shown here are an abiotic control with a 1% O_2 headspace (A), FeOB culture from Pin Oak Court (B), a SRB culture from Cedar Island (C), and an FeOB/SRB mixed culture from Cedar Island (D). For other samples see Fig. S3.4.

Chapter 4: Can you mutate it? Benzene induced mutation events in the benzene-degrading *Hydrogenophaga taeniospiralis*

Authors: Chequita N. Brooks and Erin K. Field

Prepared for Submission to: *Evolution*

Abstract

As hydrocarbon pollution events increase in frequency, continued effort is applied to removing hydrocarbons from the environment. Many of these efforts use bacteria as bioremediation agents, however, how the mutagenicity of hydrocarbons affects the functional potential of these organisms is unknown. In this work, we expose *Hydrogenophaga taeniospiralis* 2K1, a known hydrocarbon-degrading organism, with either an intensifying press or repeated pulse model of benzene perturbation. We present evidence that benzene mutates functional genes in *H. taeniospiralis* 2K1 under either an intensifying press or repeated pulse regime. Sequence analysis also indicates that mutation accruement was high enough to begin to change species identity under both intensifying press and repeated pulse conditions within a very short period of 100 experimental generations. These results not only suggest that there is strong mutagenic pressure from benzene, but that this pressure is likely realized in real-world application of organisms such as *H. taeniospiralis*. Furthermore, these conditions provide a warp-speed experimental playground for evolutionary biologists interested in random mutations toward our understanding of mechanisms of current theories such as that of evolutionary rescue.

Introduction

Hydrocarbon pollution has become an increasingly pressing issue in recent history, with dispersal events (e.g., Deepwater Horizon Oil Spill) as well as a high incidence of local-scale

events (i.e., leaking underground storage tanks). These events may be further classifiable as either pulse or press type events. Because the hydrocarbon constituents of oil, especially benzene, have marked negative effects on human health (Badham and Winn 2007) extensive research effort has been put toward removing this pollutant from the environment. Toward this end, both aerobic (Jindrova et al. 2002) and anaerobic (Edwards and Grbić-Galić 1992; Coates et al. 1999; Jahn et al. 2005; Keller et al. 2018) pathways of microbial benzene biodegradation have been studied. A variety of organisms have been identified, both in pure cultures (Coates et al. 2001) and consortia (Atashgahi et al. 2018), that exhibit benzene degradation pathways. However, it remains unknown how the mutagenic agent benzene itself impacts the organisms that we employ to degrade it. This, of course, has practical implications toward application if these organisms are susceptible to mutation in genes associated with the degradation of benzene. There are also implications toward the overall community structure, as has been explored elsewhere (Paissé et al. 2008; Abed et al. 2014; Aubé et al. 2016), and possibly to the mutation rate of that community as a whole. The effects of this, and other, pollutants may be creating model systems for studying how mutations spread throughout a bacterial population under increased mutagenic stress.

The mutagenic effects of benzene, similar to other stressors, is also likely modulated due to the nature of being a pulse or press perturbation. Press and pulse perturbation definitions originated as an ecological concept (Bender et al. 1984), and previous studies have focused primarily on the ecological impacts that these types of perturbation have on communities.

Recently, attention has shifted from a purely ecological focus of pulse and press events toward a more holistic view that incorporates evolutionary consequences (Grant et al. 2017). Moreover,

there has been work in microbial communities to understand how antibiotic resistance evolution is driven by pulse perturbation of streptomycin (Cairns et al. 2020). In this work, we have modified the pulse and press model to better reflect conditions that would be experienced within the iron mat microbial communities that inspired this study (Brooks and Field, in prep): a repeated pulse and intensifying press. A repeated pulse (many short temporal, large scale events) was used to mimic the impacts of hydrocarbons from a leaking underground storage tank during a rainy season, where periods of increased flow would temporarily decrease the concentrations of hydrocarbons. An intensifying press (long temporal, increasing magnitude event) was used to mimic the adsorptive property of iron oxyhydroxides in iron mats, which appears to lead to an increase in benzene concentration over time (Brooks and Field, in prep). In order to understand what the mutagenic effects of benzene are to prokaryotes without the introduction of confounding factors such as immigration; we have opted to focus on the effects of the intensifying press and repeated pulse perturbations on a pure culture of *Hydrogenophaga taeniospiralis* strain 2K1 (Lalucat et al.) Willems et al., which has been found previously to be capable of benzene-degradation (Fahy et al. 2006; Fahy et al. 2008). This work aims to build an understanding of how these regimes may influence mutation within this species and their functional potential.

Perturbation from anthropogenic toxicants or other sources of stress have the potential to modify populations by contributing to genetic erosion, but they also have the potential to contribute to increased genetic diversity by modulating mutation rates (van Straalen and Timmermans 2002). Unlike antibiotics, which exert selective pressure on specific genes driving mutation for survival in the presence of antibiotics, a mutagen such as benzene likely induces rapid random mutation across the entire genome and has the potential to increase variation within

the population at a more rapid rate. This random incidence of mutation throughout the genome makes standard techniques, such as Luria-Delbrück fluctuation analysis (Jones et al. 1994), untenable as they target specific functional genes. To circumvent this problem, previous studies have used whole genome sequencing (WGS) to look for single nucleotide polymorphisms (Ford et al. 2011). In eukaryotic genomes a fingerprint for benzene exposure is mutations of adenine to guanine (Billet et al. 2010; Wang et al. 2012) and it is likely that the mutations would have a similar fingerprint in prokaryotes.

To test the extent of the mutagenic effect of benzene on *H. taeniospiralis* 2K1, we exposed cultures to an intensifying press condition, beginning at 0.05 µM benzene and ending at 0.250 µM benzene. As previous data from an *in situ* microbial community under prolonged benzene perturbation indicated that the average concentration of benzene was 0.102 µM (Brooks and Field, in prep), the repeated pulse condition alternated between 0 µM benzene and 0.102 µM benzene. These two treatments were compared to that of a "wild type" that underwent no additional stress outside of the culture conditions. WGS were compared between each treatment and a reference genome extracted from the initial culture. This work builds the foundation for understanding how microbial communities in application respond to perturbation by hydrocarbons, specifically benzene, and has importance toward the understanding of such studies in the broader context of their ecology and evolution. Ultimately, this work will support ongoing efforts to understand the application of bacterial communities toward remediation of a toxic, anthropogenically produced contaminant.

Materials & Methods

Strain Information, Chemical Tested, and Culture Media

The strain *Hydrogenophaga taeniospiralis* 2K1 (Lalucat et al.) Willems et al. strain ATCC 49743 was purchased from the American Type Culture Collection (ATCC). Cultures were grown in sterile nutrient broth (NB) (remel, 9g/L) added to 60 mL serum vials capped with 20mm grey butyl septa (Fisherbrand) and shaken slowly under atmospheric oxygen. Cultures were amended with dilutions of benzene (anhydrous 99.8%, Sigma-Aldrich) in varying concentrations depending on treatment as defined in 'experimental set-up'.

Experimental Set-Up

To determine the length of time required for cultures to undergo 20 experimental generations, we used a spectrophotometric plate reader set to 30ºC that measured turbidity every 45 minutes for 48 hours in a 24-well plate. Total well volume was 500 µL, where the turbidity of both a NB control (500 µL) and *H. taeniospiralis* 2K1 (450 µL NB, 50 µL culture) were measured. Seventy-four hours was determined to be sufficient time for 20 generations to elapse based on the calculated 3.7 hour doubling time. Samples were taken every 20 generations throughout the overall 100 experimental generations, as it has been previously observed under stress regimes that the greatest number of mutations occurs within the first 100 generations (Zhou et al. 2015).

Once length of time for the experiment was established, vials were assigned in biological triplicate to one of three treatments: intensifying press, repeated pulse, or wild type (WT) (Figure 4.1). Nine cultures were grown for 20 generations to serve as reference cultures (controls) providing a baseline of the DNA make-up of the *H. taeniospiralis* 2K1 culture that was used for the experiment. One of these replicates was used for WGS. Cultures were grown for 74 hours on a shaking incubator at 30ºC. After the initial 20 generations, the cultures underwent 100

experimental generations. Cultures assigned to the "wild type" treatment were not exposed to benzene and were used to detect the background mutation rate that resulted from growth over 100 generations in the serum vial environment. Cultures assigned to the "intensifying press" treatment were exposed to increasing increments (+0.05 µM) of benzene over the course of the 100 generations. Cultures assigned to the "repeated pulse" treatment were exposed to a concentration of 0.102 µM benzene during generations 0-20, 41-60, and 81-100. For the two other sets of 20 generations the cultures were not exposed to benzene. This benzene concentration was chosen for the repeated pulse condition as it was previously determined to be the average concentration of benzene present in a real-world bacterial mat system where *Hydrogenophaga* spp. were found to be present using 16S amplicon sequencing (Brooks and Field, in prep). After 20 generations, 50 µL of culture was transferred from each vial to the corresponding vial. The remaining volume of each culture was aseptically transferred to a 50 mL centrifuge tube and pelleted (4,000 rpm for 15 minutes) for DNA extraction. Supernatant was aseptically removed, and pellets were stored at -80ºC until DNA extraction.

DNA Extraction and Sequencing

The Qiagen DNeasy PowerSoil Kit (Qiagen, Germantown, MD) was used according to the manufacturer instructions for each pellet with the following modifications: DNA was eluted in 60 µL of solution C6 and cell lysis occurred using a 10-minute cycle in a Disruptor Genie (Scientific Industries, Inc., Bohemia, NY) set to maximum speed. WGS was performed at the Comparative Genomics and Evolutionary Bioinformatics' Integrated Microbiome Resource (CGEB-IMR, Halifax, NS) using the Illumina Nextera Flex kit for MiSeq sequencing at a depth of ~100x per genome. Whole genomes were sequenced for one replicate from the reference

cultures and from nine end-generation cultures (triplicate for each treatment). All end-generation cultures were from the 81-100 generation cultures, except for one replicate from the intensifying press treatment that experienced mortality after generations 61-80, and DNA was only recoverable from generation 41-60.

Whole Genome Sequence Single Nucleotide Polymorphism Variant Calling

Sequence adapters were trimmed using Trimmomatic v. 0.36 (Bolger et al. 2014) using the options [CROP:140 LEADING:10 TRAILING:10 SLIDINGWINDOW:5:20 MINLEN:140 AVGQUAL:30]. Sequence loss was assessed using FastQC v. 0.11.5 (Andrews 2010). Reads were aligned to a reference genome of *H. taeniospiralis* accessed from Bio Project 231434 on 2021 Feb 11 using Burrows-Wheeler Aligner (bwa -mem) v. 0.7.17-r1188 (Li 2013). Alignments were indexed, sorted, suspected PCR duplicates were removed, and mapping statistics were assessed using SAMtools v. 1.9 (Li et al. 2009). The quality of the alignment was assessed using QualiMap v. 2.2.1 (García-Alcalde et al. 2012; Okonechnikov et al. 2015). Variants were called using BCFtools v. 1.7 mpileup and call (Danecek et al. 2021). Variant files were filtered using VCFtools v. 0.1.17 (Danecek et al. 2011). Genes that were annotated, but not covered by reads across their full length, were extracted using BEDTools coverage (Quinlan and Hall 2010). SNP calling from the mapped reads was used, as SNPs from assemblies are more difficult to evaluate due to issues with coverage (Olson et al. 2015).

Whole Genome Sequence Assembly

Sequences trimmed for SNP calling were assembled using SPAdes v. 3.13.0 (Bankevich et al. 2012). The quality of contig assembly was compared to the reference *H. taeniospiralis*

sequence using QUAST v. 5.0.2 (Gurevich et al. 2013). The genomes were then filtered for contig size greater than 500 base pairs and 1.5 x coverage, as in Brooks and Field (in prep). These filtered genomes were again assessed using QUAST v. 5.0.2 (Gurevich et al. 2013). Average Nucleotide Identity (ANI) was determined using JSpeciesWS (http://jspecies.ribohost.com/jspeciesws/; Accessed 2021 MAR 2) (Richter et al. 2016). ANI results were confirmed using digital DNA-DNA hybridization analysis using the Genome-to-Genome Distance Calculator (GGDC) v. 2.1 (https://ggdc-test.dsmz.de; Accessed 2021 MAR 4) (Meier-Kolthoff et al. 2013; Meier-Kolthoff et al. 2014). Codon usage indices were calculated using CodonW v. 1.4.4 (Peden 1999) on Galaxy Pasteur (Afgan et al. 2018) (toolshed.pasteur.fr/repos/khillion/codonw/codonw/1.4.4; Accessed 2021 MAR 3). Assembly completeness and contamination were determined using the CheckM v. 1.0.18 (Parks et al. 2015) lineage-specific workflow. Assemblies were annotated and GC content was calculated using RASTtk server (Aziz et al. 2008; Overbeek et al. 2014; Brettin et al. 2015) accessed 2021 March.

Unmapped Reads

It has been previously demonstrated that reads unmapped to database references can still be high-quality and data rich (Gouin et al. 2013). Given the mutated nature of our dataset, we chose to extract these reads for quality checking and subsequent analysis. The reads were re-mapped to the genome assemblies using bwa -mem (Li 2013). Unmapped reads were extracted using SAMtools view and extracted to fastq format using BEDTools bamtofastq (Quinlan and Hall 2010). FastQC v. 0.11.5 (Andrews 2010) was used to evaluate the quality of the unmapped reads and the reads were de-novo assembled using SPAdes v. 3.13.0 (Bankevich et al. 2012). Contigs were then filtered for size greater than 500 base pairs and 1.5x coverage. The quality of

unmapped reads was assessed using QUAST v. 5.0.2 (Gurevich et al. 2013). Contigs were then screened against the reference sequence using Nucleotide-Nucleotide BLAST v. 2.10.1+ (Altschul et al. 1990; Camacho et al. 2009) to verify the unmapped condition. GC content of unmapped contigs was found using Geneious Prime® 2021.0.3 (Kearse et al. 2012). Codon usage indices were calculated using CodonW v. 1.4.4 (Peden 1999) on Galaxy Pasteur (Afgan et al. 2018) (toolshed.pasteur.fr/repos/khillion/codonw/codonw/1.4.4; Accessed 2021 MAR 4). Contig sequences were annotated using prokka v. 1.14.6 (Seemann 2014) using the --*metagenome* flag. Annotated contigs were searched using an HMM previously developed (Brooks and Field, in prep) using the hmmsearch function of HMMER v. 3.2.1 (Eddy 1998). Protein sequence alignments were produced using the default methods in T-Coffee (Notredame et al. 2000) (http://tcoffee.crg.cat; Accessed 2021 MAR 17) and converted into a figure by formatting the fasta_aln using the defaults in BoxShade v. 3.21 (https://embnet.vital-it.ch/software/BOX_form.html; Accessed 2021 MAR 17).

Statistical Analysis

Analysis was performed in R v. 3.5.2 using ggpubr v. 0.4.0 (Kassambara 2020) to calculate Student's t-test and ANOVA results. Plots were produced using ggplot2 v. 3.3.2 (Wickham 2016) to generate graphical output. Color blind accessible palettes were applied to graphs using ggthemes v. 4.2.0 (Ichihara et al. 2008; Chang 2013; Arnold 2019). Plots were aligned to a grid using cowplot v. 1.1.0 (Wilke 2020).

Results

Cultures show morphological response to benzene stress

Cultures began to show morphological changes at the end of generation 41-60, where two of three biological replicates in both the intensifying press and repeated pulse conditions began to exhibit a filamentous or flocculent growth pattern in the shaken vials. The growth was long and strand-like but remained buoyant and mobile in the shaken vials. This morphology was lost in all, except for in a single intensifying press vial, in generation 61-80. This intensifying press replicate contained no growth in generation 81-100. In generation 81-100 the filamentous morphology was again observed in one intensifying press replicate and in two repeated pulse replicates. We hypothesize that the culture in the mortal intensifying press vial experienced lethal mutations to essential genes supporting our hypothesis that benzene appears to have been exerting less of a selective pressure, rather there was pressure on the entire genome equally. In this instance the DNA damage appears to have been lethal.

Genomic Features Change Under Benzene Stress

On average, the GC content of genomes was lower in the intensifying press and repeated pulse treatments than in the WT or experimental Reference (Supplemental Table 4.1) and estimated genome completeness was > 99% for all treatments. While average total reads did not vary greatly between treatments, the average percent of reads mapped decreased in the intensifying press and repeated pulse conditions from > 99% in the reference and WT treatment to 43.48% and 41.34%, respectively (Supplemental Figure 4.1). The average number of variant sites in the mapped reads also increased from 10 ± 3 (standard deviation) in the WT treatment to 413.33 ± 369.81 in intensifying press and 421 ± 357.71 in repeated pulse treatments (Figure 4.2). As there was a large number of high-quality unmapped reads assembled into contigs in the intensifying press and repeated pulse treatments, we calculated the percent guanine (%G) as it

correlated with average contig length (Figure 4.3). The %G increased with average contig length marginally within unmapped contigs ($R^2 = 0.21$, $p = 0.18$), however the %G of all unmapped contigs fell beneath the average %G for mapped contigs (33.1 ± stdev 0.40). Other nucleotide base content and information for mapped contigs can be found in Table S4.2.

The Average Nucleotide Identity (ANI) of mapped treatments was, on average, greater than the 95% identity cutoff (Figueras et al. 2014). However, one biological replicate from each of the treatments intensifying press and repeated pulse fell under the 95% identity cutoff using both BLAST+ and MUMmer based calculations (Figure 4.4). These replicates also fell beneath the 0.95 identity cutoff (Richter et al. 2016) using the tetranucleotide signature calculation. Using a digital DNA-DNA hybridization analysis, these replicates were found to fall beneath the 70% cutoff (i.e., same species) using all three formulas. The G+C difference calculated for the WGS also indicated that these and two other replicates, one from intensifying press and one from repeated pulse, were distinct species from the NCBI reference.

We compared mapped and unmapped sequences using codon usage indices (Figure 4.5). There were significant ($p < 0.05$) differences between mapped and unmapped reads when compared using the Codon Bias Index (CBI) (Bennetzen and Hall 1982), Frequency of Optimal Codons (Fop) (Ikemura 1981), and when comparing the GC content of the third position of synonymous codons. These results indicate that codon use in unmapped reads were less conserved than in the mapped reads and were less conserved in the intensifying press and repeated pulse treatments than in the WT. Unmapped reads also had a significantly greater aromaticity score than mapped reads, but there was not a significant difference between the two groups calculated using the grand average of hydropathy (GRAVY) metric (Supplemental Figure 4.2). An increase in aromatic amino acids is selectively disadvantageous to cells, as they are

expensive to manufacture (Lobry and Gautier 1994). The GRAVY score is correlated with changes in sequences that are likely associated with membrane proteins, as these are high in hydrophobic amino acids (Lobry and Gautier 1994).

Unmapped Read Annotation Indicated the Potential for Mutation in Functional Genes

Unmapped reads from the intensifying press and repeated pulse treatment genomes were annotated using a HMM to contain benzene-remediation genes nitrate reductase, 4-hydroxybenzoate octaprenyltransferase, and dimethyl sulfoxide reductase (DmsA). However, upon further inspection these genes did not appear to incur any mutations outside of differences that preexisted between the NCBI and ATCC *Hydrogenophaga taeniospiralis* genomes (Supplemental Figure 4.3). If the contigs of the unmapped reads met the quality thresholds, they were annotated with RASTtk. This annotation indicated that the unmapped sequences contained subsystems associated with resistance to antibiotics and toxic compounds (e.g., copper homeostasis), respiration (e.g., cytochrome C oxidase), and stress response (e.g., oxidative stress). Of the five samples (3 repeated pulse, 2 intensifying press) whose unmapped reads met the upload quality standards for the RASTtk pipeline, all included subsystems for phosphate metabolism. This was the only subsystem annotated for one sample's unmapped reads.

Discussion

Using a repeated pulse and intensifying press perturbation model, mutagenic effects of benzene under both models were observed that were not observed in the WT treatment. Culture growth patterns suggest that the cells may have begun to respond physiologically, for example the samples appeared to be producing exopolysaccharides (EPS), in an attempt to buffer the

effects of the benzene perturbation. Interestingly, this was observed to different extents between the intensifying press and repeated pulse treatments. Previous work found that an aerobic benzene-degrading bacterial isolate, *Pseudomonas aeruginosa* strain B5, using benzene as its sole carbon source decreased the production of EPS (Onbasli and Aslim 2009), but the authors postulate that the continued production of EPS indicated a protective effect from perturbation by benzene. The repeated pulse treatments that exhibited the flocculent morphology did so at the end of twenty generations grown under benzene perturbation (0.102 µM benzene – generations 41-60, 81-100). That the flocculation was seemingly turned off during the perturbation free generations (0 µM benzene – generations 61-80) suggests that the communities were suppressing phenotypes that were deleterious. The literature discussing mechanisms underlying how press and pulse perturbations influence genotype or phenotype is somewhat lacking, however, mathematical modeling indicates that mutations acquired during a pulse event are deleterious following the end of the pulsed perturbation (Lyberger et al. 2020). Similarly, any population that does not evolve within one generation of the pulsed perturbation can experience a deleterious effect in subsequent generations (Lyberger et al. 2020). The repeated pulse treatment may have experienced "lagging" responses every 20 generations that may have led to the growth morphology in our observations. What is less clear is why the intensifying press treatment had a seemingly more random response. Each of the three replicates exhibited different extents to their phenotypic response, where the response resulting in flocculant phenotype for forty generations resulted in mortality. Benzene, applying random pressure on the entire genome, may have induced mutations within genes that were associated with EPS production, inhibiting one of the replicates from ever exhibiting the phenotype. Ultimately, since the EPS genes have not been

annotated in the *Hydrogenophaga taeniospiralis* genome, we cannot know if there was a molecular underpinning to these observed morphological changes at this time.

Using molecular data, we were able to observe that the mutation profile in both the intensifying press and repeated pulse treatments differed greatly from the WT, as exhibited by the variance from the NCBI reference, resulting in over half of the reads from both intensifying press and repeated pulse treatments remaining unmapped and the substantial increase in single nucleotide variants. The mutations in intensifying press and repeated pulse cultures appears to have been driven toward a less-optimized profile in codon usage, in both mapped and unmapped sequences. This change was biologically relevant, as all codon usage indices indicated that the intensifying press and repeated pulse cultures had a greater skew toward random codon usage than did the reference or WT cultures. Sub-optimal codon usage can lead to a decrease in translation efficiency and accuracy (Behura and Severson 2013), which has the potential under a benzene perturbation scenario to lead to additional protein malfunction. So, when there is a mutation to a sub-optimal codon, the overall accuracy of translation decreases, which can lead to an increase in nonfunctional proteins. The codon usage indices also suggest that mutations were more evenly distributed across the three bases of each codon in the repeated pulse condition, as there was less codon usage bias for repeated pulse unmapped contigs, but less variability in the GC content of the third synonymous base of unmapped contigs. The results of the codon usage indices also indicate that the most-conserved regions in the contigs of the experimental reference appear to have gone unmapped (Figure 5). These contigs may represent differences between the ATCC representative culture and the NCBI whole genome, including the possibility of a broad host range plasmid, which have been shown to be carried by *Hydrogenophaga* spp. (Werner et al. 2020).

Using mapped contigs we were also able to compare ANI values between the three treatments, with two of the WGS falling beneath the 95% identity cutoff suggesting that they were no longer classifiable as the same species. It is very notable that both the intensifying press and repeated pulse were highly variable compared to the WT control (Figure 4.4), which is consistent with the patterns observed in the codon usage indices for both mapped and unmapped contigs (Figure 4.5). This result likely reflects the highly random nature of the benzene-resultant mutations. Species classification was confirmed using the results of our digital DNA-DNA hybridization analysis where, due primarily to GC differences, four of the cultures were annotated as distinct species and two were consistently labeled as a different species based on the DNA-DNA hybridization formulas. This result has practical implications for future studies of benzene perturbed microbial communities, as these organisms undergo speciation at an incredibly fast rate. This result suggests that future studies of microbial communities should be especially critical of any organisms that are identified beneath the genus level using sequence-based methodologies.

The high-quality, unmapped reads from the intensifying press and repeated pulse treatments have a verifiably lower %G, indicating an overall decrease in guanine in the genomes of *H. taeniospiralis* under both regimes. The number of unmapped reads increased dramatically in both the intensifying press and repeated pulse treatments, despite these reads being high quality when assessed using FastQC. The unmapped reads assembled into contigs that contained genes associated with myriad functions, including those related to benzene bioremediation. The %G of the unmapped contigs was lower than the average %G for mapped contigs in all treatments (Figure 4.3), but there was a positive correlation between %G and average contig length ($R^2 = 0.21$, $p = 0.18$). This result is unexpected, as a fingerprint of benzene exposure in

eukaryotic genomes is the mutation of adenine to guanine (Billet et al. 2010; Wang et al. 2012). Previous work, however, suggests that mutations in prokaryotic organisms are universally biased toward AT, even if the organism's genome has a high GC content (Hershberg and Petrov 2010). This has been postulated to be a reflection of the fact that adenine and thymine are "cheap" amino acids (Bohlin and Pettersson 2019). While we did not quantify the energy expenditure of the cells under benzene perturbation, it is certainly possible that there was some benefit to allowing these GC to AT mutations to happen in superfluous genes. This is further illustrated, as it was observed in the relative "safety" of the culture flasks with high-nutrient media one replicate of the intensifying press treatment still experienced mortality prior to the 100^{th} experimental generation. These results suggest that the effectiveness of microbial communities to the remediation of highly mutagenic agents such as benzene may be subject to some level of randomness, where genes that are necessary to survival may mutate causing mortality in necessary organisms. This finding certainly adds to those of microbial communities under benzene perturbation and may explain why diversity is lost and then shown to recover under pulse perturbation (Nogales et al. 2011; Sun et al. 2013). Under this scenario, organisms of a species may experience fatal mutations and be replaced with others that do not accrue these mutations.

These results suggest that the effectiveness of microbial communities to the remediation of highly mutagenic agents such as benzene may be subject to some level of randomness, where genes that are necessary to survival may mutate causing mortality in necessary organisms. This finding certainly adds to those of microbial communities under benzene perturbation and may explain why diversity is lost and then shown to recover under pulse perturbation (Nogales et al.

2011; Sun et al. 2013). Under this scenario, organisms of a species may experience fatal mutations and be replaced with others that do not accrue these mutations.

We selected *H. taeniospiralis* for this study as it has been previously found in environments under benzene perturbation, including the iron mat where *Hydrogenophaga* spp. make up a relative abundance of approximately 5% (Brooks and Field, in prep). Under conditions such as those experienced in the iron mat environment, it is likely that the standing genetic variation among *Hydrogenophaga* spp. is higher than within the strain used for this study. It is therefore probable that evolutionary rescue could occur within the population under these intensifying press conditions. Previous work has shown that evolutionary rescue can occur as early as within the first 25 generations of eukaryotes (Bell and Gonzalez 2009). The dynamics between evolutionary rescue and a highly random mutagenic stressor remain untested in prokaryotes, though these dynamics have been mathematically explored under selective pressure from antibiotics (Anciaux et al. 2019). It is most interesting, however, to consider how a benzene perturbation may increase the likelihood of evolutionary rescue. We suggest this as a potential effect as the genetic variation among both intensifying press and repeated pulse treatments increased compared to the WT treatment. Furthermore, under the ever-fluctuating conditions of environments such as iron mats, not all genes in the genome will have clear use or disuse, which may lead to an upregulated DNA repair mechanism. That said, we can assume that energy sources will not be so readily available as they were under the nutrient broth conditions, making DNA repair that much more expensive in terms of energy costs.

This study sheds significant light on the differences in mutagenicity of benzene between eukaryotic and prokaryotic organisms, reflecting similarly disparate results observed for the mutagenic agent piplartine which does not affect prokaryotes (Bezerra et al. 2009). This model

of benzene perturbation also incorporates an intensifying press and repeated pulse perturbation model, adding to the small body of literature addressing how differing regimes of perturbation change evolutionary response within prokaryotes. Finally, we suggest considerations of the mutagenic effect of benzene on functional genes in consortia applied to *in situ* benzene contamination, as we have shown that these genes may be susceptible to benzene-induced mutation.

Future Directions

Our study sets the groundwork for understanding how microorganisms under benzene perturbation, both during intensifying press and repeated pulse events, experience elevated mutation. Future work can begin to incorporate this framework into an understanding of how these mutations may be mediated by, for example, the incorporation of benzene into the metabolism of these organisms. In this study we grew these organisms aerobically so that there would be no significant change in benzene concentrations throughout the course of the twenty generations. However, this does raise interesting questions as to how the scavenging of benzene may increase or decrease its mutagenic effects to microorganisms. The mutagenicity of benzene to microorganisms also raises the question as to whether evolutionary rescue dynamics were occurring within the 100 experimental generations. This work can be further built upon by understanding what standing genetic variation exists within isolate cultures, which could inform the potential for evolutionary rescue prior to experimentation addressing one of the challenges toward our understanding of this theory (Carlson et al. 2014). Finally, we look forward to studies that use a systems-based approach by assessing bacteria from *in situ* perturbed communities to determine their resilience to environmental changes in the context of benzene perturbation.

Work is ongoing with collaborators to use electrochemical detection to track the percent mutation under both repeated pulse and intensifying press scenarios in replicate cultures with high resolution, representing percent mutation accumulation differences between generations. The differing chemistry of the varying DNA bases will be used to detect changing signatures, which are especially sensitive to mutations in the base guanine (Huffnagle et al. 2014). By pairing these methodologies we hope to further our understanding of how the mutation rates were impacted by the intensifying press and repeated pulse treatment conditions. This will further our understanding of differences between the two treatment types, as well as continue to add to the model of how benzene perturbation influences bacterial biology.

Author Contributions

CNB and EKF conceived and designed the research; CNB performed the experiments, performed the formal analysis, and wrote the manuscript. EKF provided the resources to conduct this study. All authors have read, reviewed, edited, and approved the final version of the manuscript.

Acknowledgements

We would like to acknowledge Dr. Peri Bolton for her consultation in analyzing the whole genome sequence data for this project. Funding support provided by the Graduate Women in Science National Fellowship Program Nell Mondy, Vessa Notchev, and Monique Braude Fellowship Funds to CNB.

References

Abed, R. M. M., S. Al-Kharusi, S. Prigent, and T. Headley. 2014. Diversity, Distribution and Hydrocarbon Biodegradation Capabilities of Microbial Communities in Oil-Contaminated Cyanobacterial Mats from a Constructed Wetland. PLoS ONE 9:e114570.

Afgan, E., D. Baker, B. Batut, M. van den Beek, D. Bouvier, M. Čech, J. Chilton, D. Clements, N. Coraor, B. A. Grüning, A. Guerler, J. Hillman-Jackson, S. Hiltemann, V. Jalili, H. Rasche, N. Soranzo, J. Goecks, J. Taylor, A. Nekrutenko, and D. Blankenberg. 2018. The Galaxy platform for accessible, reproducible and collaborative biomedical analyses: 2018 update. Nucleic Acids Res. 46:W537-W544.

Altschul, S. F., W. Gish, W. Miller, E. W. Myers, and D. J. Lipman. 1990. Basic local alignment search tool. J. Mol. Biol. 215:403-410.

Andrews, S. 2010. FastQC: a quality control tool for high throughput sequence data. Babraham Bioinformatics, Babraham Institute, Cambridge, United Kingdom.

Arnold, J. B. 2019. ggthemes: Extra Themes, Scales and Geoms for 'ggplot2'.

Atashgahi, S., B. Hornung, M. J. van der Waals, U. N. da Rocha, F. Hugenholtz, B. Nijsse, D. Molenaar, R. van Spanning, A. J. M. Stams, J. Gerritse, and H. Smidt. 2018. A benzene-degrading nitrate-reducing microbial consortium displays aerobic and anaerobic benzene degradation pathways. Sci. Rep. 8:4490.

Aubé, J., P. Senin, O. Pringault, P. Bonin, B. Deflandre, O. Bouchez, N. Bru, E. Biritxinaga-Etchart, C. Klopp, R. Guyoneaud, and M. Goñi-Urriza. 2016. The impact of long-term hydrocarbon exposure on the structure, activity, and biogeochemical functioning of microbial mats. Mar. Pollut. Bull. 111:115-125.

Aziz, R. K., D. Bartels, A. A. Best, M. DeJongh, T. Disz, R. A. Edwards, K. Formsma, S. Gerdes, E. M. Glass, and M. Kubal. 2008. The RAST Server: rapid annotations using subsystems technology. BMC Genomics 9:1-15.

Badham, H. J. and L. M. Winn. 2007. Investigating the role of the aryl hydrocarbon receptor in benzene-initiated toxicity in vitro. Toxicology 229:177-185.

Bankevich, A., S. Nurk, D. Antipov, A. A. Gurevich, M. Dvorkin, A. S. Kulikov, V. M. Lesin, S. I. Nikolenko, S. Pham, and A. D. Prjibelski. 2012. SPAdes: a new genome assembly algorithm and its applications to single-cell sequencing. J. Comput. Biol. 19:455-477.

Bender, E. A., T. J. Case, and M. E. Gilpin. 1984. Perturbation Experiments in Community Ecology: Theory and Practice. Ecology 65:1-13.

Bennetzen, J. L. and B. D. Hall. 1982. Codon selection in yeast. J. Biol. Chem. 257:3026-3031.

Billet, S., V. Paget, G. Garçon, N. Heutte, V. André, P. Shirali, and F. Sichel. 2010. Benzene-induced mutational pattern in the tumour suppressor gene TP53 analysed by use of a functional assay, the functional analysis of separated alleles in yeast, in human lung cells. Arch. Toxicol. 84:99-107.

Bolger, A. M., M. Lohse, and B. Usadel. 2014. Trimmomatic: a flexible trimmer for Illumina sequence data. Bioinformatics 30:2114-2120.

Brettin, T., J. J. Davis, T. Disz, R. A. Edwards, S. Gerdes, G. J. Olsen, R. Olson, R. Overbeek, B. Parrello, and G. D. Pusch. 2015. RASTtk: a modular and extensible implementation of the RAST algorithm for building custom annotation pipelines and annotating batches of genomes. Sci. Rep. 5:8365.

Cairns, J., R. Jokela, L. Becks, V. Mustonen, and T. Hiltunen. 2020. Repeatable ecological dynamics govern the response of experimental communities to antibiotic pulse perturbation. Nat Ecol Evol 4:1385-1394.

Camacho, C., G. Coulouris, V. Avagyan, N. Ma, J. Papadopoulos, K. Bealer, and T. L. Madden. 2009. BLAST+: architecture and applications. BMC Bioinformatics 10:421.

Carlson, S. M., C. J. Cunningham, and P. A. H. Westley. 2014. Evolutionary rescue in a changing world. Trends Ecol. Evol. 29:521-530.

Chang, W. 2013. R graphics cookbook. O'Reilly, Beijing.

Coates, J. D., R. Chakraborty, J. G. Lack, S. M. O'Connor, K. A. Cole, K. S. Bender, and L. A. Achenbach. 2001. Anaerobic benzene oxidation coupled to nitrate reduction in pure culture by two strains of *Dechloromonas*. Nature 411:1039-1043.

Coates, J. D., D. J. Ellis, C. V. Gaw, and D. R. Lovley. 1999. Geothrix fermentans gen. nov., sp. nov., a novel Fe(III)-reducing bacterium from a hydrocarbon-contaminated aquifer. Int. J. Syst. Evol. Microbiol. 49:1615-1622.

Danecek, P., A. Auton, G. Abecasis, C. A. Albers, E. Banks, M. A. DePristo, R. E. Handsaker, G. Lunter, G. T. Marth, S. T. Sherry, G. McVean, R. Durbin, and G. P. A. Group. 2011. The variant call format and VCFtools. Bioinformatics 27:2156-2158.

Danecek, P., J. K. Bonfield, J. Liddle, J. Marshall, V. Ohan, M. O. Pollard, A. Whitwham, T. Keane, S. A. McCarthy, R. M. Davies, and H. Li. 2021. Twelve years of SAMtools and BCFtools. GigaScience 10.

Eddy, S. R. 1998. Profile hidden Markov models. Bioinformatics (Oxford, England) 14:755-763.

Edwards, E. A. and D. Grbić-Galić. 1992. Complete mineralization of benzene by aquifer microorganisms under strictly anaerobic conditions. Appl. Environ. Microbiol. 58:2663-2666.

Fahy, A., A. Ball, G. Lethbridge, K. Timmis, and T. McGenity. 2008. Isolation of alkali-tolerant benzene-degrading bacteria from a contaminated aquifer. Lett. Appl. Microbiol. 47:60-66.

Fahy, A., T. J. McGenity, K. N. Timmis, and A. S. Ball. 2006. Heterogeneous aerobic benzene-degrading communities in oxygen-depleted groundwaters. FEMS microbiology ecology 58:260-270.

Figueras, M. J., R. Beaz-Hidalgo, M. J. Hossain, and M. R. Liles. 2014. Taxonomic Affiliation of New Genomes Should Be Verified Using Average Nucleotide Identity and Multilocus Phylogenetic Analysis. Genome Announcements 2:e00927-00914.

Ford, C. B., P. L. Lin, M. R. Chase, R. R. Shah, O. Iartchouk, J. Galagan, N. Mohaideen, T. R. Ioerger, J. C. Sacchettini, and M. Lipsitch. 2011. Use of whole genome sequencing to estimate the mutation rate of Mycobacterium tuberculosis during latent infection. Nat. Genet. 43:482.

García-Alcalde, F., K. Okonechnikov, J. Carbonell, L. M. Cruz, S. Götz, S. Tarazona, J. Dopazo, T. F. Meyer, and A. Conesa. 2012. Qualimap: evaluating next-generation sequencing alignment data. Bioinformatics 28:2678-2679.

Gouin, A., F. Legeai, P. Nouhaud, G. Rizk, J.-C. Simon, and C. Lemaitre. 2013. Whole genome re-sequencing: lessons from unmapped reads. Journées Ouvertes Biologie Informatique Mathématiques Toulouse, 1-4 July 2013:hal-00907446.

Grant, P. R., B. R. Grant, R. B. Huey, M. T. Johnson, A. H. Knoll, and J. Schmitt. 2017. Evolution caused by extreme events. Philosophical Transactions of the Royal Society B: Biological Sciences 372:20160146.

Gurevich, A., V. Saveliev, N. Vyahhi, and G. Tesler. 2013. QUAST: quality assessment tool for genome assemblies. Bioinformatics 29:1072-1075.

Huffnagle, I. M., A. Joyner, B. Rumble, S. Hysa, D. Rudel, and E. G. Hvastkovs. 2014. Dual electrochemical and physiological apoptosis assay detection of in vivo generated nickel chloride induced DNA damage in Caenorhabditis elegans. Anal. Chem. 86:8418-8424.

Ichihara, Y., M. Okabe, K. Iga, Y. Tanaka, K. Musha, and K. Ito. 2008. Color universal design: the selection of four easily distinguishable colors for all color vision types. SPIE.

Ikemura, T. 1981. Correlation between the abundance of Escherichia coli transfer RNAs and the occurrence of the respective codons in its protein genes: A proposal for a synonymous codon choice that is optimal for the E. coli translational system. J. Mol. Biol. 151:389-409.

Jahn, M. K., S. B. Haderlein, and R. U. Meckenstock. 2005. Anaerobic Degradation of Benzene, Toluene, Ethylbenzene, and *o*-Xylene in Sediment-Free Iron-Reducing Enrichment Cultures. Appl. Environ. Microbiol. 71:3355-3358.

Jindrova, E., M. Chocova, K. Demnerova, and V. Brenner. 2002. Bacterial aerobic degradation of benzene, toluene, ethylbenzene and xylene. Folia Microbiol. (Praha) 47:83-93.

Jones, M., S. Thomas, and A. Rogers. 1994. Luria-Delbrück fluctuation experiments: design and analysis. Genetics 136:1209-1216.

Kassambara, A. 2020. ggpubr: 'ggplot2' Based Publication Ready Plots.

Kearse, M., R. Moir, A. Wilson, S. Stones-Havas, M. Cheung, S. Sturrock, S. Buxton, A. Cooper, S. Markowitz, C. Duran, T. Thierer, B. Ashton, P. Meintjes, and A. Drummond. 2012. Geneious Basic: An integrated and extendable desktop software platform for the organization and analysis of sequence data. Bioinformatics 28:1647-1649.

Keller, A. H., S. Kleinsteuber, and C. Vogt. 2018. Anaerobic benzene mineralization by nitrate-reducing and sulfate-reducing microbial consortia enriched from the same site: Comparison of community composition and degradation characteristics. Microb. Ecol. 75:941-953.

Li, H. 2013. Aligning sequence reads, clone sequences and assembly contigs with BWA-MEM. arXiv:1303.3997v1302 [q-bio.GN].

Li, H., B. Handsaker, A. Wysoker, T. Fennell, J. Ruan, N. Homer, G. Marth, G. Abecasis, R. Durbin, and G. P. D. P. Subgroup. 2009. The Sequence Alignment/Map format and SAMtools. Bioinformatics 25:2078-2079.

Lobry, J.R. and C. Gautier. 1994. Hydrophobicity, expressivity and aromaticity are the major trends of amino-acid usage in 999 *Escherichia coli* chromosome-encoded genes. Nucleic Acids Research 22:3174-3180.

Lyberger, K., M. Osmond, and S. Schreiber. 2020. Is evolution in response to extreme events good for population persistence? bioRxiv:2020.2004.2002.014951.

Meier-Kolthoff, J. P., A. F. Auch, H.-P. Klenk, and M. Göker. 2013. Genome sequence-based species delimitation with confidence intervals and improved distance functions. BMC Bioinformatics 14:60.

Meier-Kolthoff, J. P., H.-P. Klenk, and M. Göker. 2014. Taxonomic use of DNA G+C content and DNA–DNA hybridization in the genomic age. Int. J. Syst. Evol. Microbiol. 64:352-356.

Nogales, B., M. P. Lanfranconi, J. M. Piña-Villalonga, and R. Bosch. 2011. Anthropogenic perturbations in marine microbial communities. FEMS Microbiol. Rev. 35:275-298.

Notredame, C., D. G. Higgins, and J. Heringa. 2000. T-coffee: a novel method for fast and accurate multiple sequence alignment. J. Mol. Biol. 302:205-217.

Okonechnikov, K., A. Conesa, and F. García-Alcalde. 2015. Qualimap 2: advanced multi-sample quality control for high-throughput sequencing data. Bioinformatics 32:292-294.

Olson, N. D., S. P. Lund, R. E. Colman, J. T. Foster, J. W. Sahl, J. M. Schupp, P. Keim, J. B. Morrow, M. L. Salit, and J. M. Zook. 2015. Best practices for evaluating single nucleotide variant calling methods for microbial genomics. Frontiers in Genetics 6.

Onbasli, D. and B. Aslim. 2009. Effects of some organic pollutants on the exopolysaccharides (EPSs) produced by some *Pseudomonas* spp. strains. J. Hazard. Mater. 168:64-67.

Overbeek, R., R. Olson, G. D. Pusch, G. J. Olsen, J. J. Davis, T. Disz, R. A. Edwards, S. Gerdes, B. Parrello, and M. Shukla. 2014. The SEED and the Rapid Annotation of microbial genomes using Subsystems Technology (RAST). Nucleic Acids Res. 42:D206-D214.

Paissé, S., F. Coulon, M. Goñi-Urriza, L. Peperzak, T. J. McGenity, and R. Duran. 2008. Structure of bacterial communities along a hydrocarbon contamination gradient in a coastal sediment. FEMS Microbiol. Ecol. 66:295-305.

Parks, D. H., M. Imelfort, C. T. Skennerton, P. Hugenholtz, and G. W. Tyson. 2015. CheckM: assessing the quality of microbial genomes recovered from isolates, single cells, and metagenomes. Genome Res. 25:1043-1055.

Peden, J. F. 1999. Analysis of Codon Usage. Pp. 215. Department of Genetics. University of Nottingham.

Quinlan, A. R. and I. M. Hall. 2010. BEDTools: a flexible suite of utilities for comparing genomic features. Bioinformatics 26:841-842.

Richter, M., R. Rosselló-Móra, F. Oliver Glöckner, and J. Peplies. 2016. JSpeciesWS: a web server for prokaryotic species circumscription based on pairwise genome comparison. Bioinformatics (Oxford, England) 32:929-931.

Seemann, T. 2014. Prokka: rapid prokaryotic genome annotation. Bioinformatics 30:2068-2069.

Sun, M. Y., K. A. Dafforn, E. L. Johnston, and M. V. Brown. 2013. Core sediment bacteria drive community response to anthropogenic contamination over multiple environmental gradients. Environ. Microbiol. 15:2517-2531.

van Straalen, N. M. and M. J. T. N. Timmermans. 2002. Genetic Variation in Toxicant-Stressed Populations: An Evaluation of the “Genetic Erosion” Hypothesis. Human and Ecological Risk Assessment: An International Journal 8:983-1002.

Wang, L., X. He, Y. Bi, and Q. Ma. 2012. Stem cell and benzene-induced malignancy and hematotoxicity. Chem. Res. Toxicol. 25:1303-1315.

Werner, J., E. Nour, B. Bunk, C. Spröer, K. Smalla, D. Springael, and B. Öztürk. 2020. PromA Plasmids Are Instrumental in the Dissemination of Linuron Catabolic Genes Between Different Genera. Front. Microbiol. 11.

Wickham, H. 2016. ggplot2: Elegant Graphics for Data Analysis. Springer-Verlag New York.

Wilke, C. O. 2020. cowplot: Streamlined Plot Theme and Plot Annotations for 'ggplot2'.

Zhou, A., K. L. Hillesland, Z. He, W. Schackwitz, Q. Tu, G. M. Zane, Q. Ma, Y. Qu, D. A. Stahl, J. D. Wall, T. C. Hazen, M. W. Fields, A. P. Arkin, and J. Zhou. 2015. Rapid

selective sweep of pre-existing polymorphisms and slow fixation of new mutations in experimental evolution of Desulfovibrio vulgaris. ISME J 9:2360-2372.

Figures

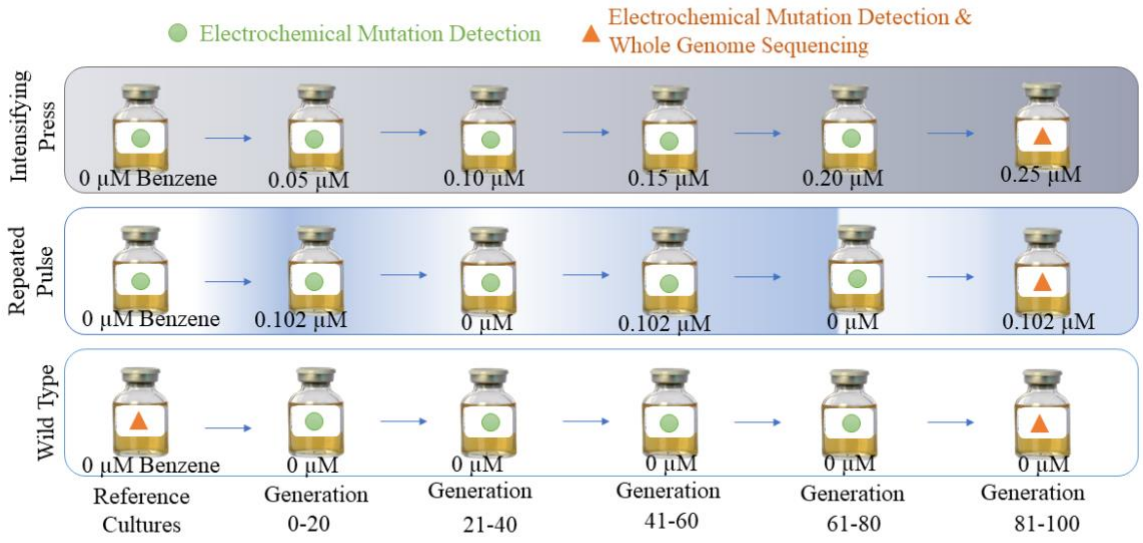

Figure 4.1: An artistic rendition of the experimental set-up used for this experiment. Serum vials in each treatment (Wild Type, Intensifying Press, Repeated Pulse) represent a set of biological triplicates. Green circles indicate serum vials where only electrochemical mutation detection will be used (work ongoing with collaborators). Orange triangles indicate serum vials where both electrochemical mutation detection and whole genome sequencing was used to detect mutation profiles. Samples were transferred and destructively sampled every twenty generations so that mutation rates within the first 100 generations would be highly characterized, as the first 100 generations have been previously observed under perturbation conditions to reflect the greatest mutation rate (Zhou et al. 2015).

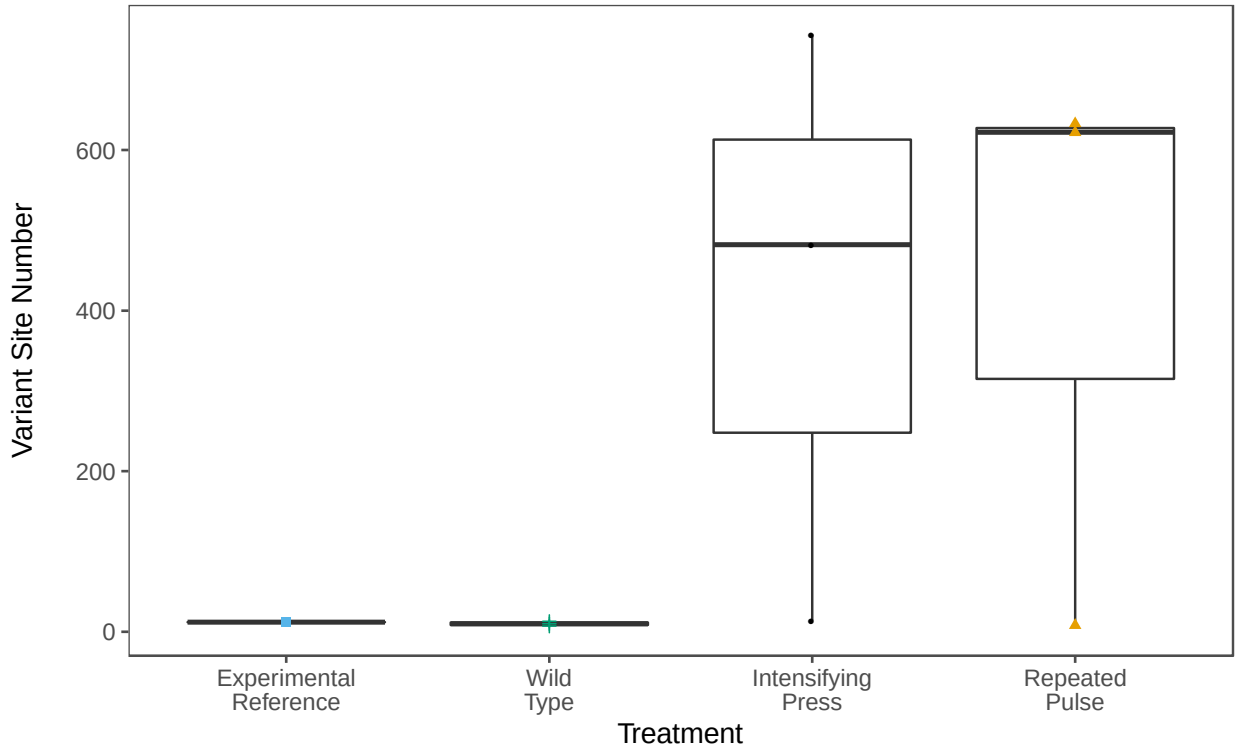

Figure 4.2: The average number of variant sites in each treatment set (wild type (green cross), intensifying press (black circle), and repeated pulse (yellow triangle)) as compared to the number of variants in the experimental reference (blue square). Variant site number was found using BCFtools v. 1.7 mpileup and call (Danecek et al. 2021). The average number of variant sites in intensifying press (413.33 ± 369.81) and repeated pulse (421 ± 357.71) treatments was much greater than in the WT (10 ± 3).

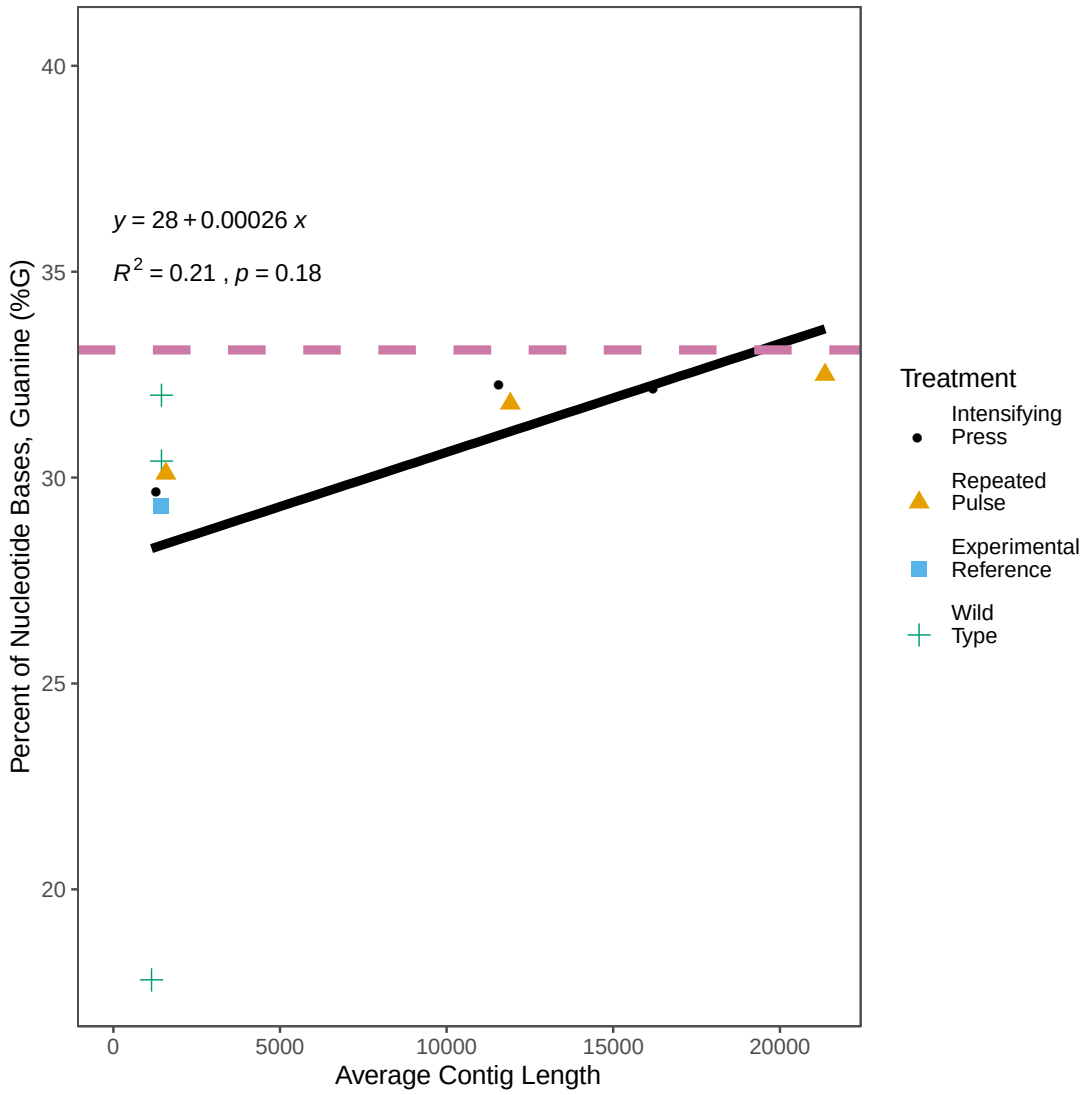

Figure 4.3: The percent guanine (%G) and average contig length of the unmapped contigs for each sample was calculated using Geneious Prime® 2021.0.3 (Kearse et al. 2012). The experimental reference percent guanine (blue square), WT (green cross), intensifying press (black circle), and repeated pulse (yellow triangle) are plotted. There is a non-significant positive correlation between an increased %G and average contig length ($R^2 = 0.21$, $p = 0.18$). These results that the unmapped contigs in the intensifying press and repeated pulse treatments are both high-quality and long. These unmapped contigs, however, had a lower %G than the average for all treatments' mapped contigs (pink) (avg 33.1 ± stdev 0.40).

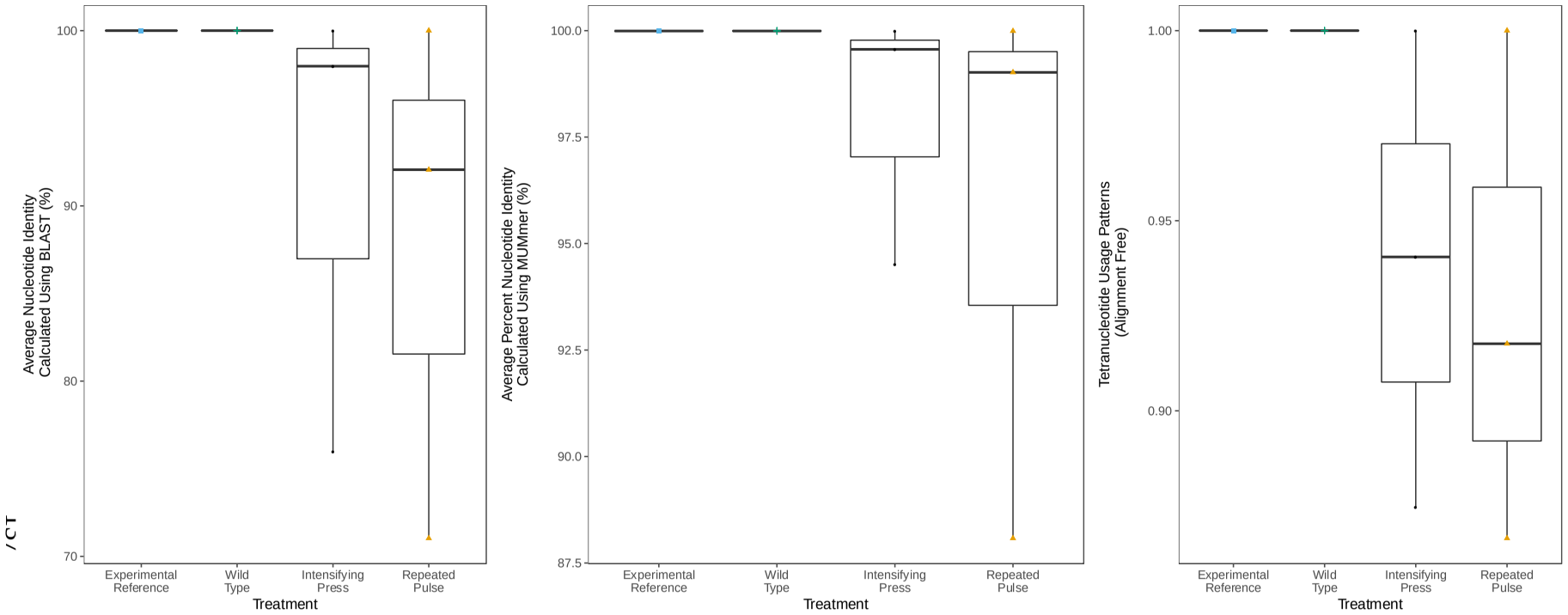

Figure 4.4: Average Nucleotide Identity (ANI) for mapped sequences from each treatment was determined using JSpeciesWS (Richter et al. 2016). Plots from left to right are ANI calculated using BLAST (%), ANI calculated using MUMmer (%), and Tetranucleotide Usage Patterns (alignment free) for mapped contigs. The experimental reference ANI is plotted in blue, WT in green, intensifying press in black, and repeated pulse in yellow.

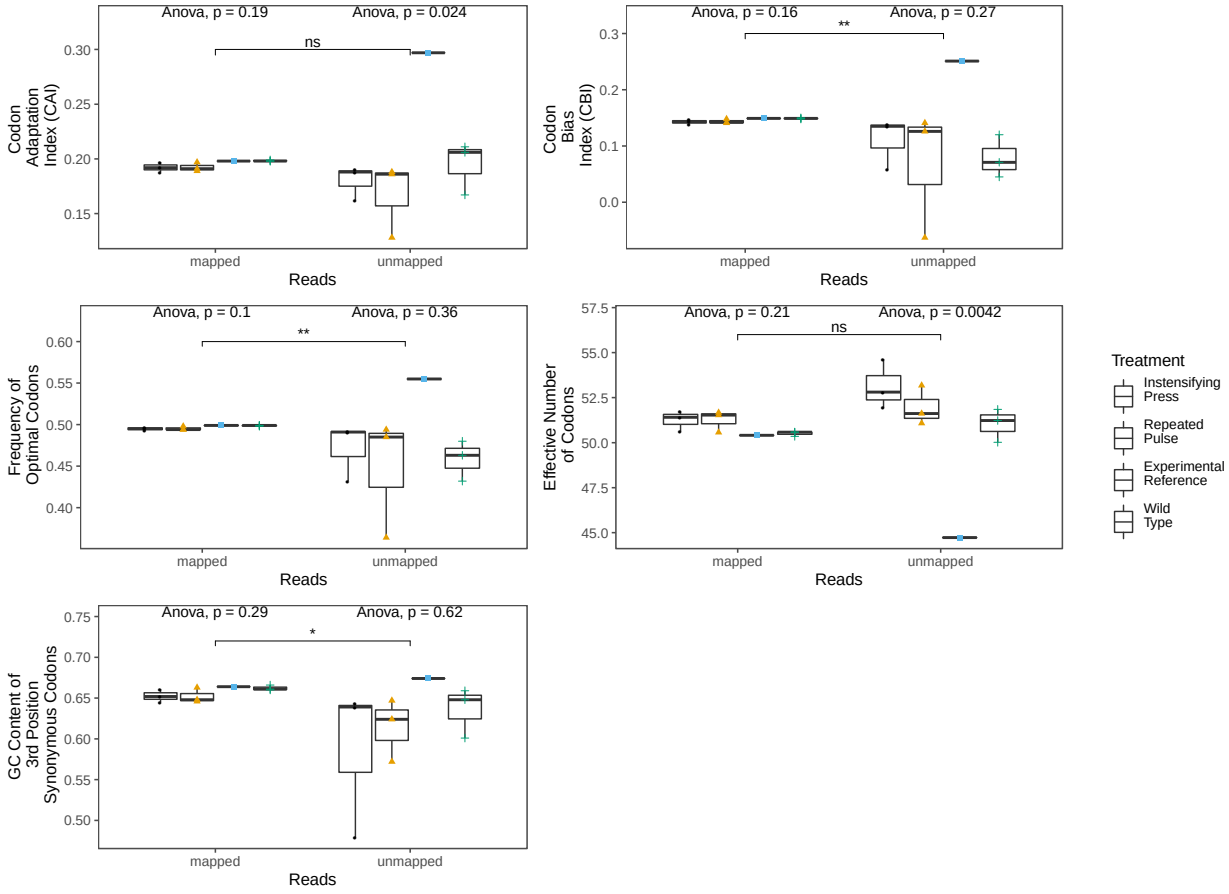

Figure 4.5: Codon usage indices for mapped and unmapped contigs of each treatment were calculated using CodonW v. 1.4.4 (Peden 1999) and mapped and unmapped contigs were compared. Significance values (ns = $p>0.05$, * = $p\leq0.05$, **= $p\leq0.01$) indicate what statistically significant differences exist between mapped and unmapped contigs. ANOVA values on the left of each plot indicate difference between mapped contigs, and on the right indicate difference between unmapped contigs. The experimental reference (blue square), wild type (green cross), intensifying press (black circle), and repeated pulse (yellow triangle) treatments are plotted for the Codon Adaptation Index (CAI), Codon Bias Index (CBI), Frequency of Optimal Codons (Fop), Effective Number of Codons, and the GC content of 3rd position synonymous codons.

Chapter 5: Conclusions & Future Directions

The microaerophilic iron-oxidizing bacteria (FeOB) has captured generations of microbiologists' imaginations since they were first enriched in 1888 by Winogradsky. The isolation of FeOB would not come until much later, through the invention of the gradient tube in 1957[1; 2]. Since then, the study of FeOB has led to a greater understanding of a metabolism that is a race against not only the need of other organisms for reduced iron but against autocatalysis (where iron is oxidized through abiotic means). Even as our understanding of FeOB has grown, our knowledge of the complex microenvironments that form within the iron mat, the structure produced by FeOB in freshwater systems, has remained stagnant. In this work, we have sought to answer unsettled questions about the contribution of the iron mat community as a whole to biogeochemical cycling. Furthermore, we asked new questions about how the bacteria in these communities have extrinsic value in remediating freshwater oil contamination.

One previously underexplored idea was that other types of iron-oxidizing bacteria besides the microaerophiles might be present. We have presented evidence that nitrate-reducing iron-oxidizing bacteria and photoferrotrophs are present in iron mat communities. These functional groups are seemingly sensitive to different conditions than those of their microaerophilic counterparts (e.g., photoferrotrophs are more sensitive to irradiance). However, this work did not address the distance of association (i.e., how far apart are these organisms spatially), which would greatly enhance our understanding of whether there is competition between these functional groups in the freshwater iron mat. However, the high concentration of reduced iron associated with seep type iron mats suggests that these interactions may be further complicated by association with mat type (our work showed differences between flocculent and seep type mats).

Another outstanding question about the iron mat regarding the microbial community was what organisms outside of the bacteria were present, and if there was variation within those taxa. Using two different creeks in Greenville, NC, we found three phyla within Archaea were consistently present but with varying degrees of relative abundance between iron mats in each creek[3]. Within this data set, we were also able to identify Archaea that carry out functions related to methane cycling. These and future results will help tie other cycles, such as carbon, to the iron mat community and help build a fuller understanding of the biogeochemical cycles connected by these microorganisms.

To further progress our understanding of the interconnectedness of cycles within the iron mat, we developed a method for co-culturing FeOB and sulfate-reducing bacteria (SRB) from the same source inoculum[4]. This opens avenues for characterizing the first of many relationships present in iron mat communities, and other communities with FeOB (e.g., biocorrosion biofilms). We found a distinction in the cultures between the FeOB and SRB that was not related to dissolved oxygen, which raises questions about the nature of the relationship between FeOB and SRB. Our understanding of these relationships is critical as iron mats and other microbial communities face unprecedented environmental changes due to anthropogenic actions.

One such environmental change was experienced by the iron mats' microbial communities in Town Creek, Greenville, NC where iron mats are impacted by underground storage tanks leaking oil into the creek. As this type of perturbation is widespread, yet understudied in iron mat communities, we sought to understand what impact the oil had on community composition, structure, and function. Mats downstream of the tanks (exposed) had a lower alpha diversity and had a greater relative abundance of Proteobacteria than iron mats upstream (unexposed). We also found that the community structure of the iron mats was

primarily driven by dissolved oxygen, pH, and benzene concentration. These results suggest that perturbation by oil may impact as-yet-unknown relationships within the iron mat. However, the iron mat community was able to respond functionally. Genes for benzene degradation such as 4-hydroxybenzoate octaprenyltransferase and formate dehydrogenase-O major subunit were found in higher abundance in the downstream (exposed) metagenomic sequences. Furthermore, benzene-degrading taxa, such as *Hydrogenophaga* spp., were identified from both up- and downstream iron mats. Overall, while the iron mats may suffer a loss of some ecosystem functions, they are resilient to hydrocarbon perturbation and may be appliable to other hydrocarbon leaks in the future. Future studies may not only build upon our understanding of hydrocarbons in iron mats, but use a similar approach in understanding what ecosystem trade-offs are inherent in the application of iron mats to other contaminants (e.g., copper[5]).

To further our understanding of how hydrocarbon perturbations impact bacterial communities, we tested how two different ecologically relevant regimes, repeated pulse and intensifying press, of benzene influenced the mutation profile of the isolate *Hydrogenophaga taeniospiralis* 2K1. We found that under both regimes, *H. taeniospiralis* genomes had an increase in single nucleotide variations and a decrease in percent guanine. These mutations were so great in magnitude that, after 100 culture generations, some of the cultures were identified as different species based on average nucleotide identity and digital DNA-DNA hybridization. These results suggest that hydrocarbon perturbation influences not only the ecology but the evolution of microbial communities. Further work is ongoing to characterize how pulse and press perturbation changed mutation rates using electrochemical analysis. This added information will provide critical information in understanding how microorganisms' evolution is impacted in these hydrocarbon perturbed communities.

How the presence of anthropogenically derived contaminants influences the ecosystem functions and evolutionary trajectory of iron mat microbial communities remains a field rich for study. We anticipate future studies will find connections with implications that will extend from the local environment to global impacts. The iron mat microbial community contributes to global biogeochemical cycles such as iron, sulfur, carbon, and nitrogen and the connections of these cycles within the iron mat community have only just begun to be explored in this work.

References

1. Kucera, S, and Wolfe, R (1957). A selective enrichment method for *Gallionella ferruginea*. J Bacteriol *74*, 344.

2. Emerson, D, and Moyer, C (1997). Isolation and characterization of novel iron-oxidizing bacteria that grow at circumneutral pH. Appl Environ Microbiol *63*, 4784-4792.

3. Brooks, CN, and Field, EK (2020). Iron Flocs and the Three Domains: Microbial Interactions in Freshwater Iron Mats. mBio *11*, e02720-02720.

4. Brooks, CN, and Field, EK (2021). Orange leads to black: evaluating the efficacy of co-culturing iron-oxidizing and sulfate-reducing bacteria to discern ecological relationships. Environ Microbiol Rep *n/a*.

5. Field, HR, Whitaker, AH, Henson, JA, and Duckworth, OW (2019). Sorption of copper and phosphate to diverse biogenic iron (oxyhydr) oxide deposits. Sci Total Environ *697*, 134111.

APPENDIX A: Copyright Permission - Chapter One

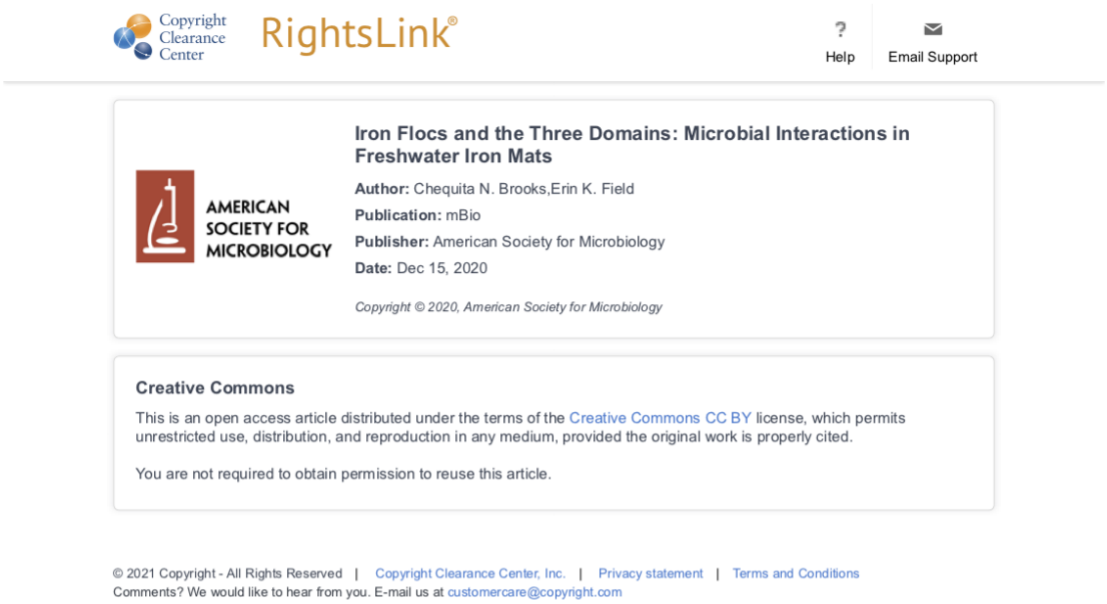

Copyright Clearance Center RightsLink®

Help Email Support

AMERICAN SOCIETY FOR MICROBIOLOGY

Iron Flocs and the Three Domains: Microbial Interactions in Freshwater Iron Mats

Author: Chequita N. Brooks,Erin K. Field

Publication: mBio

Publisher: American Society for Microbiology

Date: Dec 15, 2020

Copyright © 2020, American Society for Microbiology

Creative Commons

This is an open access article distributed under the terms of the Creative Commons CC BY license, which permits unrestricted use, distribution, and reproduction in any medium, provided the original work is properly cited.

You are not required to obtain permission to reuse this article.

APPENDIX B: Supplemental Tables & Figures – Chapter Two

Supplemental Table 2.1: Geochemical conditions from each site at Town Creek, Greenville, NC. Iron mats were categorized by location as upstream (U), downstream A (Da), or downstream B (Db). Samples for geochemical analysis were also collected from a water sample that was taken downstream of the leaking underground storage tank (W). Measurements are displayed as averages ± standard deviation across all timepoints. Raw data can be found in the attached spreadsheet.

Site	**Upstream (U)**	**Downstream A (Da)**	**Downstream B (Db)**	**Water (W)**
Reduced Iron (µM)	74.20 ± 23.32	217.52 ± 74.35	94.21 ± 39.14	35.29 ± 5.49
Oxidized Iron (µM)	1388.36 ± 128.06	3242.85 ± 772.52	1922.80 ± 43.31	10.54 ± 2.37
Total Iron (µM)	1462.56 ± 150.66	3460.37 ± 787.53	2017.01 ± 82.45	45.83 ± 6.49
Benzene (mg/L)	0.000 ± 0.000	0.012 ± 0.002	0.007 ± 0.001	0.0067 ± 0.0006
Ethylbenzene (mg/L)	0.000 ± 0.000	0.0054 ± 0.0012	0.0007 ± 0.0001	0.001 ± 0.000
Xylene (mg/L)	0.000 ± 0.000	0.028 ± 0.006	0.002 ± 0.000	0.003 ± 0.001
Toluene (mg/L)	0.000 ± 0.000	0.008 ± 0.005	0.000 ± 0.000	0.000 ± 0.000
Non-Particulate Organic Carbon (NPOC) (mg/L)	4.72 ± 0.76	3.04 ± 0.11	4.36 ± 0.86	3.29 ± 0.27
Total Nitrogen (TN) (mg/L)	0.57 ± 0.14	0.48 ± 0.17	0.73 ± 0.01	0.73 ± 0.19
Nitrates & Nitrites (mg/L)	1.95 ± 0.82	0.66 ± 0.24	0.97 ± 0.00	26.55 ± 5.64
Phosphate (PO_4) (mg/L)	0.0023 ± 0.0015	0.0023 ± 0.0019	0.0050 ± 0.0000	0.0168 ± 0.0054
Water Temperature (ºC)	20.10 ± 4.45	21.25 ± 2.46	11.65 ± 0.35	18.89 ± 3.43
Air Temperature (ºC)	17.4 ± 6.8	17.4 ± 6.8	5.8 ± 2.8	17 ± 7.2
Salinity (ppt)	0.17 ± 0.00	0.21 ± 0.00	0.19 ± 0.00	0.18 ± 0.01
Dissolved Oxygen (DO) (mg/L)	5.44 ± 1.49	2.23 ± 0.65	6.30 ± 0.02	5.88 ± 0.29
pH	6.6 ± 0.3	6.4 ± 0.1	6.5 ± 0.0	6.5 ± 0.2

Supplemental Table 2.2: The genera of iron-reducing bacteria present in 16S amplicon sequences from the iron mat samples. Averages of the percent relative abundance of each genera from downstream and upstream of the leaking underground storage tank are represented below. References used to hypothesize function of genera as iron-reducers are in the "Reference" column.

Genus	Downstream Average (% relative abundance)	Upstream Average (% relative abundance)	Reference
Geobacter	0.558	0.738	(1)
Shewanella	0.002	0.011	(1)
Rhodoferax	0.004	0.006	(1)
Geobacteraceae (family – unclassified genus)	0.0005	0	(1)
Geothrix	0.179	0.211	(2)
Desulfuromonas	0.011	0.005	(3)

Supplemental Table 2.3: The genera of sulfate-reducing bacteria present in 16S amplicon sequences from the iron mat samples. Averages of the percent relative abundance of each genera from downstream and upstream of the leaking underground storage tank are represented below. References used to hypothesize function of genera as sulfate-reducers are in the "Reference" column.

Genus	Downstream Average	Upstream Average	Reference
Desulfobacter	0.0005	0	(4)
Desulfobacterium	0.002	0.004	(4)
Desulfobacula	0.003	0.001	(5)
Desulfobulbus	0.023	0.049	(5)
Desulfomonile	0.001	0.022	(4)
Desulfosporosinus	0.007	0.0007	(5)
Desulfovibrio	0.032	0.012	(5)
Thermodesulfovibrio	0.003	0.003	(5)
Desulfomicrobium	0.006	0.024	(5)
Desulfobacteraceae (family – unclassified genus)	0.013	0.037	(5)
Desulfobacterales (family – unclassified genus)	0.025	0.017	(5)
Desulfuromonadales (family – unclassified genus)	0.008	0.019	(6)
Desulfatirhabdium	0.01	0.009	(7)
Desulforegula	0.005	0.0007	(8)
Desulfatiferula	0.002	0.001	(9)
Desulfopila	0.001	0.0003	(10)
Desulfovibrionales (family – unclassified genus)	0	0.001	(5)
Desulfovibrionaceae (family – unclassified genus)	0.0004	0	(11)
Syntrophobacteer	0.0006	0.008	(12)

Supplemental Table 2.4: Description of high-quality metagenome assembled genomes (MAGs) obtained from iron mats in Town Creek, Greenville, NC. MAG completeness and contamination were calculated using CheckM v. 1.0.18 (13). All MAGs were assigned taxonomy using MetaSanity v. 1.2.0 (14). MAG size and GC content were calculated using RASTtk (15-17).

MAG#	Sample Location	Bin Method	Complete (%)	Contamination (%)	Identification (g=genus, f=family, c=class)	Genome Size (Mbp)	GC Content (%)
1	U – SE 2	Concoct	78.34	5.02	*Phycorickettsia* (g)	1.09	34.5
2	U – SE 2	Maxbin	93.25	1.1	*Gallionella* (g)	2.53	52.9
3	U – SE 3	Concoct	95.73	2.02	Burkholderiaceae (f)	3.16	64.7
4	U – SE 3	Concoct	92.97	1.63	Beijerinckiaceae (f)	3.08	67.0
5	U – SE 3	Concoct	65.35	4.32	*Leadbetterella* (g)	2.98	38.0
6	U – SE 3	Concoct	96.92	0.74	*Cloacibacterium* (g)	3.06	32.8
7	U – SE 4	Concoct	99.76	1.94	*Acinetobacter* (g)	3.75	38.3
8	U – SE 4	Concoct	84.73	2.83	*Thermomonas* (g)	2.12	70.5
9	U – SE 4	Concoct	73.34	4.67	Sphingomonadaceae (f)	2.71	57.8
10	U – SE 4	Concoct	95.34	6.64	*Phycorickettsia* (g)	1.40	34.5
11	U – SE 4	Concoct	72.41	5.17	*Sphingomonas(A)* (g)	1.76	66.2
12	Da – SE 1	Concoct	66.17	2.83	*Pelomonas* (g)	3.14	70.0
13	Da – SE 1	Concoct	84.87	1.17	Burkholderiaceae (f)	3.23	64.1
14	Da – SE 1	Metabat	59.5	9.8	Methylomonadaceae (f)	2.42	44.1
15	Da – SE 1	Metabat	97.71	4.67	Burkholderiaceae (f)	2.84	61.0
16	Da – SE 2	Maxbin	99.35	1.87	Burkholderiaceae (f)	2.74	61.0
17	Da – SE 3	Concoct	91.43	3.35	*Gallionella* (g)	2.22	62.6
18	Da – SE 3	Concoct	99.81	2.04	Burkholderiaceae (f)	3.53	63.9
19	Da – SE 4	Concoct	95.66	0.21	*Gallionella* (g)	2.30	53.2
20	Da – SE 4	Concoct	70.09	0.95	Gracilibacteria (c)	1.22	39.5
21	Da – SE 4	Concoct	95.32	0.69	Methylomonadaceae (f)	2.91	41.3
22	Da – SE 4	Concoct	99.58	3.57	Burkholderiaceae (f)	3.41	64.3
23	Da – SE 4	Concoct	94.22	0.35	Methylomonadaceae (f)	2.96	41.3
24	Db – SE 1	Concoct	88.13	3.13	*Gallionella* (g)	2.09	53.6
25	Db – SE 1	Concoct	94.33	6.87	*Gallionella* (g)	2.12	51.0
26	Db – SE 1	Concoct	96.57	0.98	Burkholderiaceae (f)	2.75	61.0
27	Db – SE 2	Concoct	98.17	1.67	*Gallionella* (g)	2.25	51.0
28	Db – SE 2	Concoct	93.51	0.76	Burkholderiaceae (f)	2.58	61.0
29	Db – SE 2	Maxbin	87.13	3.24	*Gallionella* (g)	2.35	53.3

Supplemental Table 2.5: Putative Leptothrix spp. MAGs searched for iron oxidation genes using the HMMs in FeGenie (18). Possible iron oxidation genes with HMMs are Cyc1, Cyc2_repCluster1, Cyc2_repCluster2, Cyc2_repCluster3, FoxA, FoxB, FoxC, FoxE, FoxY, FoxZ, MtoA, MtrB_TIGR03509, and suflocyanin. Here we present the MAGs that were classified by MetaSanity as being in the family Burkholderiaceae, with each X representing an open reading frame in that MAG as being the gene in the first row.

MAG #	Cyc1	Cyc2_repCluster1	MtrB_TIGR03509	MtoA
3		X		
13				
15	X	X	X	X
16	X	X		
18	X	X		
22	X	X		
26	X	X		
28	X	X		

Supplemental Table 2.6: Metagenome assembly quality statistics calculated using the MetaQUAST function in QUAST v. 5.0.2 (19). The interpretation of each value can be read about in the QUAST manual (http://quast.sourceforge.net/docs/manual.html; Accessed 2021JAN26). Briefly, the "Genome Fraction (%)" is the percentage of aligned bases to the reference genome. As no reference genome was provided, MetaQUAST called BLASTN to align contigs to the SILVA 16S rRNA database and the 50 reference genomes with the top alignment scores were chosen.

Sample	Genome Fraction (%)	# Misassemblies	# Contigs	# Contigs ≥ 1,000 bp	# Contigs ≥ 50,000 bp	Largest Contig (bp)	Total Length (bp)	N50	L50
U1	78.804	10	73,668	15,862	1	56,329	70,497,637	929	18,194
U2	0.248	11	94,743	15,437	5	68,160	81,932,399	796	26,850
U3	0.419	20	146,638	26,524	32	357,575	134,208,763	855	38,458
U4	0.173	14	123,682	29,277	21	357,707	123,454,918	1017	28,398
Da1	56.622	3	116,521	20,427	12	131,329	103,617,361	827	32,208
Da2	22.942	22	29,106	4,644	5	96,818	26,093,544	813	7,344
Da3	34.084	13	142,409	32,539	49	452,140	145,282,894	1,009	31,954
Da4	37.425	11	163,329	33,808	116	587,965	166,293,253	975	35,766
Db1	21.919	13	76,123	16,525	14	141,907	76,414,582	980	16,905
Db2	23.388	23	90,221	22,283	24	174,066	92,447,762	1050	20,501
Average± Standard Error	27.60 ±8.11	14 ±1.94	105,644 ±12,872.08	21,687.3 ±2872.78	27.9 ±10.80	242,399.6 ± 58,046.75	102,024,311 ± 13,085,240	925.1 ± 29.88	25,657.8 ± 3,076.44

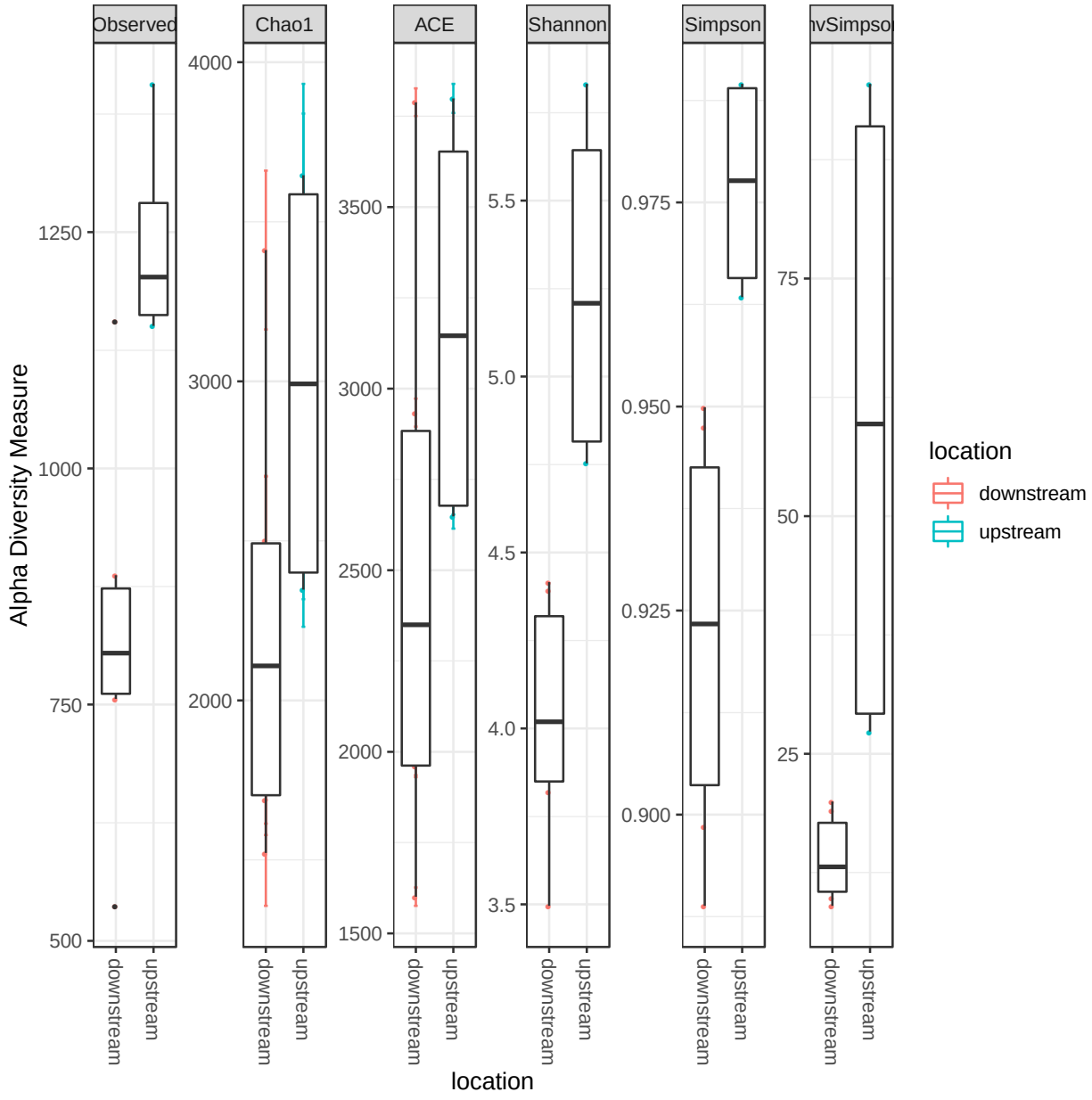

Supplemental Figure 2.1: Alpha diversity indices for up- and downstream iron mats were compared using a Mann-Whitney-Wilcoxon test in R v. 3.5.2. Observed Species Richness (U = 1, p = 0.02518), Shannon Diversity Index (U = 0, p = 0.01421), Simpsons Diversity Index (U = 0, p = 0.01421), and Inverse Simpsons Diversity Index (U = 0, p = 0.1421) were all significantly different between upstream and downstream iron mats. Also plotted are Chao1 and ACE alpha diversity indices.

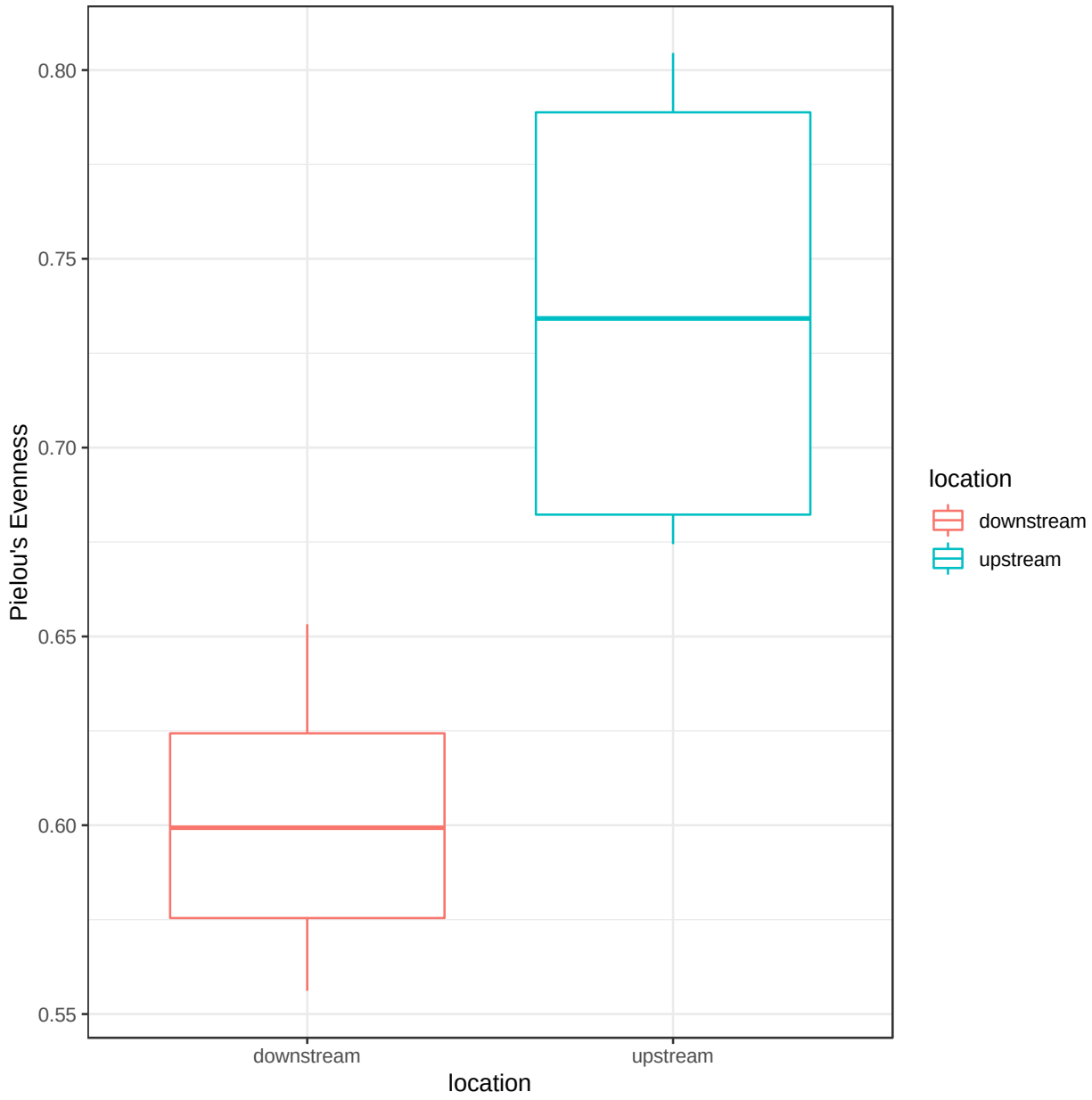

Supplemental Figure 2.2: Pielou's evenness, plotted here for downstream (red) and upstream (blue) iron mat microbial communities, was significantly different between upstream and downstream iron mats (ANOVA F = 17.43, p = 0.0031).

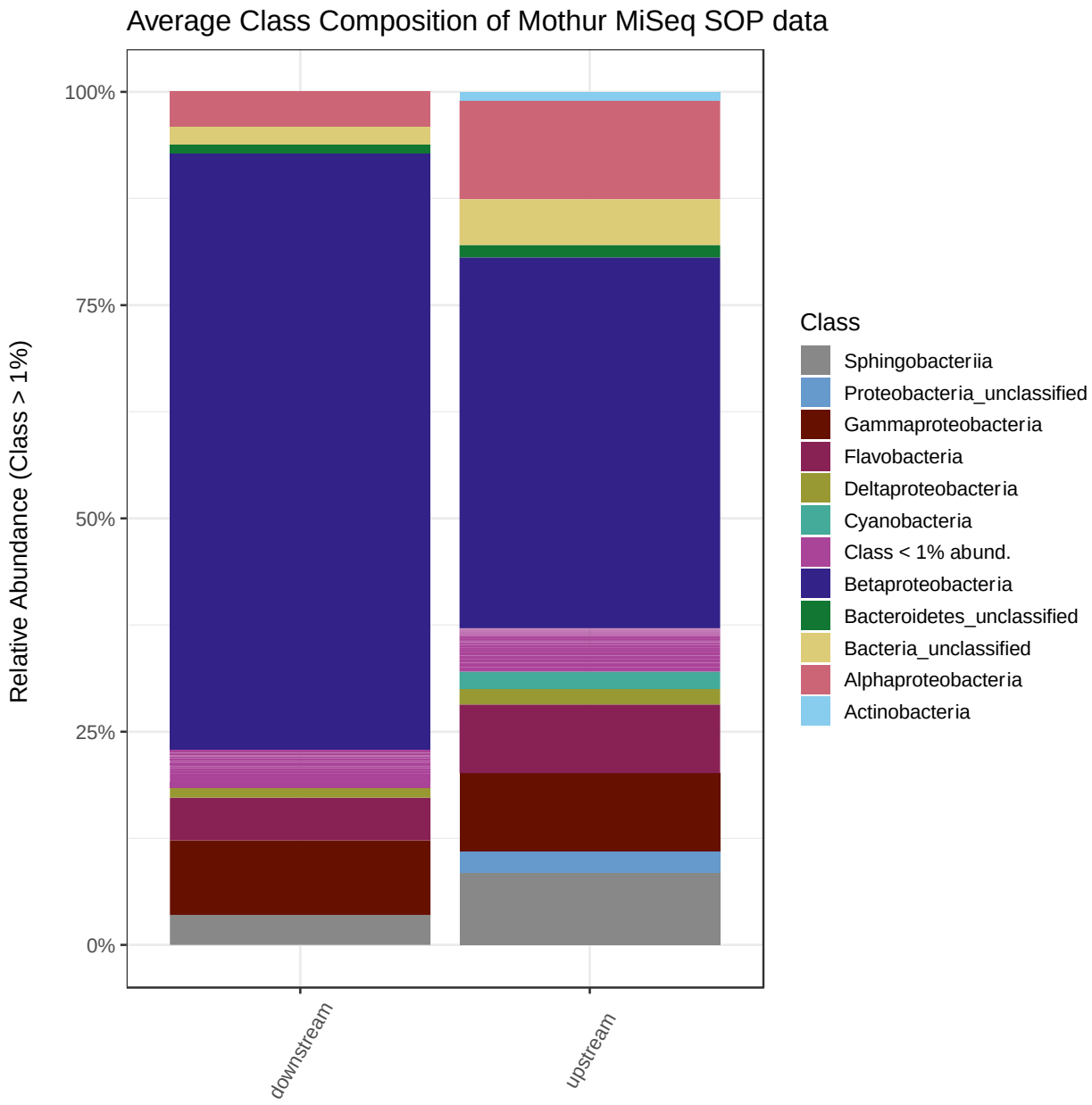

Supplemental Figure 2.3: Relative abundances of each class calculated and averaged by location (up- or downstream). Classes < 1% relative abundance were grouped above under the magenta color. The class Betaproteobacteria had the greatest average relative abundance both up- and downstream from the leaking underground storage tank.

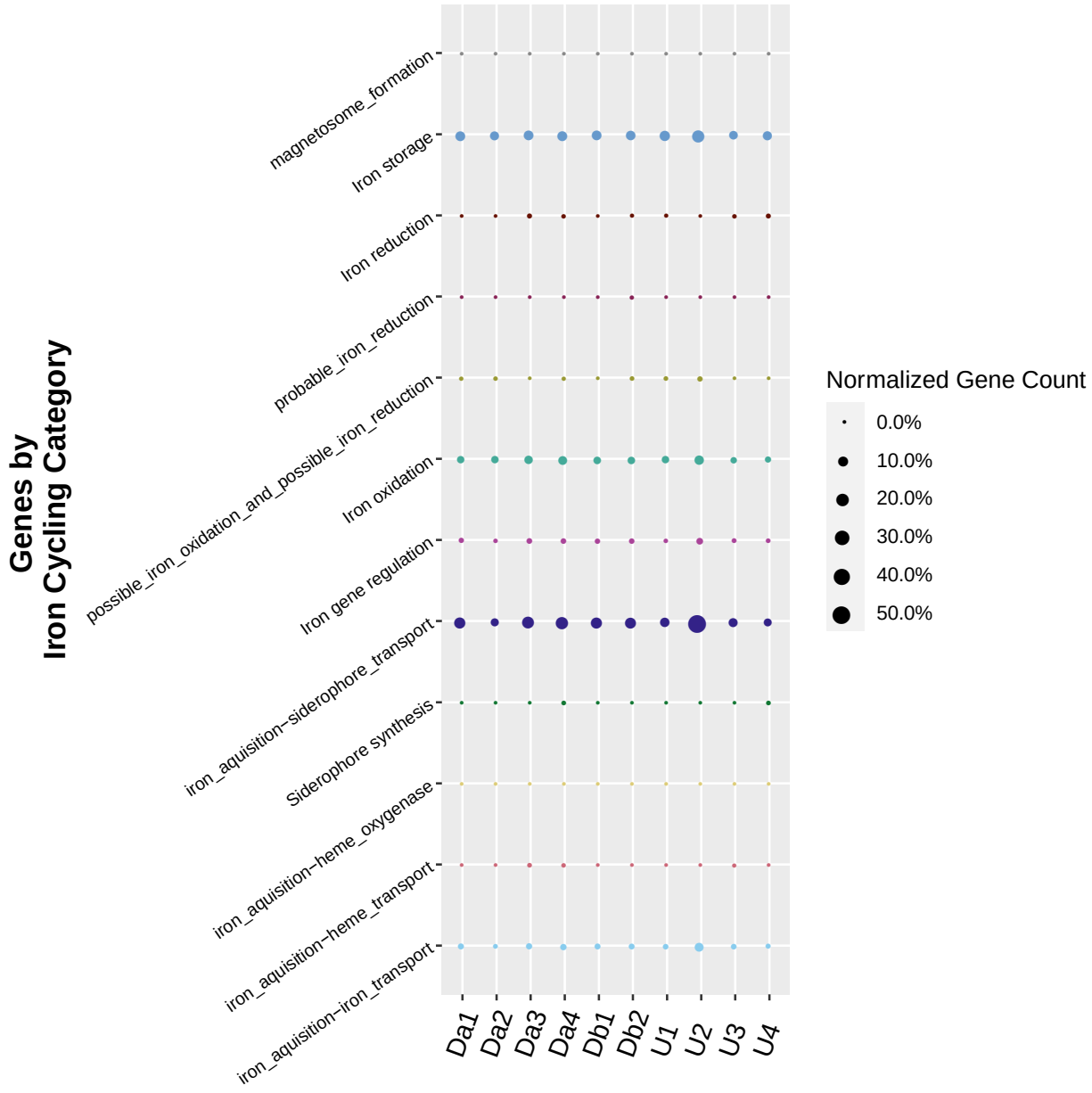

Supplemental Figure 2.4: Metagenome contig assembly iron-cycling gene count. Metagenome contig assemblies were assessed for iron-cycling genes using FeGenie v. 1 (18). All assemblies returned 0 heme oxygenase or magnetosome sequences, suggesting a paucity of magnetotactic

organisms. However, all other iron-cycling gene sequences targeted by the program returned relatively high proportions of total open reading frames (ORFs) in the assemblies. Siderophore transport was the highest at 50% of U2 ORFs.

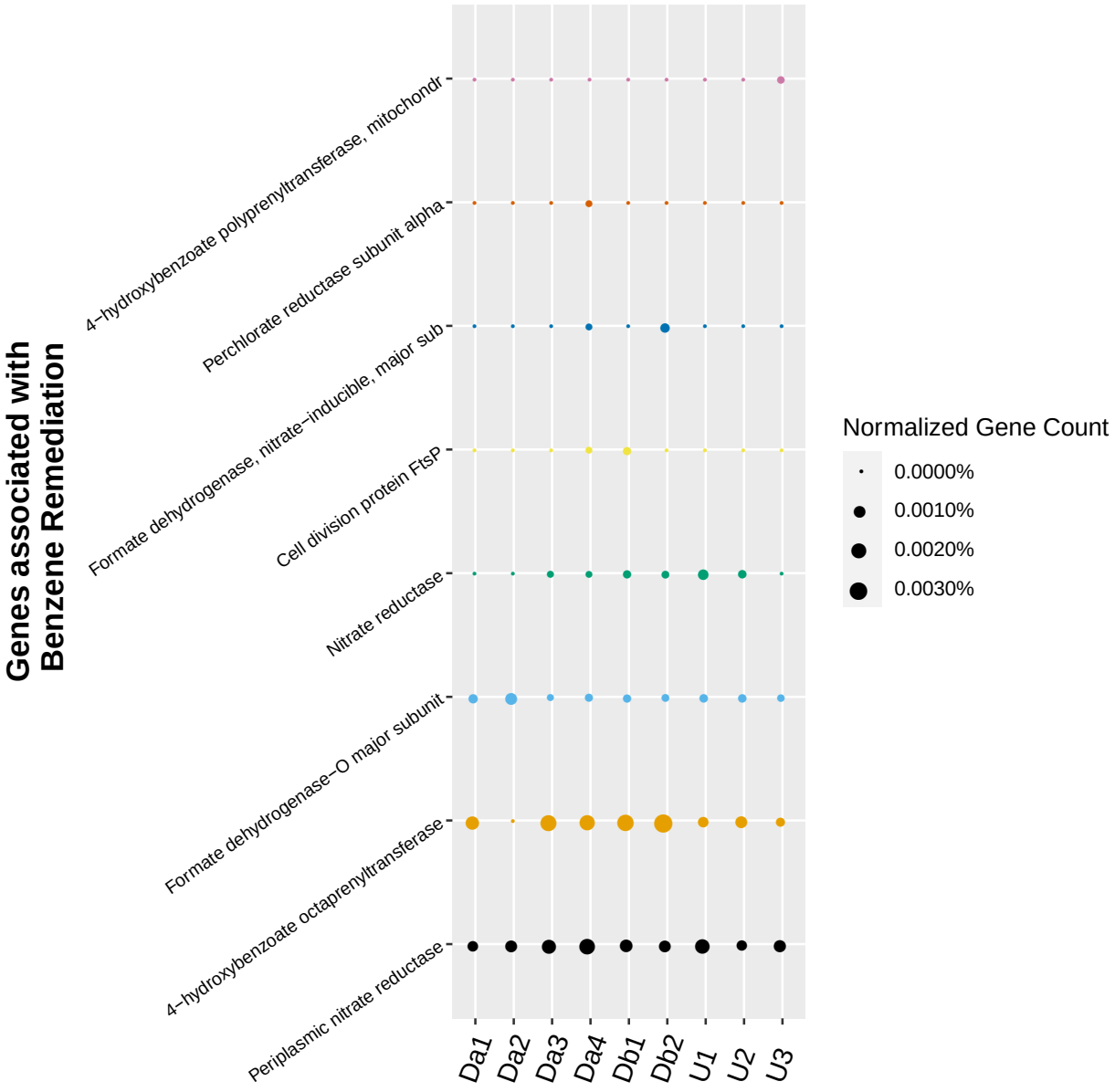

Supplemental Figure 2.5: Metagenome contig assembly benzene-remediation gene count. Metagenome contig assemblies were assessed for benzene-remediation associated genes using a hidden markov model. Gene counts were normalized for total open reading frames (ORFs). The

normalized abundance of benzene-remediation genes was very low, which correlates with the very low relative abundance of 16S sequences associated with benzene-remediating taxa.

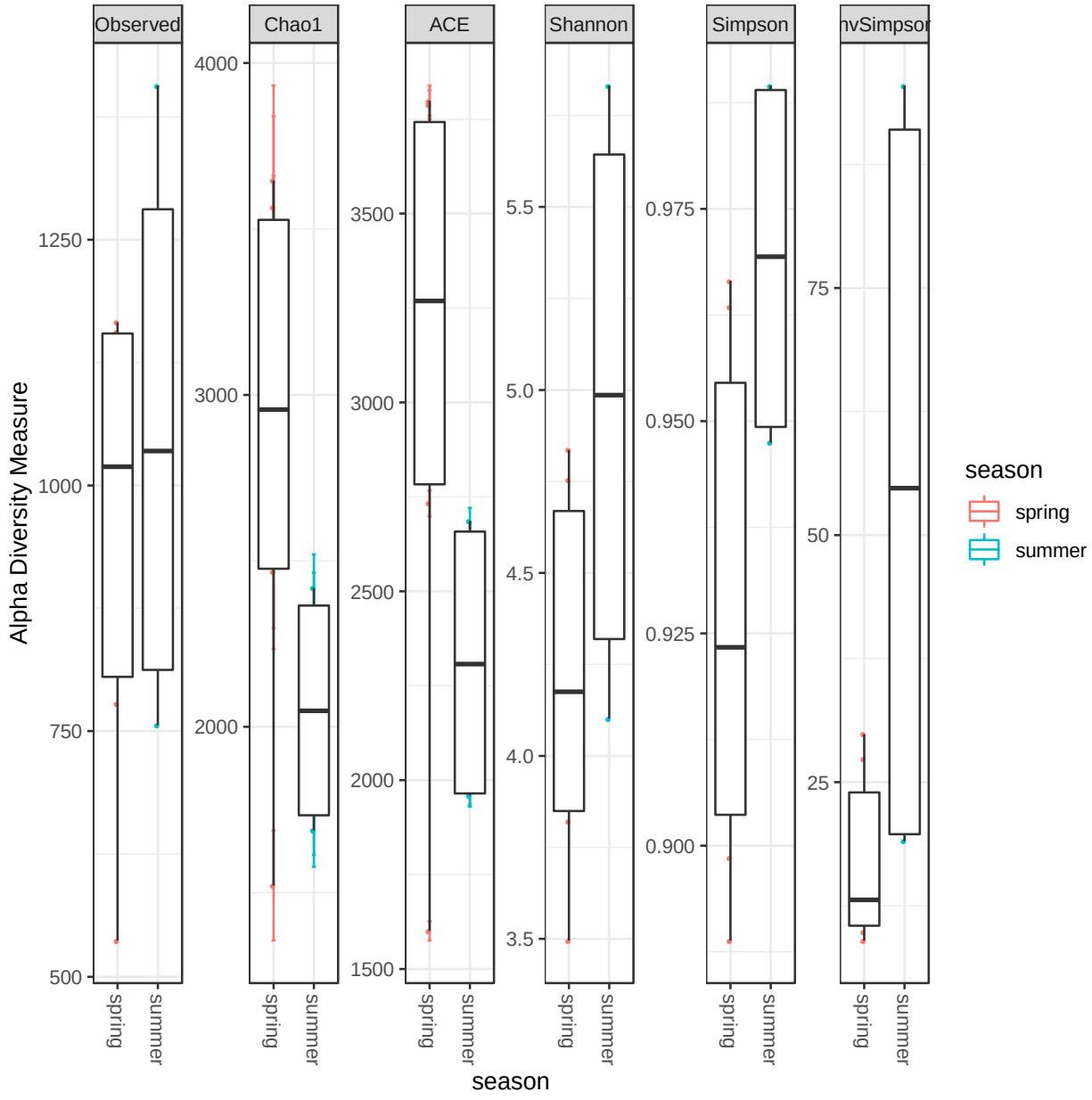

Supplemental Figure 2.6: Alpha diversity indices compared by season using a Mann-Whitney-Wilcoxon test in R v. 3.5.2. There were no significant differences observed between seasons.

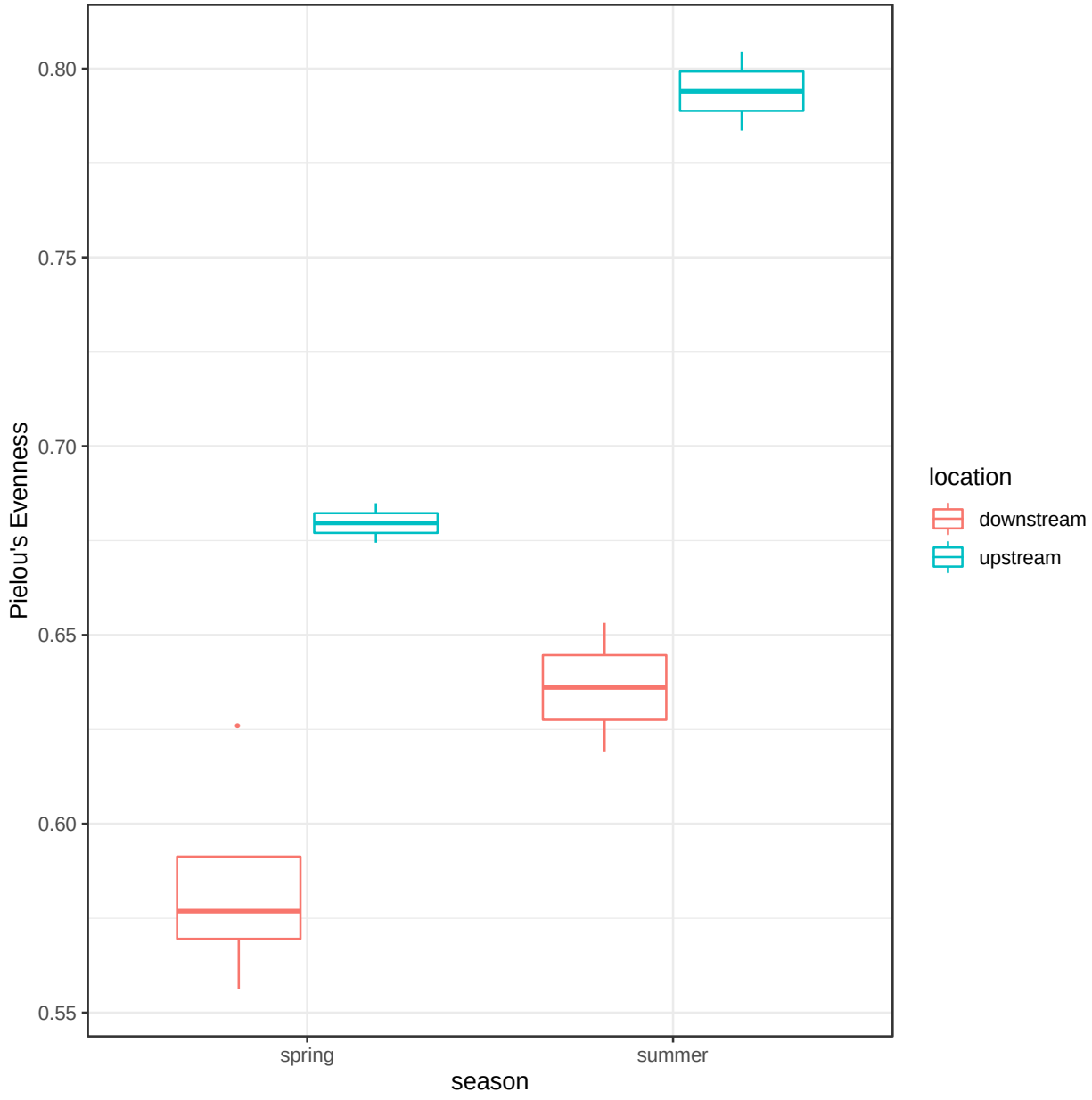

Supplemental Figure 2.7: Pielou's Evenness compared by season. Pielou's Evenness was not significantly different when seasons were compared, however significance was preserved using a model for both season and location (aov(pielou ~ season + location)) (ANOVA season F = 28.77, p = 0.001, location F = 42.58, p = 0.0003).

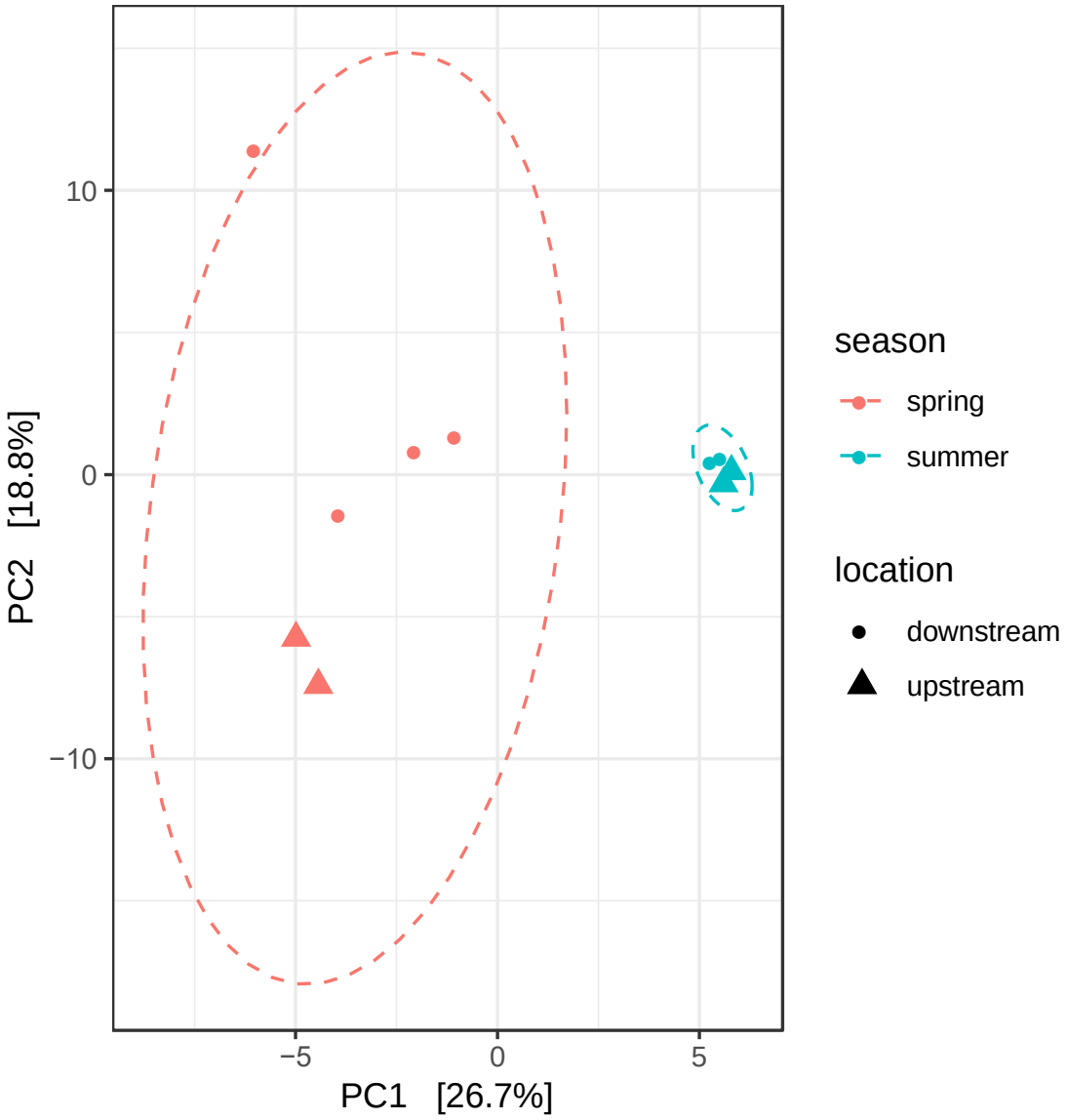

Supplemental Figure 2.8: Principle components analysis (PCA) of up- and downstream mats by season performed using a redundancy analysis (RDA) of the nine possible axes for the iron mat community data, showing the first two components which explain 26.7% and 18.8% of the total variance explainable by the data collected. Differences between seasons was significant (ADONIS R^2 = 0.25393, p = 0.004, strata = season) suggesting that iron mat communities have a strong signature of species change between seasons.

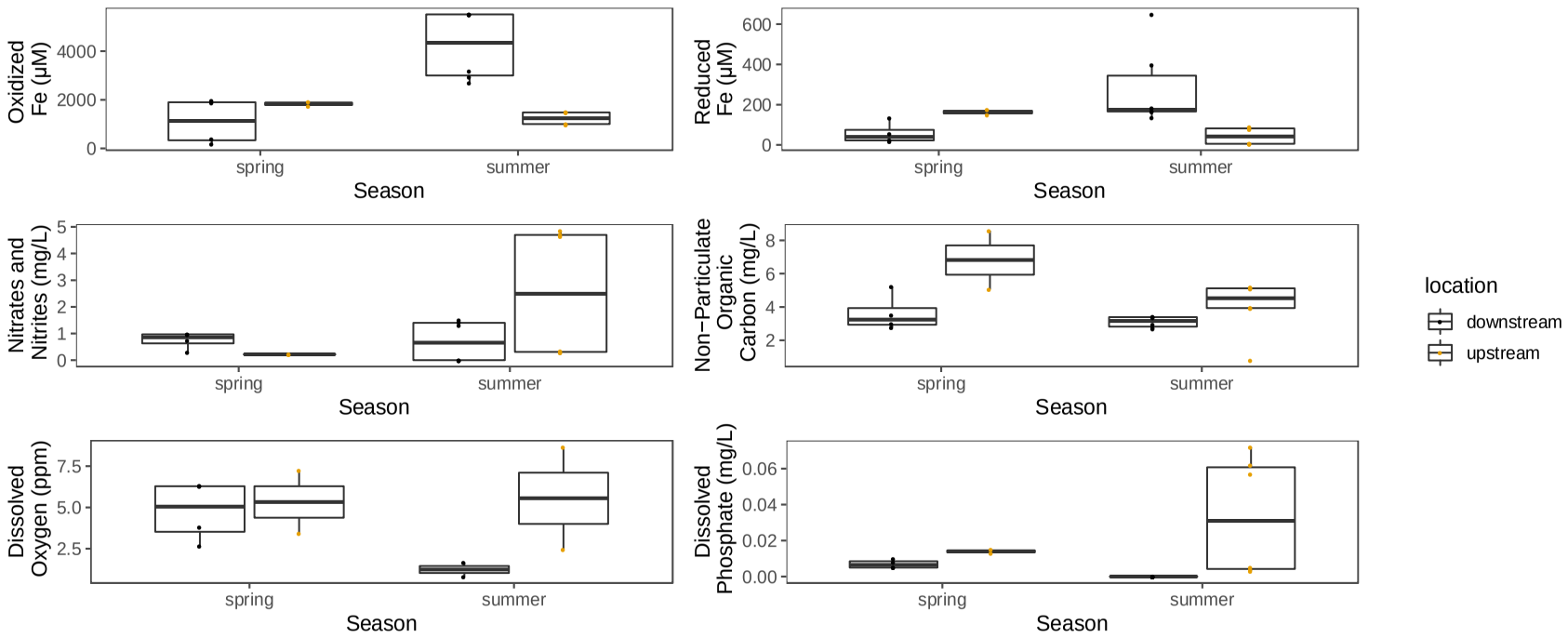

Supplemental Figure 2.9: Comparison of geochemistry between up- and downstream iron mats by season. Both up- (yellow) and downstream (black) mat types were grouped by season, spring (S1 and S2) or summer (S3 and S4) (water samples were excluded) and plotted by concentration of oxidized iron, reduced iron, nitrates and nitrites, non-particulate organic carbon, dissolved oxygen, and dissolved phosphate. Downstream mats had lower concentrations of oxidized and reduced iron in spring samples than downstream mats from the summer. However, downstream spring mats had higher concentrations dissolved oxygen than downstream summer mats. There was greater variation in concentrations of nitrates and nitrites and dissolved phosphate among the summer upstream mats than the spring upstream mats. The increased difference in concentrations of dissolved oxygen between upstream and downstream mats in the summer may have contributed to the community structuring observed using canonical correspondence analysis.

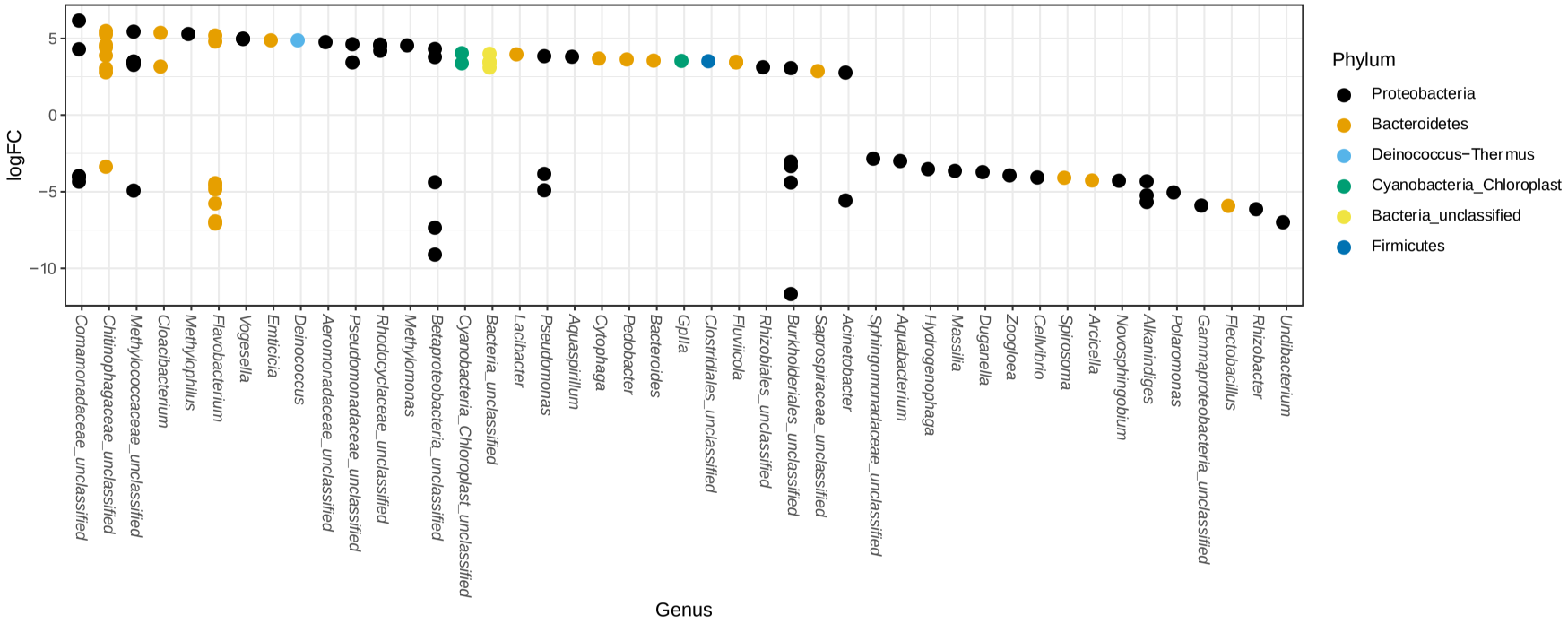

Supplemental Figure 2.10 : Differential abundances of taxa between iron mats sampled in spring and summer were calculated from an independently filtered data set. Genera with differential abundances with an alpha < 0.001 were plotted. Each point on the plot represents a single OTU sequence. Points with a log Fold Change greater than zero are over-expressed in the summer sampled iron mat communities, whereas OTUs with a log-fold change less than zero are over-expressed in spring communities.

References

1. Kim S-J, Koh D-C, Park S-J, Cha I-T, Park J-W, Na J-H, Roh Y, Ko K-S, Kim K, Rhee S-K. 2012. Molecular analysis of spatial variation of iron-reducing bacteria in riverine alluvial aquifers of the Mankyeong River. The Journal of Microbiology 50:207-217.
2. Coates JD, Ellis DJ, Gaw CV, Lovley DR. 1999. Geothrix fermentans gen. nov., sp. nov., a novel Fe(III)-reducing bacterium from a hydrocarbon-contaminated aquifer. Int J Syst Evol Microbiol 49:1615-1622.
3. Coates JD, Lonergan DJ, Philips EJP, Jenter H, Lovley DR. 1995. *Desulfuromonas palmitatis* sp. nov., a marine dissimilatory Fe(III) reducer that can oxidize long-chain fatty acids. Arch Microbiol 164:406-413.
4. Li X, Lan S-m, Zhu Z-p, Zhang C, Zeng G-m, Liu Y-g, Cao W-c, Song B, Yang H, Wang S-f, Wu S-h. 2018. The bioenergetics mechanisms and applications of sulfate-reducing bacteria in remediation of pollutants in drainage: A review. Ecotoxicol Environ Saf 158:162-170.
5. Leloup J, Fossing H, Kohls K, Holmkvist L, Borowski C, Jørgensen BB. 2009. Sulfate-reducing bacteria in marine sediment (Aarhus Bay, Denmark): abundance and diversity related to geochemical zonation. Environ Microbiol 11:1278-1291.
6. Greene AC. 2014. The Family *Desulfuromonadaceae*, p 143-155. *In* Rosenberg E, DeLong EF, Lory S, Stackebrandt E, Thompson F (ed), The Prokaryotes: Deltaproteobacteria and Epsilonproteobacteria doi:10.1007/978-3-642-39044-9_380. Springer Berlin Heidelberg, Berlin, Heidelberg.
7. Balk M, Altinbaş M, Rijpstra WI, Sinninghe Damsté JS, Stams AJ. 2008. *Desulfatirhabdium butyrativorans* gen. nov., sp. nov., a butyrate-oxidizing, sulfate-

reducing bacterium isolated from an anaerobic bioreactor. Int J Syst Evol Microbiol 58:110-5.

8. Rees GN, Patel BK. 2001. *Desulforegula conservatrix* gen. nov., sp. nov., a long-chain fatty acid-oxidizing, sulfate-reducing bacterium isolated from sediments of a freshwater lake. Int J Syst Evol Microbiol 51:1911-1916.

9. Cravo-Laureau C, Labat C, Joulian C, Matheron R, Hirschler-Réa A. 2007. *Desulfatiferula olefinivorans* gen. nov., sp. nov., a long-chain n-alkene-degrading, sulfate-reducing bacterium. Int J Syst Evol Microbiol 57:2699-2702.

10. Suzuki D, Ueki A, Amaishi A, Ueki K. 2007. Desulfopila aestuarii gen. nov., sp. nov., a Gram-negative, rod-like, sulfate-reducing bacterium isolated from an estuarine sediment in Japan. Int J Syst Evol Microbiol 57:520-526.

11. Kuever J. 2014. The Family *Desulfovibrionaceae*, p 107-133. *In* Rosenberg E, DeLong EF, Lory S, Stackebrandt E, Thompson F (ed), The Prokaryotes: Deltaproteobacteria and Epsilonproteobacteria doi:10.1007/978-3-642-39044-9_272. Springer Berlin Heidelberg, Berlin, Heidelberg.

12. Mizuno K, Morishita Y, Ando A, Tsuchiya N, Hirata M, Tanaka K. 2012. Genus-specific and phase-dependent effects of nitrate on a sulfate-reducing bacterial community as revealed by dsrB-based DGGE analyses of wastewater reactors. World Journal of Microbiology and Biotechnology 28:677-686.

13. Parks DH, Imelfort M, Skennerton CT, Hugenholtz P, Tyson GW. 2015. CheckM: assessing the quality of microbial genomes recovered from isolates, single cells, and metagenomes. Genome Res 25:1043-1055.

14. Neely CJ, Graham ED, Tully BJ. 2020. MetaSanity: an integrated microbial genome evaluation and annotation pipeline. Bioinformatics 36:4341-4344.

15. Brettin T, Davis JJ, Disz T, Edwards RA, Gerdes S, Olsen GJ, Olson R, Overbeek R, Parrello B, Pusch GD. 2015. RASTtk: a modular and extensible implementation of the RAST algorithm for building custom annotation pipelines and annotating batches of genomes. Sci Rep 5:8365.

16. Overbeek R, Olson R, Pusch GD, Olsen GJ, Davis JJ, Disz T, Edwards RA, Gerdes S, Parrello B, Shukla M. 2014. The SEED and the Rapid Annotation of microbial genomes using Subsystems Technology (RAST). Nucleic Acids Res 42:D206-D214.

17. Aziz RK, Bartels D, Best AA, DeJongh M, Disz T, Edwards RA, Formsma K, Gerdes S, Glass EM, Kubal M. 2008. The RAST Server: rapid annotations using subsystems technology. BMC Genomics 9:1-15.

18. Garber AI, Nealson KH, Okamoto A, McAllister SM, Chan CS, Barco RA, Merino N. 2020. FeGenie: A Comprehensive Tool for the Identification of Iron Genes and Iron Gene Neighborhoods in Genome and Metagenome Assemblies. Front Microbiol 11.

19. Gurevich A, Saveliev V, Vyahhi N, Tesler G. 2013. QUAST: quality assessment tool for genome assemblies. Bioinformatics 29:1072-1075.

APPENDIX C: Supporting Experimental Procedures & Figures – Chapter Three

Site Descriptions and Sampling

Sediment samples were taken from two study sites, along the Neuse River (Supplemental Figure S1, Supplemental Table S1). Sediment samples for the co-culture experiment were collected from Cedar Island and Fisher's Landing from the top centimeter of sediment. These sediment samples were chosen for inoculation as both FeOB and SRB are known to be present in coastal sediments and where visual orange oxides and black sulfides, the waste products of their metabolism, were present. Additional environmental samples were collected from stainless steel coupons deployed for 6-8 weeks at Wright's Creek (35.390018, -76.583338) and Pin Oak Court (34.954849, -76.707440) (Garrison et al., 2019). These samples were chosen for inclusion as previous studies indicated FeOB and SRB are both present on steel (Lv et al., 2019).

Media Preparation

Gradient tubes were prepared for inoculation following Emerson and Floyd (2005). Briefly, sterilized glass tubes contained a 500 µL bottom layer that consisted of agarose-stabilized iron-sulfide (FeS). Once the bottom layer had hardened (approximately 10 minutes) 3.7 mL of semi-solid top layer media, either Estuary Media (EM), which is approximately 18 ppt, or Modified Wolfe's Mineral Media (MWMM), which is approximately 0 ppt, was added. EM is an approximately 50/50 mixture of MWMM and Artificial Seawater (Emerson and Floyd, 2005; Field et al., 2016). There was 0.2 g and 3.49g $MgSO_4 \cdot 7H_2O$ per liter of MWMM and EM, respectively. No additional sulfate addition was necessary in modifying either media to induce SRB growth. The media in all of the gradient tubes was stabilized to pH 6. The iron and oxygen

gradients were allowed to stabilize overnight at 25ºC with a 100% N_2 headspace prior to inoculation.

Sample Culturing

The same day as sample collection, 100 µL of sediment slurry was inoculated from either Cedar Island or Fisher's Landing in each gradient tube. Two of each sediment type were left at ambient atmospheric oxygen (21% O_2) and four of each sediment type were sparged for 30 seconds 1% O_2 gas mix (1% O_2 / 4% CO_2 / 95% N_2). This procedure was repeated once in tubes using Estuary Media and once in tubes using MWMM. After one week's incubation half of the 1% O_2 tubes were opened for 30 seconds to allow for the oxygen in the headspace to return to atmospheric levels (Table 1).

DNA Extraction

Gradient tubes were inoculated and incubated for one week prior to DNA extraction. One week of incubation was all that was needed for the propagated cultures which had previously undergone dilution to extinction to begin forming visible precipitates. All of the media from ten replicate tubes was transferred to a 15 mL conical tube and homogenized. 1 mL of the homogenized sample was transferred to a 1.5 mL centrifuge tube and heated for 5 minutes at 70ºC to melt the low-melt agarose. Samples were then centrifuged at 14,000 rpm for 10 minutes. The supernatant was removed, and the sample pellet was resuspended in either 1 mL of sterile Estuary or Modified Wolfe's Mineral Media. Again, the sample was centrifuged at 14,0000 rpm for 8 minutes and the supernatant was removed. 250 µL of pellet was transferred to a bead beater tube from the Qiagen DNeasy PowerSoil Kit (Qiagen, Germantown, MD). The kit was then used

according to manufacturer instructions with the following modification: DNA was eluted in 60 µL of 10 µM TRIS buffer, pH 8.

16S rDNA sequencing, and phylogenetic analysis

16S rDNA sequencing of the V1-V3 region was performed at RTL Genomics (Lubbock, TX, USA) using Illumina MiSeq. Sequences were processed using mothur v. 1.39.5 (Schloss et al., 2009; Schloss et al., 2011; Kozich et al., 2013) and the MiSeq SOP accessed 2017 October 25 (https://mothur.org/wiki/miseq_sop/) to identify present taxa (97% OTU threshold). Graphs were generated using the phyloseq package (McMurdie and Holmes, 2013) in R v. 3.5.2.

Microsensor Profiling

Samples were incubated for 2 weeks prior to microsensor profile characterization (Table S1). A profile of the oxygen and H_2S in each gradient tube was characterized using a H_2S microsensor (sensor type: H2S-50, outside tip diameter 50µm (Unisense A/S, Denmark)) and an oxygen microsensor (sensor type: OX-50, outside tip diameter 50µm (Unisense A/S, Denmark)). The Unisense instruments were calibrated and operated according to the manufacturer's instructions. Profiles were made by first introducing the microsensor to the surface of the estuary media at the top of the gradient tube where the signal was allowed to stabilize for at least 30 seconds. Each microsensor was used to measure concentrations in 5 mm intervals to create a profile throughout the growth media. H_2S (µmol/L) profiles were made first, followed by the O_2 (µmol/L) profiles. One gradient tube was profiled for each media/sample/headspace combination. Since the microsensors are very sensitive to vibrations, the measurements were

made on a heavy platform, which the micromanipulator, used to move the microsensors, was mounted on.

Supplemental Figure S3.1: Map of sampling sites. The green pins indicate sampling sites (see Tables 1, S1) on the Neuse and Pamlico Rivers in North Carolina. Inset images were taken on the day of sampling at the corresponding site. Map obtained from Google Earth Pro 7.3.2.776 and modified with site locations (green markers) and inset images.

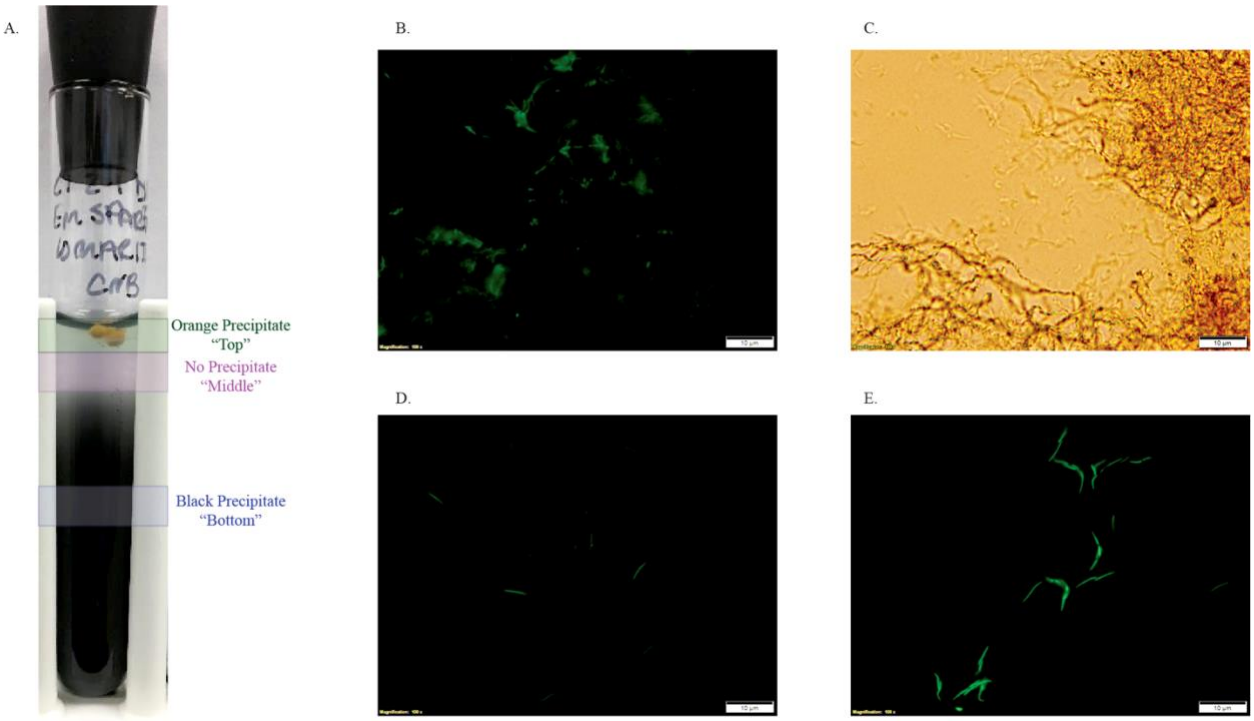

Supplemental Figure S3.2: Microbial growth in precipitate bands was confirmed using an Olympus BX-41 (Olympus, Melville, NY, USA) and SYTO-13. Subsamples from precipitate "bands" were taken as in A) at the top, middle, and bottom. Microscopy of the top layer B) indicated that there was microbial growth associated with C) the iron-oxides present in the culture. The middle D) also showed cells, but they exhibited cell morphology different from that in E) the bottom, where the black precipitate was being produced. All microscopy images were taken using cellSens (Olympus, Melville, NY, USA) at 100x magnification and the scale bar represents 10 µm.

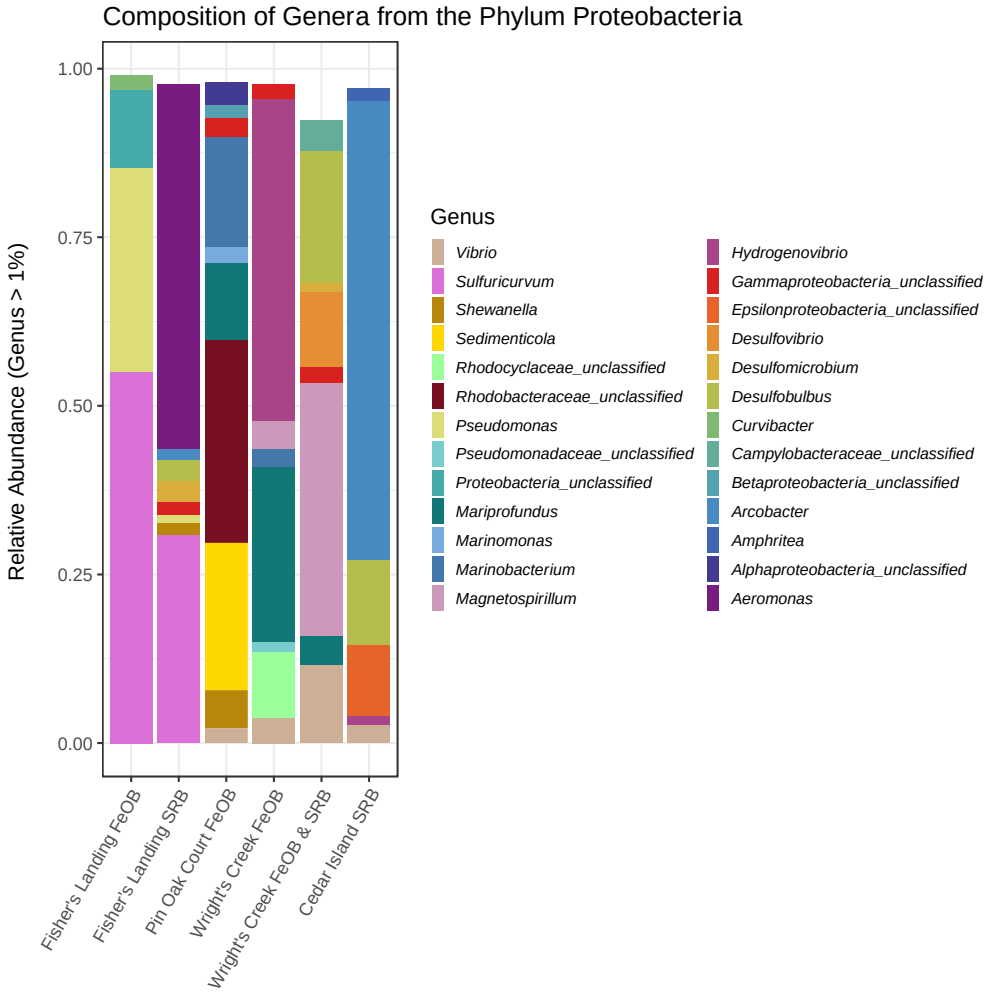

Supplemental Figure S3.3: The relative abundance of genera in the phylum Proteobacteria are represented here for samples from all four sampling sites. As the Fisher's Landing sample was not representative of estuarine community profiles it was not included in the O_2 and H_2S profiling. All other samples that demonstrated iron-oxide precipitates demonstrate *Mariprofundus* spp. presence. Cultures with black precipitate both demonstrated the presences of *Desulfobulbus* spp., which may be the representative SRB in those cultures.

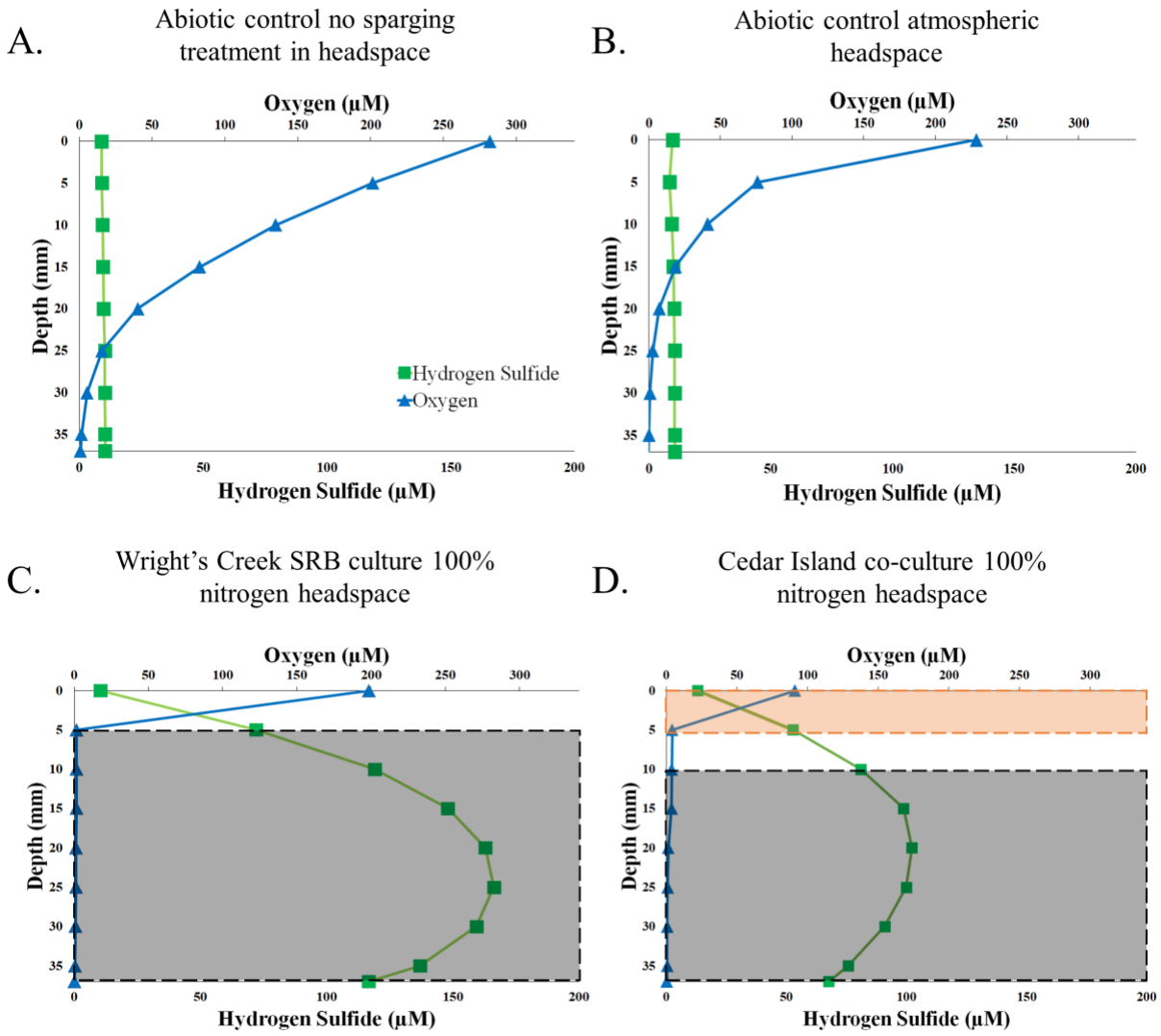

Supplemental Figure S3.4: Measurements of the (green) H2S and (blue) O2 concentrations (µmol/L) at depth in the gradient tube starting at the surface (0 mm). In panels representing cultures with (D) FeOB the orange shaded box indicates presence of iron-oxide precipitate (Fe(III) oxyhydroxides). Cultures with (C, D) SRB have a black shaded box indicating the presence of a black precipitate (FeS). The (A) abiotic control with no sparging treatment was tested the same length of time from gradient tube manufacture as the other gradient tubes. As the gradient tubes are not made anoxic, the concentration of O_2 throughout the depth of the gradient

tube steadily increased post-manufacture. The (B) abiotic control with an atmospheric headspace was exposed for 30 seconds to the atmosphere during the inoculation period. The (C, D) inoculated samples with a 100% nitrogen headspace were sparged with a 100% N_2 gas mix for 30 seconds following inoculation of the media, rather than atmospheric exposure or sparging with the 1% O_2 gas mix. The 100% N_2 sparged samples still exhibit O_2 resulting from that which was dissolved in the gradient tubes prior to inoculation.

References

Emerson, D., and Floyd, M.M. (2005) Enrichment and isolation of iron-oxidizing bacteria at neutral pH. *Methods in enzymology* **397**: 112-123.

Field, E., Kato, S., Findlay, A., MacDonald, D., Chiu, B., Luther III, G., and Chan, C. (2016) Planktonic marine iron oxidizers drive iron mineralization under low-oxygen conditions. *Geobiology* **14**: 499-508.

Garrison, C.E., Price, K.A., and Field, E.K. (2019) Environmental Evidence and Genomic Insight of Iron-oxidizing Bacteria Preference Towards More Corrosion Resistant Stainless Steel at Higher Salinities. *Appl Environ Microbiol*: AEM. 00483-00419.

Kozich, J.J., Westcott, S.L., Baxter, N.T., Highlander, S.K., and Schloss, P.D. (2013) Development of a dual-index sequencing strategy and curation pipeline for analyzing amplicon sequence data on the MiSeq Illumina sequencing platform. *Appl Environ Microbiol* **79**: 5112-5120.

Lv, M., Du, M., Li, X., Yue, Y., and Chen, X. (2019) Mechanism of microbiologically influenced corrosion of X65 steel in seawater containing sulfate-reducing bacteria and iron-oxidizing bacteria. *Journal of Materials Research and Technology* **8**: 4066-4078.

McMurdie, P.J., and Holmes, S. (2013) phyloseq: an R package for reproducible interactive analysis and graphics of microbiome census data. *PloS one* **8**.

Schloss, P.D., Gevers, D., and Westcott, S.L. (2011) Reducing the effects of PCR amplification and sequencing artifacts on 16S rRNA-based studies. *PloS one* **6**.

Schloss, P.D., Westcott, S.L., Ryabin, T., Hall, J.R., Hartmann, M., Hollister, E.B. et al. (2009) Introducing mothur: open-source, platform-independent, community-supported software for describing and comparing microbial communities. *Appl Environ Microbiol* **75**: 7537-7541.

APPENDIX D: Supplemental Table – Chapter Three

Table S3.1: Cultures used for H2S and O2 profiling included two SRB, one from Cedar Island and one from Wright's Creek, an FeOB from Pin Oak Court, and a mixed culture (FeOB and SRB) from Cedar Island. The gas headspace, sample type, and salinity at time of sampling of each culture are included. Where noted culture types were measured under multiple head space regimes.

Culture Type	Abiotic Control	Abiotic Control	Abiotic Control	Cedar Island SRB	Wright's Creek SRB	Pin Oak Court FeOB	Cedar Island Mixed Culture	Cedar Island Mixed Culture
Gas Headspace	Atmospheric (21% O_2)	100% N_2	1% O_2 / 4% CO_2 / 95% N_2	1% O_2 / 4% CO_2 / 95% N_2	100% N_2	1% O_2 / 4% CO_2 / 95% N	Atmospheric (21% O_2)	100% N_2
Sample Type	N/A	N/A	N/A	Sediment	Stainless Steel Coupon	Stainless Steel Coupon	Sediment	Sediment
Sample Salinity	N/A	N/A	N/A	10.5 ppt	9.0 ppt	9.2 ppt	10.5 ppt	10.5 ppt

APPENDIX E: Copyright Permissions – Chapter Three

JOHN WILEY AND SONS LICENSE
TERMS AND CONDITIONS

Feb 24, 2021

This Agreement between East Carolina University -- Chequita Brooks ("You") and John Wiley and Sons ("John Wiley and Sons") consists of your license details and the terms and conditions provided by John Wiley and Sons and Copyright Clearance Center.

License Number	5015550261714
License date	Feb 24, 2021
Licensed Content Publisher	John Wiley and Sons
Licensed Content Publication	Environmental Microbiology Reports
Licensed Content Title	Orange leads to black: evaluating the efficacy of co-culturing iron-oxidizing and sulfate-reducing bacteria to discern ecological relationships
Licensed Content Author	Chequita N. Brooks, Erin K. Field
Licensed Content Date	Feb 7, 2021
Licensed Content Volume	0
Licensed Content Issue	0

Licensed Content Pages	8
Type of use	Dissertation/Thesis
Requestor type	Author of this Wiley article
Format	Electronic
Portion	Full article
Will you be translating?	No
Title	Bacteria of a feather floc together: Microbial interactions and function within iron-oxidizing bacterial communities
Institution name	East Carolina University
Expected presentation date	Apr 2021
Requestor Location	East Carolina University 227 Turkey Creek 6237 NW 109th Place ALACHUA, FL 32615 United States Attn: East Carolina University
Publisher Tax ID	EU826007151
Total	0.00 USD

Terms and Conditions

APPENDIX F: Supplemental Tables & Figures – Chapter Four

Supplemental Table 4.1: Description of whole genome sequences (WGS) obtained from experimental cultures. WGS completeness, contamination, genome size, and GC content for mapped contigs were calculated using CheckM v. 1.0.18 (Parks et al. 2015). GC content of unmapped contigs was calculated using Geneious Prime® 2021.0.3 (Kearse et al. 2012).

Sample	Contamination (%)	Completeness (%)	Genome Size	GC Content (%) (mapped)	GC Content (%) (unmapped)
Experimental Reference	0.00	99.14	5285765	66.8	63.5
WT – 1	0.00	99.14	5282451	66.7	61.3
WT – 2	0.00	99.14	5284082	66.7	60.8
WT - 3	0.00	99.14	5287610	66.7	61.5
Intensifying Press – 1	0.00	99.14	5286193	66.7	65.1
Intensifying Press – 2	5.39	99.54	6650761	65.2	61.4
Intensifying Press – 3	76.57	100.00	9598156	65.6	63.7
Repeated Pulse – 1	2.35	99.67	6407628	65.2	60.4
Repeated Pulse – 2	0.00	99.14	5289573	66.7	64.5
Repeated Pulse – 3	43.90	100.00	8381078	65.4	64.5
Avg. WT	**0.00 ± 0.00**	**99.14 ± 0.00**	**5284714 ± 2636**	**66.7 ± 0.0**	**61.2 ± 0.4**
Avg. Intensifying Press	**27.32 ± 42.74**	**99.56 ± 0.43**	**7178370 ± 2203868**	**65.8 ± 0.8**	**63.4 ± 1.9**
Avg. Repeated Pulse	**15.42 ± 24.70**	**99.60 ± 0.43**	**6692760 ± 1565352**	**65.8 ± 0.8**	**63.13 ± 2.4**

Supplemental Table 4.2: Description of the mapped and unmapped nucleotide base content, number of contigs, and minimum and maximum contig length for the experimental reference (Reference), wild type (WT), intensifying press (Press), and repeated pulse (Pulse). These data were collected using Geneious Prime® 2021.0.3 (Kearse et al. 2012).

Sample	Mapping Status	A%	T%	C%	G%	GC%	N%	Number of Contigs	Min Contig Length	Max Contig Length	Mean Contig Length
Reference	Mapped	16.7	16.6	33.2	33.5	66.7	0	80	678	487745	66072
Reference	Unmapped	16.2	20.3	34.2	29.3	63.5	0	4	846	1891	1430
WT - 1	Mapped	16.6	16.7	33.1	34.0	66.7	0	52	678	514978	101586
WT - 1	Unmapped	17.7	20.9	29.2	32.0	61.3	0	6	726	2237	1443
WT - 2	Mapped	16.6	16.7	33.3	33.4	66.7	0	44	708	514968	120093
WT - 2	Unmapped	21.4	29.6	31.2	17.8	60.8	0	6	744	1484	1144
WT - 3	Mapped	16.6	16.7	33.2	33.5	66.7	0	53	528	503071	99766
WT - 3	Unmapped	17.8	20.7	31.1	30.4	61.5	0	5	995	2153	1443
Pulse - 1	Mapped	18.0	17.4	32.6	32.5	65.2	0	210	500	348894	30153
Pulse - 1	Unmapped	17.0	17.5	32.6	32.5	65.1	0	293	523	137263	21356
Pulse - 2	Mapped	16.7	33.2	33.5	33.2	66.7	0	45	678	516179	117546
Pulse - 2	Unmapped	21.6	17.0	31.3	30.1	61.4	0	4	973	2145	1578
Pulse - 3	Mapped	17.2	17.4	32.6	32.7	65.4	0	2997	500	104406	2797
Pulse - 3	Unmapped	18.2	18.2	31.8	31.8	63.7	0	121	515	133521	11910
Press - 1	Mapped	16.8	16.5	33.6	33.1	66.7	0	67	528	503071	78898
Press - 1	Unmapped	16.3	23.3	30.7	29.7	60.4	0	5	1051	1814	1336
Press - 2	Mapped	17.5	17.4	32.6	32.6	65.2	0	637	500	256207	10441
Press - 2	Unmapped	17.7	17.8	32.3	32.2	64.5	0	287	505	215208	16247
Press - 3	Mapped	17.1	17.3	32.7	32.9	65.6	0	4094	500	103157	2344
Press - 3	Unmapped	17.7	17.9	32.2	32.3	64.5	0	165	508	76727	11620

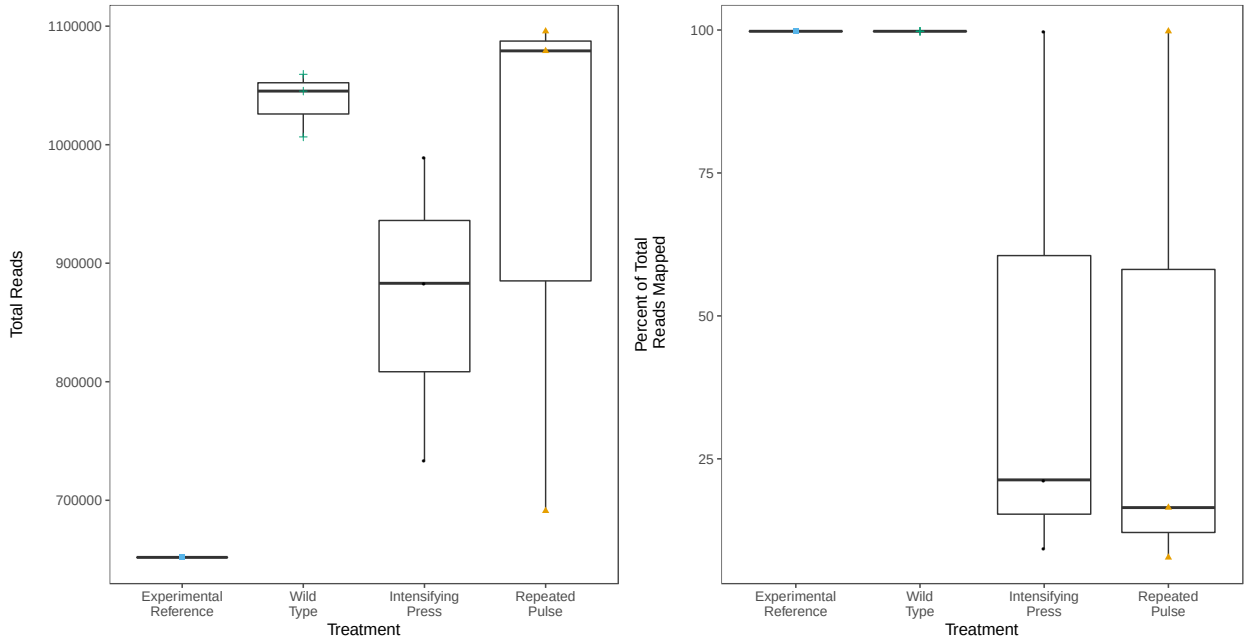

Supplemental Figure 4.1: The total number of reads and percentage of mapped reads was found using QualiMap v. 2.2.1 (García-Alcalde et al. 2012; Okonechnikov et al. 2015). The experimental reference (blue square), wild type (WT) (green cross), intensifying press (black circle), and repeated pulse (yellow triangle) are plotted for both total reads (left plot) and percent of reads mapped (right plot). While the total number of reads did not, on average, vary that greatly between the three treatments, the percentage of reads that mapped decreased dramatically in the press and pulse conditions.

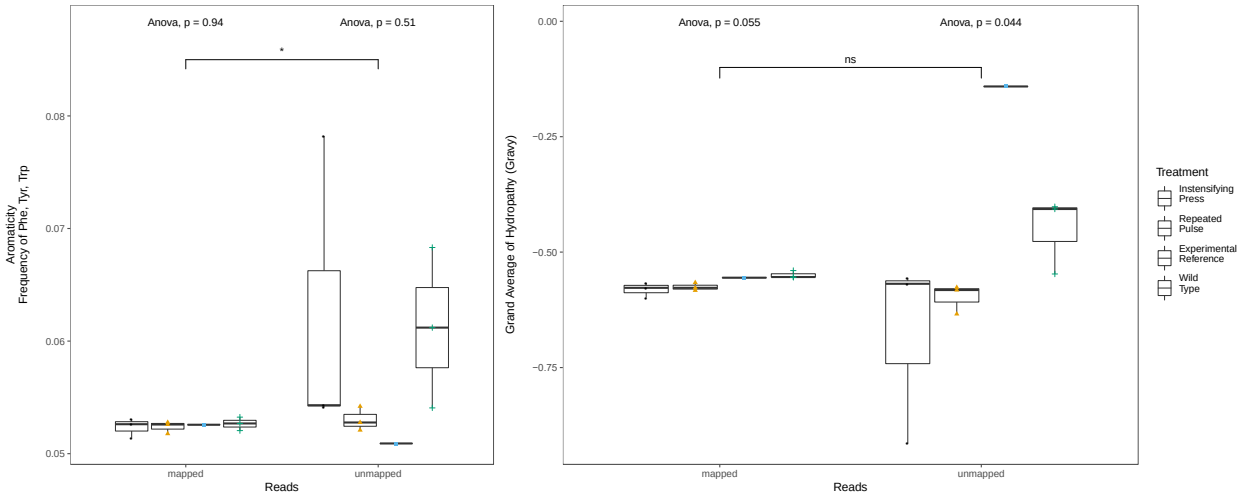

Supplemental Figure 4.2: Scores for aromaticity and the grand average of hydropathy (GRAVY) were calculated using CodonW v. 1.4.4 (Peden 1999) on Galaxy Pasteur (Afgan et al. 2018) and mapped and unmapped contigs were compared. Significance values (ns, *, **) indicate statistically significant differences ($p > 0.05$, $p \leq 0.05$, $p \leq 0.01$) between mapped and unmapped contigs. ANOVA values on the left of each plot indicate difference between mapped contigs and on the right indicate difference between unmapped contigs. The experimental reference (blue square), WT (green cross), intensifying press (black circle), and repeated pulse (yellow triangle) are plotted for aromaticity (left plot) and GRAVY (right plot).

Supplemental Figure 4.3: Alignment comparison of prokka v. 1.14.6 (Seemann 2014) annotations between the NCBI genome and unmapped contigs from a repeated pulse and intensifying press treatment sample for 4-hydroxybenzoate octaprenyltransferase.

References

Afgan, E., D. Baker, B. Batut, M. van den Beek, D. Bouvier, M. Čech, J. Chilton, D. Clements, N. Coraor, B. A. Grüning, A. Guerler, J. Hillman-Jackson, S. Hiltemann, V. Jalili, H. Rasche, N. Soranzo, J. Goecks, J. Taylor, A. Nekrutenko, and D. Blankenberg. 2018. The Galaxy platform for accessible, reproducible and collaborative biomedical analyses: 2018 update. Nucleic Acids Res. 46:W537-W544.

García-Alcalde, F., K. Okonechnikov, J. Carbonell, L. M. Cruz, S. Götz, S. Tarazona, J. Dopazo, T. F. Meyer, and A. Conesa. 2012. Qualimap: evaluating next-generation sequencing alignment data. Bioinformatics 28:2678-2679.

Kearse, M., R. Moir, A. Wilson, S. Stones-Havas, M. Cheung, S. Sturrock, S. Buxton, A. Cooper, S. Markowitz, C. Duran, T. Thierer, B. Ashton, P. Meintjes, and A. Drummond. 2012. Geneious Basic: An integrated and extendable desktop software platform for the organization and analysis of sequence data. Bioinformatics 28:1647-1649.

Okonechnikov, K., A. Conesa, and F. García-Alcalde. 2015. Qualimap 2: advanced multi-sample quality control for high-throughput sequencing data. Bioinformatics 32:292-294.

Parks, D. H., M. Imelfort, C. T. Skennerton, P. Hugenholtz, and G. W. Tyson. 2015. CheckM: assessing the quality of microbial genomes recovered from isolates, single cells, and metagenomes. Genome Res. 25:1043-1055.

Peden, J. F. 1999. Analysis of Codon Usage. Pp. 215. Department of Genetics. University of Nottingham.